Lecture notes CT3320 – (217)

Groundwater *mechanics*, *flow* and *transport*

March 2006

Faculty of Civil Engineering and Geosciences

Prof. dir. ir. F.B.J. Barends
Dr. ir. G.J.M. Uffink

TU Delft Delft University of Technology

69310966
Bestelnummer: 06917290021

Preface

These lecture notes are treating the principles of groundwater *mechanics*, *flow* and *transport*. *Flow* of groundwater is relevant in several civil engineering problems such as river and coastal defense structures, de-watering systems, land reclamation, irrigation/drainage of agricultural land or drinking water supply. Groundwater *mechanics* deals with stability and flexibility of foundations and slopes, subjected to forces induced by earthquakes and high water levels. Another aspect of groundwater mechanics is the de-watering of temporary building pits or permanent underground structures, such as tunnels, metro stations etc. Groundwater *flow* refers to problems where changes in groundwater heads and groundwater flux are introduced. For instance, civil engineering projects such as river and coastal defense structures, de-watering systems, land reclamation, irrigation/drainage of agricultural land or groundwater pumping for drinking water supply. Strictly speaking, flow of groundwater is a form of transport through a porous medium, but usually the term *groundwater transport* is reserved to refer to a category of problems where the displacement of solutes comes into play: e.g. the leaching of contaminant from landfills, the impact of the agricultural use of fertilizers and pesticides on groundwater quality, etc.

The present text is organized as follows. First we start with the basics of *Groundwater Flow* (part 1), before introducing in part 2 S*olute Transport* processes. Part 3 (*Dike Technology*) gives a more historical review of the struggle of the Dutch people against the water. Finally several subjects in which forces (mechanics) and stability aspects are important are collected and discussed in part 4 under the title *Breakwater Technology*.

CONTENTS

PART 1

PART 3

PART 4

PART 1

Fundamentals of Flow

The continuum approach.

Sand bodies consist of a solid matrix of grains and a system of connected pores. The pores may be completely or partly saturated with water (or any other fluid). In this text only fully saturated soils are considered and attention is focused on the flow of the water through the pores and the transport of solutes (e.g. contaminants). The two separate phases, solid matrix and pore fluid may be distinguished explicitly. However, such a microscopic *approach* is seldom used to describe the flow of groundwater. Usually, a higher scale, the macroscopic scale, is introduced on which new macroscopic quantities are defined. For instance, instead of the individual pores, one uses the *porosity*, which is the ratio of the pore volume V_p over the total volume V (pores and grains). The porosity is denoted by the letter n, which represents a dimensionless number [-]:

$$n = \frac{V_p}{V} \tag{1}$$

The value of n is assigned to a point in space, whether the point falls inside or outside a pore. Since the pore volume is always smaller than the total volume, the value of n always lies between 0 and 1. Practical values for n are in the range of .3 to .4 for alluvial sediments. For rubble rock n is 0.42, for sandstone 0.15. For clays the porosity may be higher, up to 0.6.

A macroscopic approach is also followed to describe the fluid flow through the pores. Consider a plane with surface A, [L^2], where A is large compared to the dimensions of a single pore. When the volume of water through this plane, per unit of time is denoted by Q , [$L^3 T^{-1}$], then the *specific discharge* q is defined as:

$$q = Q/A \tag{2}$$

In words: the volume of water flowing across a unit area per unit time. An alternative name for specific discharge is *volume flux density*. Its dimension is that of a velocity [$L T^{-1}$]. Specific discharge is also a macroscopic quantity, so q exists in every point in space, whether it coincides

with a pore or a grain in a microscopic view. In a Cartesian coordinate system (x, y, z) the specific discharge is represented by a vector $\vec{q}$ with components q_x, q_y and q_z.

The specific discharge should not be confused with the *groundwater velocity*, although it has the same dimension. Since groundwater flows only through the pores, which takes only a part n of the total cross section surface A, the average fluid velocity, v, is equal to $Q/(nA)$, or:

$$\vec{q} = n\vec{v} \tag{3}$$

The actual velocity inside the pore can be quite different from the average velocity. We will take a closer look at this in the chapters on groundwater transport. The average velocity is important when the displacement of solutes is considered. The macroscopic approach as described in this section is also known as the *continuum approach.*

Fluid properties

Fluid properties as *density* ρ [M L^{-3}] and *specific weight* γ [M L^{-2} T^{-2}], where $\gamma = \rho g$, play a gravitational role. In principle, the density of groundwater may vary. It depends among others on the temperature, chemical content and the pressure, but in most applications the variations are small and ρ is considered as a constant.

The *pressure* p [M L^{-1} T^{-2}] and its distribution is important for the occurrence of flow. Pressure is always expressed with atmospheric pressure as a zero reference pressure. The water table or phreatic surface is defined as the surface where the pressure equals atmospheric pressure or $p = 0$. Groundwater flow can be described in terms of pressure, as we will see later in this chapter, but in most cases where the fluid density is constant, a simpler description is possible in terms of the *piezometric head* φ (see figure 1):

$$\varphi = \frac{p}{\rho g} + z \tag{4}$$

φ is also called *hydraulic head, groundwater head* or simply *head.* Its dimension is length. Heads are used more often than pressures, although the use of heads implies a limitation: the head can be defined only when the fluid has a constant density. The advantage of using heads is that they can

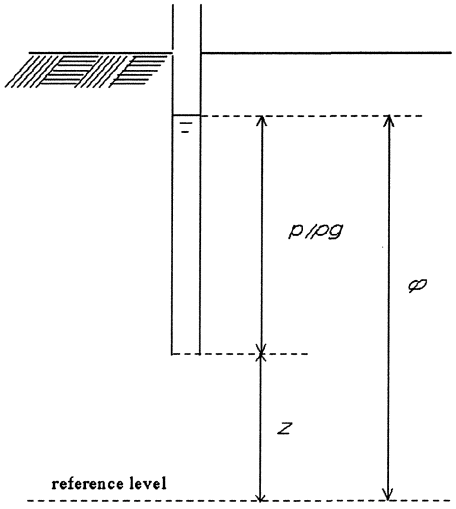

Figure 1 Definition of groundwater head, pressure head and elevation head.

easily be measured in a borehole with a measuring tape. The terms at the right hand side of (4) each have their own name. The quantity $p/\rho g$ is called *pressure head*, while z is the *elevation head*. Elevation head is defined with respect to a certain horizontal datum level, which may be chosen freely. In the Netherlands the standard datum level for regional studies is NAP (Nieuw Amsterdams Peil). For problems on a local scale some other datum level may be more convenient, for example the local soil surface. It follows from (4) that for a constant head and density the pressure distribution is a linear function of z: $p = \rho g(\varphi - z)$. This is the *hydrostatic pressure distribution*. In this case a vertical equilibrium exists and no vertical flow occurs. When between two points a head difference occurs groundwater starts to flow, so head differences are the driving force to groundwater flow.

The head difference $\Delta\varphi = \varphi_2 - \varphi_1$ is always associated with a certain distance $\Delta x = x_2 - x_1$. It is common to speak of the head difference over a certain distance Δx, or we can use the head difference per unit of length. This is the *head gradient*, often denoted by i:

$$i = \frac{\varphi_2 - \varphi_1}{x_2 - x_1} = \frac{\Delta\varphi}{\Delta x} \tag{5}$$

Darcy's law

The head gradient is the driving force for groundwater flow. Darcy's law says how much fluid flows at a certain head gradient and in a given sand formation. To be more precise, a linear relation exists between q and i:

$$q = -k\,i \tag{6}$$

The coefficient k is the *permeability*, or *hydraulic conductivity*. The dimension of k is length over time [$L\ T^{-1}$], equal to the dimension of a velocity. It is a property of the sand (or clay) body.

A modern version of Darcy's law arises when Δx approaches zero and $\Delta\varphi/\Delta x$ is replaced by $\partial\varphi/\partial x$. In three dimensions Darcy's law becomes:

$$q_x = -k\frac{\partial\varphi}{\partial x};\quad q_y = -k\frac{\partial\varphi}{\partial y};\quad q_z = -k\frac{\partial\varphi}{\partial z} \tag{7}$$

or, in vector notation:

$$\vec{q} = -k\nabla\varphi \tag{8}$$

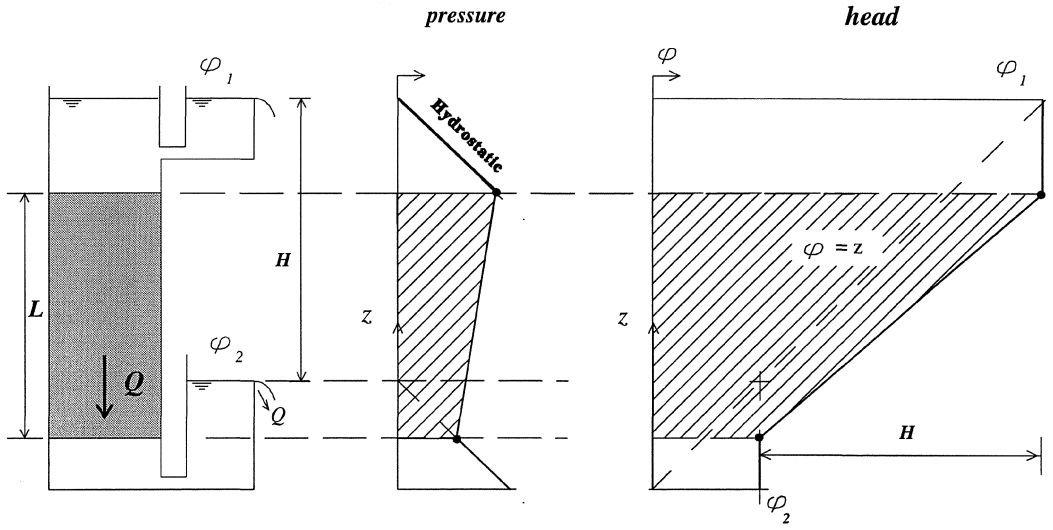

Figure 2 Darcy's experiment in a column and the vertical distribution of pressure and head.

Figure 2 shows schematically the experiment carried out by Darcy and the vertical distribution of both pressure and head. To obtain these distributions proceed as follows. Start with the elevations A and B, where the head is φ_1 and φ_2 , respectively and the pressure is zero. From these points we can construct lines corresponding to the hydrostatic situation, which means a linear pressure distribution and a constant head. On these lines we can find the pressure and heads for the points C and D, etc, etc.

The table below gives the order of magnitude for the permeability of sand/gravel/clay in m/s.

Coarse gravel	10^{-1} - 10^{-2}
Sand and gravel	10^{-2} - 10^{-5}
Fine sands, silt, loess	10^{-5} - 10^{-9}
Clay, shale.	10^{-9} - 10^{-13}

For very coarse material like gravel or rubble rock Darcy's law does not apply, since the flow can become turbulent. In non-saturated soils the permeability is a function of the moisture content and special laws apply.

Intrinsic permeability

The formulation of Darcy's law by (7) or (8) is not correct for all cases. E.g. for fluids with a variable density the definition of heads does not work and one can only use the pressure p. Moreover, the permeability appears to depend on the density and the viscosity of the fluid. Experiments have shown that k is proportional to the quotient γ/μ:

$$k = \kappa \frac{\gamma}{\mu} = \kappa \frac{\rho g}{\mu} \tag{9}$$

where μ is the *dynamic viscosity* of the fluid, [M L^{-1} T^{-1}]. The coefficient κ is a property of the soil only, called the *intrinsic permeability*. It has the dimension of an area [L^2]. With the intrinsic permeability and the pressure p Darcy's law can be written in the following form:

$$q_x = -\frac{\kappa}{\mu}\frac{\partial p}{\partial x}; \quad q_y = -\frac{\kappa}{\mu}\frac{\partial p}{\partial y}; \quad q_z = -\frac{\kappa}{\mu}\left(\frac{\partial p}{\partial z} + \rho g\right) \tag{10}$$

or in vector-notation:

$$\vec{q} = -\frac{\kappa}{\mu}(\nabla p + \rho g \nabla z) \tag{11}$$

The formulation above holds for an arbitrary fluid and is not restricted to fluids with a constant density. For instance, it is commonly used in the oil industry. In groundwater flow the expression in φ is still widely used, not only because it is easier to work with, but also because in most engineering problems the differences in density or viscosity are extremely small or absent. Another reason is that φ is easily measured in a well, either by a stick or a measuring tape, while pressure measurements require more sophisticated tools. Groundwater situations where density differences play a role are encountered e.g. in coastal aquifers (salt/fresh water), or in groundwater polluted with hydrocarbons (lighter than water). Viscosity effects occur when differences in groundwater temperature are present, e.g. thermal heat projects, storage of cooling water, etc.

Carman-Kozeny

Darcy's law is an empirical law. Much research has been done to find a more satisfying theoretical explanation, but with little success. Well-known is the work by Kozeny and Carman, who used Poisseuille's law for flow through a tube as an analogy for porous media flow. Carman and Kozeny derived a relation between κ and several geometric parameters:

$$\kappa = c\frac{n^3}{\tau(1-n)^2 S^2} \tag{12}$$

Here n is the porosity, S the *specific surface* of the grains (grain surface over grain volume). τ is a measure for the *tortuosity* of a streamline through the pores. The idea behind the use of this parameter was that it could be determined by sending electric currents through the pores. c is a factor that varies with the shape of the grains. For pure spheres c = 1/2, but for natural sands this factor may vary considerably. The Carman-Kozeny relation throws some light on the physical background of the process, although it still contains empirical constants. For instance, the specific surface indicates the role of resistance by friction. The specific surface is directly related to the mean grain diameter. For grains in the shape of spheres with a uniform diameter d, the specific surface S becomes $\pi d^2/(\pi d^3/6) = 6/d$. It indicates that the finer the grains, the higher the specific surface, thus the more resistance to flow and less permeable. (Note that one cm^3 of fine sand may

have an internal surface in the order of 1 m^2; 1 cm^3 of clay up to 20 m^2 and more). When we substitute $S = 6/d$ in (12) it appears that the permeability varies quadratic with the effective grain size d. The relation also indicates the importance of porosity. However, the natural variations of porosity are small. For sand formations the porosity is always around .35, varying from .32 to .38.

Equation of groundwater flow

Groundwater flow problems can be solved mathematically in several ways, but they all start with the basic differential equation, also called the groundwater flow equation. To set up the groundwater flow equation we need, in addition to Darcy's law, a physical principle such as the principle of mass conservation. This principle says that per unit of time the difference between the mass flowing into the system $I(t)$ and the mass flowing out of the system $O(t)$ must be equal to the increase of mass stored in the system $M(t)$. As a differential equation this reads:

$$I(t) - O(t) = \frac{dM}{dt} \tag{13}$$

This holds for every small element we consider. In this chapter we shall restrict ourselves to stationary groundwater flow, so I and O are constant in time and the changes of storage in time are zero:

$$I - O = 0 \tag{14}$$

Let us now describe the terms I and O in more detail. Consider a small volumetric element during a unit time interval ($\Delta t = 1$). Fig. 5 shows such an element and the volume flux across the faces of the element. For the in and out going flux we obtain:

$$I = \rho q_x \Delta y \Delta z + \rho q_y \Delta x \Delta z + \rho q_z \Delta x \Delta y \tag{15}$$

$$O = \left(\rho q_x + \frac{\partial (\rho q_x)}{\partial x} \Delta x \right) \Delta y \Delta z + \left(\rho q_y + \frac{\partial (\rho q_y)}{\partial y} \Delta y \right) \Delta x \Delta z + \left(\rho q_z + \frac{\partial (\rho q_z)}{\partial z} \Delta z \right) \Delta x \Delta y \tag{16}$$

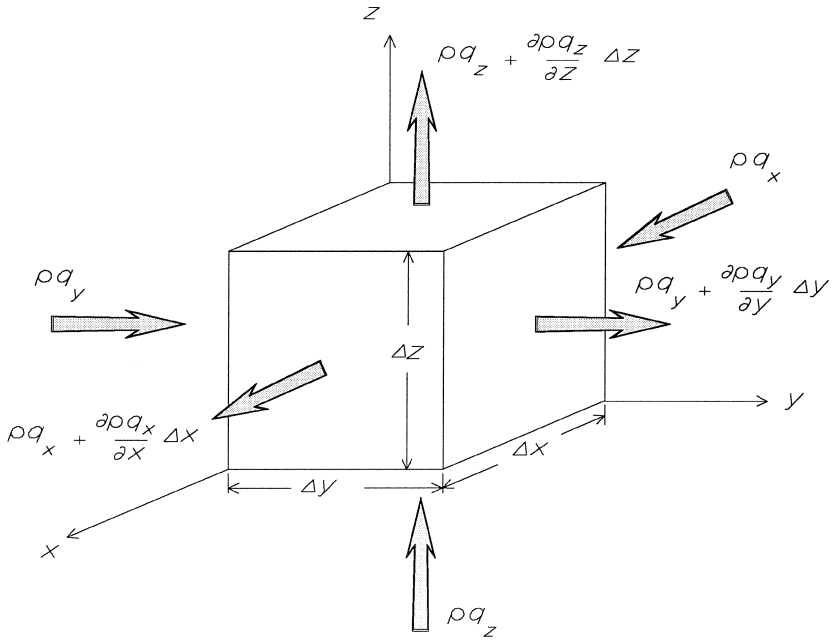

Figure 3 Elementary volume and in and out going flux

The difference $I - O$ is

$$I - O = -\left(\frac{\partial(\rho q_x)}{\partial x} + \frac{\partial(\rho q_y)}{\partial y} + \frac{\partial(\rho q_z)}{\partial z} \right) \Delta x \Delta y \Delta z = 0 \qquad (17)$$

If the fluid is incompressible, ρ is constant and we obtain:

$$\frac{\partial q_x}{\partial x} + \frac{\partial q_y}{\partial y} + \frac{\partial q_z}{\partial z} = 0 \qquad (18)$$

This is the *continuity equation* for incompressible fluids. When Darcy's law is substituted we obtain:

$$\frac{\partial}{\partial x}\left(k \frac{\partial \varphi}{\partial x} \right) + \frac{\partial}{\partial y}\left(k \frac{\partial \varphi}{\partial y} \right) + \frac{\partial}{\partial z}\left(k \frac{\partial \varphi}{\partial z} \right) = 0 \qquad (19)$$

which is the *groundwater flow equation* for a steady state. For a homogeneous aquifer (k = constant) the flow equation reduces to:

$$\frac{\partial^2 \varphi}{\partial x^2} + \frac{\partial^2 \varphi}{\partial y^2} + \frac{\partial^2 \varphi}{\partial z^2} = 0 \tag{20}$$

which is known as the *Laplace equation.*

Boundary conditions

The flow equation (19) applies to an extensive class of groundwater flow problems. For a particular problem the solution is found by solving the differential equation using the prevailing boundary conditions to determine the unknown integration constants. Several types of boundary conditions can be distinguished:

- head is given (***Dirichlet***), e.g:

$$\varphi = f(s) \tag{21}$$

  where s is a coordinate along the boundary and $f(s)$ a given function.

- flux is given (***Neumann***), e.g:

$$\frac{\partial \varphi}{\partial n} = f(s) \tag{22}$$

  where n is the coordinate perpendicular to the boundary.

- A combination of the head and the flux is given (***Rayleigh***), e.g:

$$\varphi + \beta \frac{\partial \varphi}{\partial n} = f(s) \tag{23}$$

In the next section we discuss some cases, where the differential equation can be solved easily by analytical means.

Exercise 1 Darcy's law and heterogeneity (I)

A permeameter is filled with two types of sand (see figure), with conductivities k_1 and k_2. The height of the sand samples is L_1 and L_2. The cross-section of the permeameter is A and the amount of water through the apparatus is Q. Suppose $k_1 = 2k_2$ and $L_1 = 3L_2/2$. Calculate the head at the intersection between the two types of sand.

Denote the discharge through the samples by Q_1 and Q_2. Continuity requires $Q_1 = Q_2$. Applying Darcy's law:

$$Q_1 = k_1 A H_1 / L_1$$
$$Q_2 = k_2 A H_2 / L_2$$

where $H_1 = \phi_0 - \phi_1$ and $H_2 = \phi_1 - \phi_2$. Both ϕ_0 and ϕ_2 are known, i.e. ϕ_0 is taken zero and ϕ_2 is equal to $-H$. ϕ_1 needs to be calculated. Combination of continuity and Darcy yields:

$$(k_1/L_1)\,(\phi_0 - \phi_1) = (k_2/L_2)\,(\phi_1 - \phi_2)$$

or

$$\phi_1 = \frac{(k_1/L_1)\,\phi_0 + (k_2/L_2)\phi_2}{(k_1/L_1) + (k_2/L_2)} = \frac{4\phi_0 + 3\phi_2}{7} = -\frac{3}{7}H$$

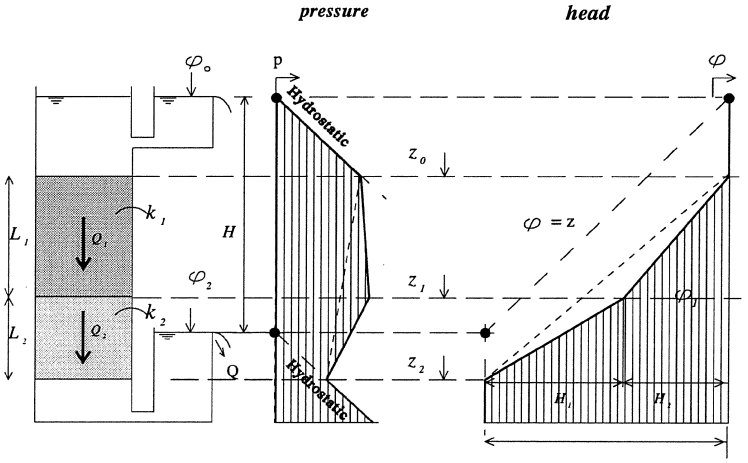

Assume the following numerical values:

$L_1 = .3$ m $\quad L_2 = .2$m $\quad H = .65$ m $\quad \gamma = 10^4$ N/m^3 $\quad z_0 = -.2$ m $\quad z_1 = -.5$ m $\quad z_2 = -.7$ m

and calculate head and pressure at $z = z_0$, $z = z_1$ and $z = z_2$.

$z = z_0$ $\quad \phi = \phi_0 = 0$ (choice of reference) $\quad p_0 = \gamma(\phi_0 - z_0) = 0.20\ 10^4$ N/m^2

$z = z_1$ $\quad \phi = \phi_1 = -\frac{3}{7}H = -.278$ m $\quad p_1 = \gamma(\phi_1 - z_1) = 0.22\ 10^4$ N/m^2

$z = z_2$ $\quad \phi = \phi_2 = -H = -.65$ m $\quad p_2 = \gamma(\phi_2 - z_2) = 0.05\ 10^4$ N/m^2

Exercise 2 Darcy's law and heterogeneity (II)

A situation similar to exercise 1, but with horizontal flow (see figure 2). Let k_1 = 5 m/day and k_2 = 20 m/day, L_1 = 10 cm and L_2 = 20 cm, H = 60 cm, while the cross-section A = 40 cm^2. Calculate ϕ_1, which is the head at the intersection of the two bodies of sand and the discharge Q.

Again, continuity and combined with Darcy yields $k_1AH_1/L_1 = k_2AH_2/L_2$ which, as above, leads to:

$$\phi_1 = \frac{(k_1/L_1)\phi_0 + (k_2/L_2)\phi_2}{(k_1/L_1) + (k_2/L_2)}$$

Substitution of $\phi_0 = 0$ (choice of reference level) and $\phi_2 = H = 6$ cm, leads to:

$$\phi_1 = 4 \text{ cm.}$$

To calculate Q apply Darcy's law:

$$Q = k_1A\phi_1/L_1 = 0.008 \text{ m}^3\text{/day}$$

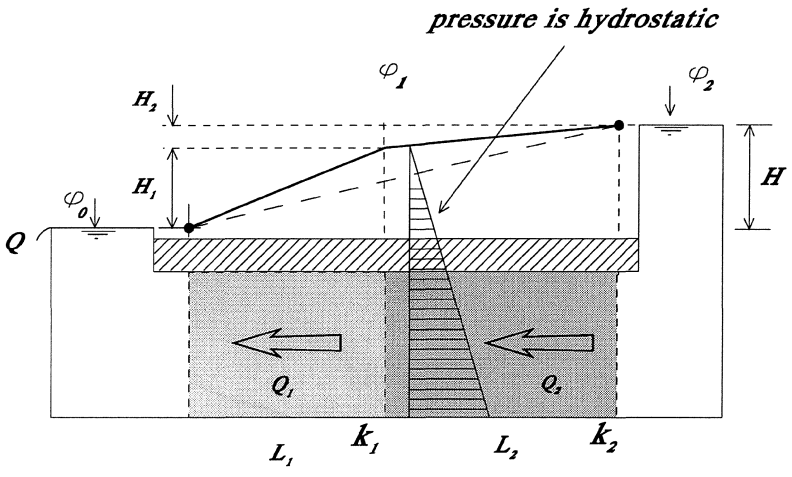

Exercise 3 Heterogeneity and effective permeability (I)

Consider the situation of exercise 2. This heterogeneous sand body consists of two different types of sand. We can replace this heterogeneous block by a homogeneous block with an equivalent or effective permeability k_{eff}. This is the permeability that produces the same discharge Q_{eff} under the same drop in piezometric head $\Delta\varphi_{eff} = \varphi_2 - \varphi_0$. The length L of the block with the equivalent permeability is equal to the sum of the lengths of the heterogeneous blocks, so $L = L_1 + L_2$ Give a formula for the effective permeability.

Answer: Our equations are Darcy in the blocks with k_1, k_2 and in the equivalent medium. Additionally we have equations that express that the pressure drop over the effective medium with k_{eff} equals that over the heterogeneous one and that the resulting discharges are equal:

Darcy heterogeneous case: $$Q_1 = k_1 A \frac{\varphi_1 - \varphi_0}{L_1}$$

$$Q_2 = k_2 A \frac{\varphi_2 - \varphi_1}{L_2}$$

Darcy equivalent medium: $$Q_{eff} = k_{eff} A \frac{\varphi_2 - \varphi_0}{L}$$

Equivalent discharge: $$Q_{eff} = Q_1 = Q_2$$

Equivalent drop in head: $$(\varphi_2 - \varphi_0) = (\varphi_2 - \varphi_1) + (\varphi_1 - \varphi_0)$$

We start with the last equation and write the terms as gradients:

$$\frac{(\varphi_2 - \varphi_0)}{L} = \frac{(\varphi_2 - \varphi_1)}{L_2}\frac{L_2}{L} + \frac{(\varphi_1 - \varphi_0)}{L_1}\frac{L_1}{L}$$

Now substitute the gradients using the expressions given by Darcy's law:

$$\frac{Q_{eff}}{k_{eff} A} = \frac{Q_2}{k_2 A}\frac{L_2}{L} + \frac{Q_1}{k_1 A}\frac{L_1}{L}$$

Since all Q's are equal, they cancel out together with A and we obtain:

$$\frac{1}{k_{eff}} = \frac{1}{L}\left\{\frac{L_1}{k_1} + \frac{L_2}{k_2}\right\}$$

This is the formula for the (weighted) harmonic mean.

Exercise 4 Heterogeneity and effective permeability (II)

A similar question as exercise 3, but now the medium with total thickness D, consists of two horizontal layers, with thick nesses d_1 and d_2 respectively (see figure). We consider that in the direction perpendicular to the paper, the thickness is 1.

Again, we have Darcy for the layers with k_1 and k_2 and for the equivalent medium:

Heterogeneous case:

$$Q_1 = k_1 d_1 \frac{\varphi_2 - \varphi_1}{L}$$

$$Q_2 = k_2 d_2 \frac{\varphi_2 - \varphi_1}{L}$$

Equivalent medium:

$$Q_{eff} = k_{eff} D \frac{\varphi_2 - \varphi_1}{L}$$

We must now use an expression that says that the total discharge through the layers, which is the sum of the discharge through the individual layer, must be the same in the equivalent case, so:

$$Q_{eff} = Q_1 + Q_2$$

Substitution with the Darcy's law expressions gives:

$$k_{eff} D \frac{\varphi_2 - \varphi_1}{L} = k_1 d_1 \frac{\varphi_2 - \varphi_1}{L} + k_2 d_2 \frac{\varphi_2 - \varphi_1}{L}$$

and finally this reduces to:

$$k_{eff} = \frac{1}{D}\{k_1 d_1 + k_2 d_2\}$$

This is the formula for the (weighted) arithmetic mean.

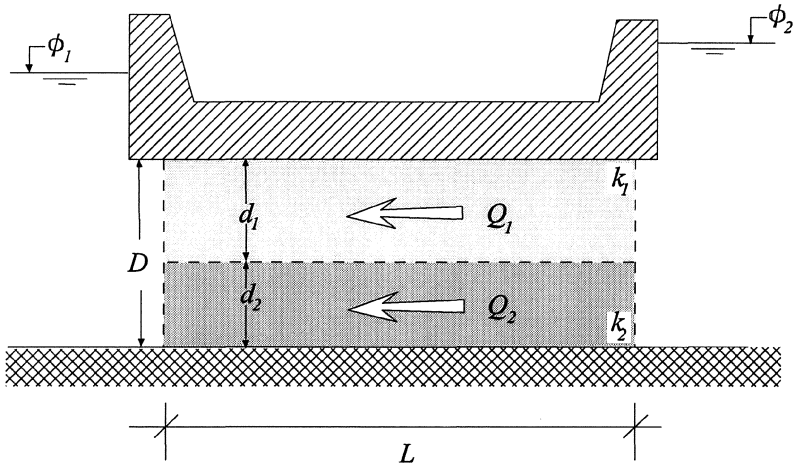

Steady Flow in One Dimension

In this chapter some elementary one-dimensional solutions are presented for several aquifer types: confined (artesian), unconfined (phreatic) and semi-confined (leaky).

Confined aquifer, linear case

An aquifer with an impervious layer at the top and the bottom is referred to as *confined*. Also used is the term *artesian* aquifer. In figure 4 an example of a linear flow in a confined aquifer is shown. A dam is located between two bodies of surface water with fixed heads φ_1 and φ_2, respectively. H denotes the aquifer thickness. The differential equation can be obtained by reducing the general equation (19), or it can be derived from scratch. As an exercise we shall derive the flow equation for this particular case.

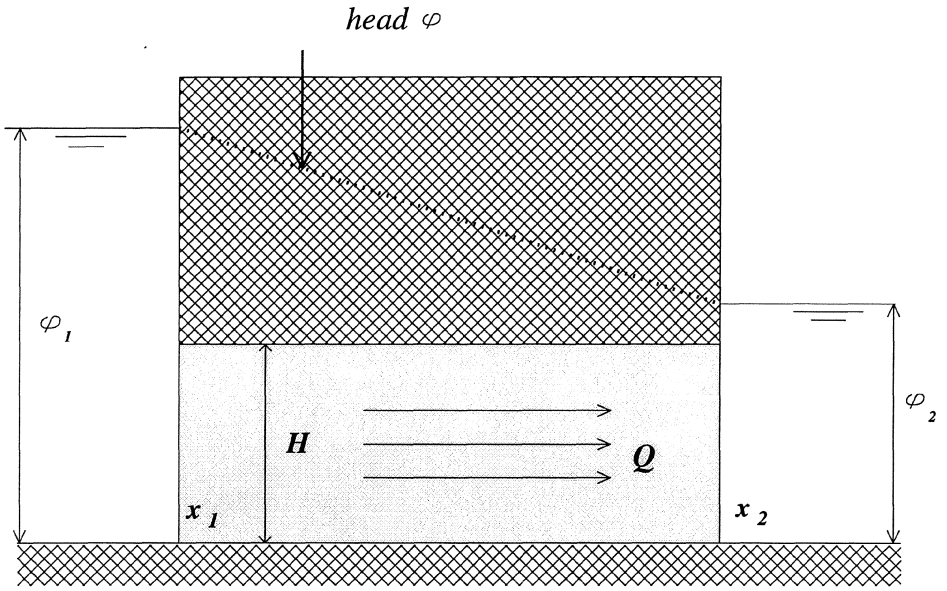

Figure 4. Flow through a dam in a confined aquifer

We start by writing down the continuity equation. If Q is the total flux through the layer ($Q = qH$), then the principle of continuity says that Q does not change in x-direction or:

$$\frac{dQ}{dx} = 0 \tag{24}$$

For Q we write, using Darcy's law:

$$Q = qH = -kH\frac{d\varphi}{dx} \tag{25}$$

Combination of continuity (eq. 24) and Darcy's law (eq. 25), gives:

$$\frac{d^2\varphi}{dx^2} = 0 \tag{26}$$

This is the one-dimensional version of the Laplace equation (19). Integration gives:

$$\varphi = Ax + B \tag{27}$$

where A and B are integration constants that must be determined from the boundary conditions. For the present case the boundary conditions are of the Dirichlet type, which means that heads are given:

$$\begin{aligned} x = x_1;\quad \varphi = \varphi_1 \\ x = x_2;\quad \varphi = \varphi_2 \end{aligned} \tag{28}$$

Substitution into (27) leads to $A = (\varphi_2 - \varphi_1)/(x_2 - x_1)$ and $B = (\varphi_1 x_2 - \varphi_2 x_1)/(x_2 - x_1)$. With this, the solution becomes:

$$\varphi = \frac{\varphi_2(x - x_1) - \varphi_1(x - x_2)}{x_2 - x_1} \tag{29}$$

The flux Q through the dam is found by applying Darcy's law, using (29):

$$Q = -kH\frac{\varphi_2 - \varphi_1}{x_2 - x_1} \tag{30}$$

The product kH, often denoted as T, is called the *transmissivity*.

Confined aquifer, radial flow

Consider a well with discharge Q in the center of a circular island. The radius of the island is R. The head of the water surrounding the island is φ_0 (figure 5).

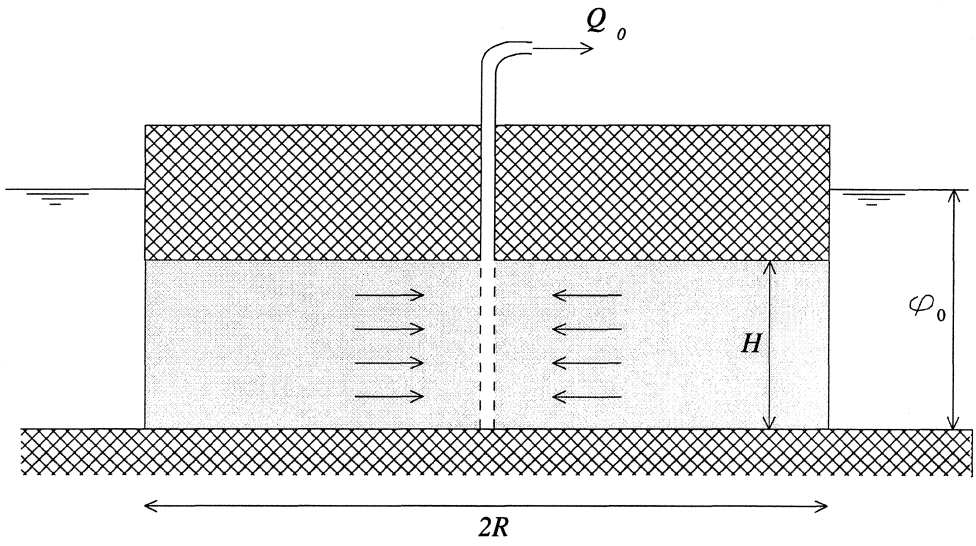

Figure 5 Well in a circular island and confined aquifer

Since the problem is axial-symmetric, it is convenient to use polar coordinates en write the flow equation as:

$$\frac{d^2\varphi}{dr^2}+\frac{1}{r}\frac{d\varphi}{dr}=0 \qquad (31)$$

This equation is obtained by the substitution $x = r\cos\theta$ and $y = r\sin\theta$ and ignoring the derivatives to θ (radial symmetry). The general solution to (31) is:

$$\varphi = A\ln r + B \qquad (32)$$

A and B follow from the boundary conditions. The first condition is of the Dirichlet type and the second of the Neuman type:

$$r = R \quad ; \varphi = \varphi_0 \qquad (33)$$

$$r \to 0; \frac{d\varphi}{dr} = \frac{Q_0}{2\pi kHr} \tag{34}$$

where Q_0 is the discharge of the well. The sign of Q_0 is taken positive when the well is pumping. This corresponds with a positive gradient $d\varphi/dr$ just outside the well. Substitution of (34) into (32) leads to:

$$A = \frac{Q_0}{2\pi kH} \tag{35}$$

Use of (33) gives:

$$B = \varphi_0 - \frac{Q_0}{2\pi kH} \ln R \tag{36}$$

The final solution becomes:

$$\varphi = \varphi_0 + \frac{Q_0}{2\pi kH} \ln \frac{r}{R} \tag{37}$$

The concept of a circular island is somewhat artificial, but the formula can be used also when the flow is radial and at a distance, e.g. at $r = r_0$, the head is given as φ_0. In that case in (37) one must write $R = r_0$.

Unconfined Flow and the Dupuit-Forchheimer assumption

Situations with a free groundwater surface are called unconfined or *phreatic*. Strictly speaking, in unconfined aquifers the flow is not 1-dimensional, because both a horizontal and a vertical velocity component exists. The vertical component, however, is always much smaller than the horizontal one. One may object that this doesn't show in the picture, but in vertical cross-sections the vertical dimension is usually exaggerated in comparison with the horizontal. A classical simplification is to assume that the head remains constant in vertical direction, which, of course, is only true when the vertical flow is zero. This assumption is known as the ***Dupuit-Forchheimer approximation***. It enables us to simplify the case to a one-dimensional problem.

Consider the flow between two canals with different water levels, similar to figure 6, but without the confining layer on top. Also, a groundwater recharge N is included (figure 6). To establish the flow equation we combine again continuity and Darcy's law. Continuity gives:

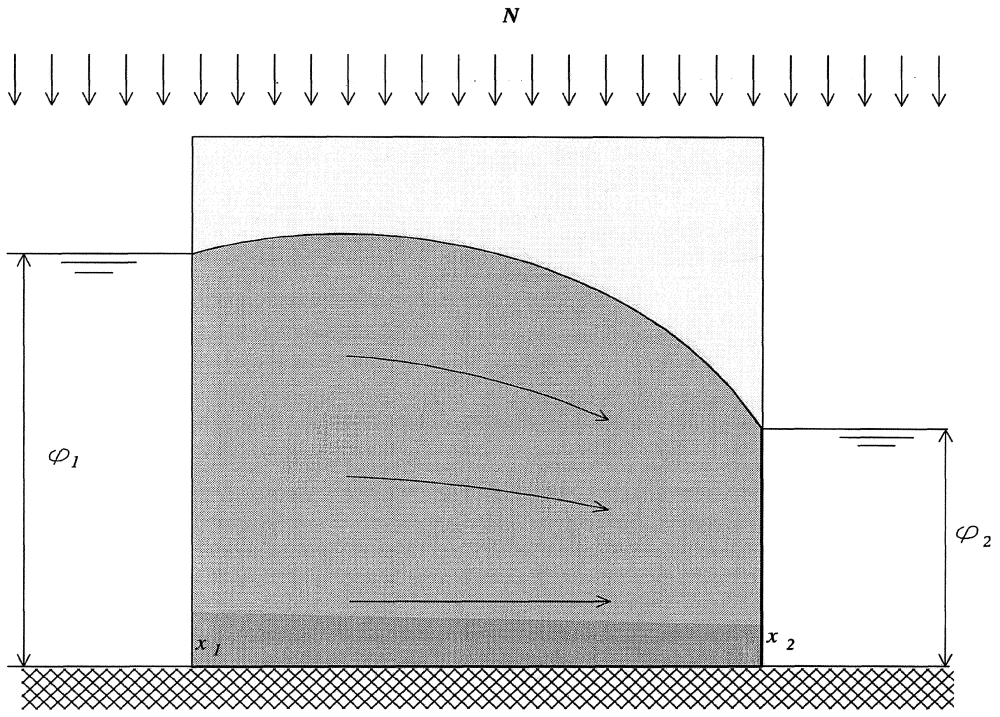

Figure 6 Flow in unconfined aquifer with rain.

$$\frac{dQ}{dx} = N \tag{38}$$

where $Q = \varphi q$ is the total flow in horizontal direction. Note, that here we must use the base of the aquifer as reference level for φ. Substitution of Darcy's law leads to the following flow equation:

$$\frac{d}{dx}\left(\varphi \frac{d\varphi}{dx}\right) = -\frac{N}{k} \tag{39}$$

In contradiction to (26), the equation is non-linear in φ. The non-linearity is easily dealt with by considering φ^2 as independent variable. Eq. (39) is then written as:

$$\frac{d^2\varphi^2}{dx^2} = -2\frac{N}{k} \tag{40}$$

The general solution becomes:

$$\varphi^2 = -\frac{N}{k}x^2 + Ax + B \tag{41}$$

The boundary conditions are:

$$\begin{aligned} x &= x_1 \quad ; \quad \varphi = \varphi_1 \\ x &= x_2 \quad ; \quad \varphi = \varphi_2 \end{aligned} \tag{42}$$

Substitution into (41) and solving A and B gives:

$$A = \frac{\varphi_2^2 - \varphi_1^2}{x_2 - x_1} + \frac{N}{k}(x_2 + x_1) \tag{43}$$

$$B = \frac{\varphi_2^2 x_1 - \varphi_1^2 x_2}{x_2 - x_1} - \frac{N}{k}x_1 x_2 \tag{44}$$

The final solution becomes:

$$\varphi^2 = -\frac{N}{k}(x - x_1)(x - x_2) + \frac{\varphi_2^2(x - x_1) - \varphi_1^2(x - x_2)}{x_2 - x_1} \tag{45}$$

Note, that for $N = 0$ the solution resembles that of the confined case as given by (29). The difference is that φ is re placed by φ^2. The discharge through the dam $Q = - k\varphi\, d\varphi/dx$ becomes, (still for $N = 0$):

$$Q = -\frac{k}{2}\frac{\varphi_2^2 - \varphi_1^2}{x_2 - x_1} \tag{46}$$

As a matter of fact, the same expression is found when the problem is solved fully 2-dimensionally, (without the Dupuit-Forchheimer assumption).

Phreatic aquifer with rain, radial flow

Consider a well in a circular island with recharge N from the top (figure 7). For the total discharge Q at a distance r we have $Q(r) = 2\pi r\varphi\, q$ or:

$$Q(r) = -2\pi rk\varphi\frac{d\varphi}{dr} = -\pi rk\frac{d\varphi^2}{dr} \tag{47}$$

The base of the aquifer is taken as reference. The discharge Q is no longer constant with increasing r due to the recharge N. To establish the continuity equation we consider an elementary volume consisting of a cylinder with radius r, thickness dr and height equal to the aquifer thickness. The change in discharge, denoted as dQ, is equal to the recharge infiltrating that at the top, or $2\pi\, rdrN$. Thus, continuity gives:

$$\frac{dQ}{dr} = 2\pi rN \tag{48}$$

Substitution by (47) leads to:

$$\frac{d^2\varphi^2}{dr^2} + \frac{1}{r}\frac{d\varphi^2}{dr} = -\frac{2N}{k} \tag{49}$$

with a general solution:

$$\varphi^2 = -\frac{N}{2k}r^2 + A\ln r + B \tag{50}$$

The boundary conditions are of the Dirichlet type (at $r = R$) and the Neumann type (for $r \to 0$):

$$\begin{aligned} r = R \quad &; \quad \varphi = \varphi_0 \\ r \to 0 \quad &; \quad \frac{d\varphi^2}{dr} = \frac{Q_0}{\pi kr} \end{aligned} \tag{51}$$

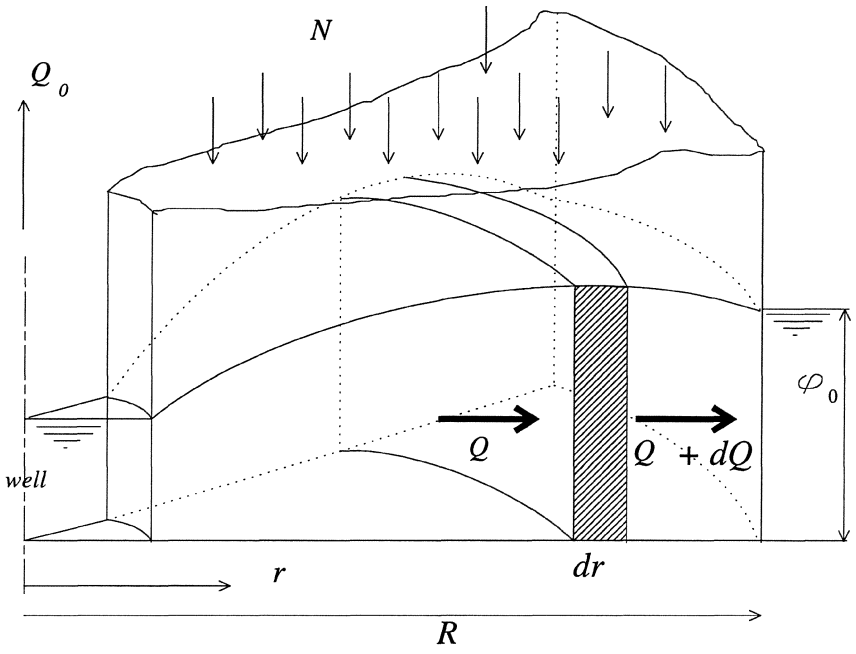

Figure 7 Flow to a well in an unconfined aquifer

where Q_0 is the discharge of the well. The constants A and B are solved using the boundary conditions. The final solution for solution for φ^2 then becomes:

$$\varphi^2 = \varphi_0^2 + \frac{N}{2k}(R^2 - r^2) + \frac{Q_0}{\pi k}\ln\frac{r}{R} \qquad (52)$$

Semi confined

A confined aquifer becomes *semi-confined*, if one or both confining layers are not impervious, but semi-pervious. These aquifers are also known as *leaky aquifers*. Often, the semi-pervious layer on top is overlain by a second aquifer, in which the head is not influenced by the flow in the main aquifer. Such cases are found in polder areas, where the head in the upper aquifer is regulated by a detailed drainage/irrigation system. As an example we consider a canal with a water level above the *polder-level* φ_0 (figure 8).

To establish the flow equation we need the amount of leakage through the clay layer q_0. The leakage is induced by the head loss φ - φ_0 over the clay layer, with a thickness d. Darcy's law here, for purely vertical flow, gives:

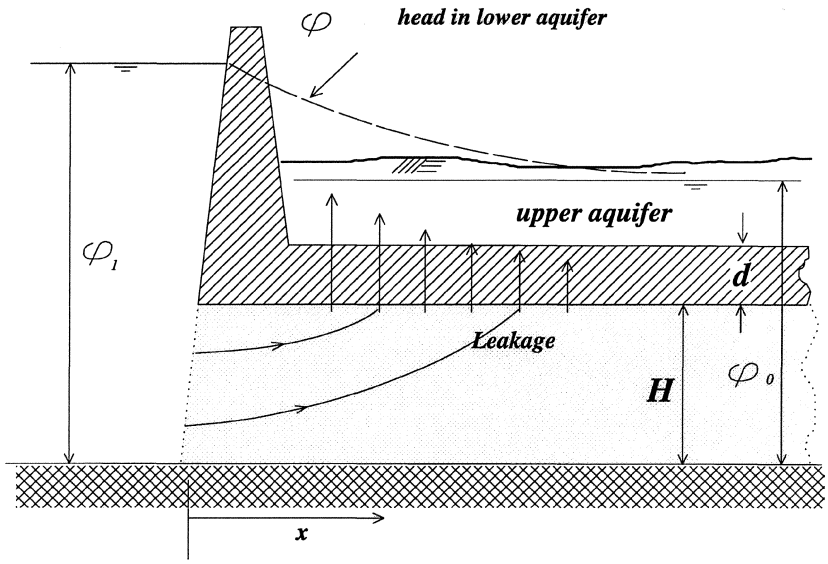

Figure 8 Flow in semi-confined aquifer

$$q_0 = k_0 \frac{\varphi - \varphi_0}{d} \tag{53}$$

where k_0 is the permeability of the clay layer. The properties of the clay layer are usually combined in the so-called *resistance c*:

$$c = \frac{d}{k_0} \tag{54}$$

The resistance has the dimension of time and is usually expressed in days. The continuity equation now becomes $dQ/dx = - q_0$, leading to:

$$kH \frac{d^2\varphi}{dx^2} = \frac{\varphi - \varphi_0}{c} \tag{55}$$

or:

$$\frac{d^2\varphi}{dx^2} = \frac{\varphi - \varphi_0}{\lambda^2} \tag{56}$$

where, $\lambda = \sqrt{(kHc)}$ is called the *leakage factor*. The general solution has the form:

$$\varphi - \varphi_0 = A\exp(x/\lambda) + B\exp(-x/\lambda) \tag{57}$$

The constants A and B are determined from the (Dirichlet-type) boundary conditions:

$$\begin{aligned} x \to \infty \quad &; \quad \varphi = \varphi_0 \\ x = 0 \quad &; \quad \varphi = \varphi_1 \end{aligned} \tag{58}$$

Substitution gives $A = 0$ and $B = (\varphi_1 - \varphi_0)$ and the solution becomes:

$$\varphi - \varphi_0 = (\varphi_1 - \varphi_0)\exp(-x/\lambda) \tag{59}$$

We can see from (59) that it is the *leakage factor* λ that determines the spatial distribution of the head. The leakage-factor, with the dimension of length, indicates to what extent away from the canal the influence of the higher head in the canal is still felt. At a distance of 3 λ the head difference (ϕ_1 - ϕ_0) is reduced by *exp* (- 3), which is a reduction of 98 %. A closer look at the flow lines in the aquifer shows that leakage is leaving at the top of the aquifer in vertical direction. This implies that in the aquifer a vertical flow component exists, so in reality the problem is two-dimensional. As in the case of unconfined flow, the head distribution is simplified by assuming that *in the aquifer* the vertical flow does not produce vertical head differences (*Dupuit-Forchheimer assumption*).

Leaky aquifer, radial flow

When pumping takes place in a leaky aquifer, the head difference over the semi-pervious layer, created by the drawdown in the pumped aquifer, produces a flow through the clay layer $q_0 = -(\varphi_0 - \varphi)/c$, where φ_0 is the polder level, φ the head in the pumped aquifer and c the resistance of the semi-pervious layer. Again, to obtain the final differential equation we follow a continuity approach on a cylinder at distance r with a thickness dr. The discharge $Q(r)$ through the cylinder is given by:

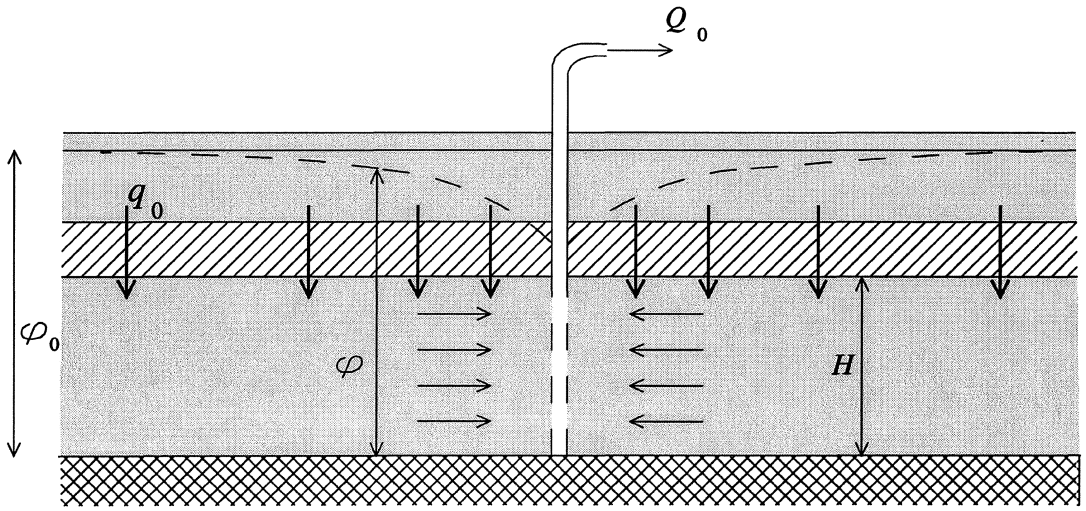

Figure 9 Radial flow in an infinite semi-confined aquifer

$$Q(r) = -2\pi rkH\frac{d\varphi}{dr} \tag{60}$$

Continuity says that the increase dQ of the discharge over a distance dr, must be equal to the amount of water entering through the clayer layer or $-2\pi r dr\, q_0$:

$$\frac{dQ}{dr} = -2\pi r q_0 \tag{61}$$

Combination of (60) and (61) gives:

$$\frac{d^2\varphi}{dr^2} + \frac{1}{r}\frac{d\varphi}{dr} = \frac{q_0}{kH} \tag{62}$$

or, with the *leakage-factor* $\lambda = \sqrt{(kHc)}$, and using (53):

$$\frac{d^2\varphi}{dr^2} + \frac{1}{r}\frac{d\varphi}{dr} = \frac{\varphi - \varphi_0}{\lambda^2} \tag{63}$$

of zero order, and of the first and second kind, denoted as I_0 and K_0. These functions cannot be expressed in known functions such as exponentials or cosine and sine. Series expansions exist and tables can be found in several mathematical handbooks (also see appendix A). The functions $K_0(r)$ and $I_0(r)$ are no direct solutions to (63), but to the following equation:

$$\frac{d^2\varphi}{dr^2}+\frac{1}{r}\frac{d\varphi}{dr}=\varphi \tag{64}$$

Equation (63) can easily be reduced to (64) by the substitution $\varphi'=\varphi-\varphi_0$. The solution to (63) becomes:

$$\varphi-\varphi_0 = A\,I_0(r/\lambda)+BK_0(r/\lambda) \tag{65}$$

Figure 10 shows graphs of $I_0(r)$, and $K_0(r)$, as well as the modified Bessel functions of the order one: $I_1(r)$ and $K_1(r)$. The functions of order one and order zero are related by:

$$\frac{d}{dr}I_0(r)=I_1(r) \tag{66}$$

$$\frac{d}{dr}K_0(r)=-K_1(r) \tag{67}$$

To determine the integration constants A and B in (65), we need boundary conditions. For the present case they are:

$$\begin{aligned} &r\to\infty \;\;;\;\; \varphi=\varphi_0 \\ &r\to 0 \;\;;\;\; \frac{d\varphi}{dr}=\frac{Q_0}{2\pi rkH} \end{aligned} \tag{68}$$

where Q_0 is the discharge of the well. The first condition can be satisfied only if the contribution by I_0 is zero, since I_0 goes to infinity for $r\to\infty$ (figure 10). Therefore, $A = 0$. For the second boundary condition we differentiate the solution and use (66) and (67):

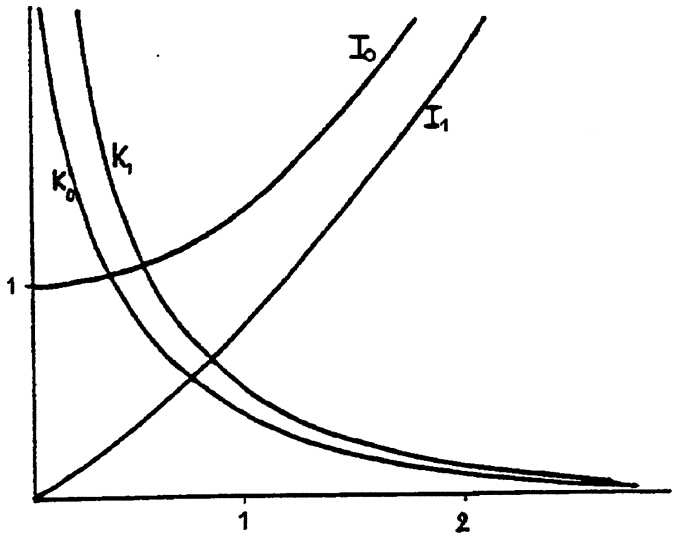

Figure 10 Modified Bessel functions of order zero and one

$$\frac{d\varphi}{dr} = B\frac{d}{dr}K_0(r/\lambda) = -\frac{B}{\lambda}K_1(r/\lambda) \tag{69}$$

There exists a useful approximation for $K_1(r)$ as $r \rightarrow 0$:

$$r \rightarrow 0 \quad ; \quad K_1(r) \approx \frac{1}{r} \tag{70}$$

Then, $K_1(r/\lambda) \approx \lambda/r$ for $r/\lambda \rightarrow 0$. Finally we find $B = -Q_0/(2\pi kH)$. The solution becomes:

$$\varphi - \varphi_0 = -\frac{Q_0}{2\pi kH}K_0(r/\lambda) \tag{71}$$

For $r/\lambda < 0.2$ the Bessel-function $K_0(r/\lambda)$ is, in approximation, equal to $ln\ (1.123\ \lambda/r)$, giving:

$$\varphi - \varphi_0 = \frac{Q_0}{2\pi kH}\ln\left(\frac{r}{1.123\lambda}\right) \tag{72}$$

Note the great similarity between (72) and (37).

Exercise 5 Confined Flow

A well is in the center of a circular island with radius R (see figure). The head at R is φ_R. The aquifer is confined with conductivity k. The radius of the well is r_w, while the borehole, in which the well screen is placed, has a radius r_b ($r_b > r_w$). After installation of the well screen, the space between r_w and r_b is filled with coarse sand with a conductivity k_b. The question is:

a) calculate the drawdown ($\varphi_R - \varphi_w$)

b) calculate the travel time from the edge of the island to the well

Use the following numerical values:

$k = 0.0001$ m/s	$k_b = 0.01$ m/s
$Q = 10^{-3}$ m^3/s	$H = 10$ m
$n = 0.4$	$R = 2000$ m
$r_b = 1.0$ m	$r_w = 0.2$ m

a) Calculation of drawdown:

Choose φ_R as reference level, so $\varphi_R = 0$. Calculate φ_b from:

$$\varphi_b = \frac{Q}{2\pi kH}\ln\left(\frac{r_b}{R}\right) = -1.212\,m$$

Accordingly, φ_w is found by using $\varphi = \varphi_b$ for $r = r_b$ as a boundary condition and considering the borehole as a separate, very small, aquifer:

$$\varphi_w - \varphi_b = \frac{Q}{2\pi k_b H}\ln\left(\frac{r_w}{r_b}\right)$$

b) Calculation of travel time:

Suppose a contaminant is spilled on the surface and leaks to the aquifer. It may be necessary to know when the contaminant reaches the well, so measures can be taken in time.

General procedure:

The velocity $v_r = dr/dt$ is equal to the specific discharge q_r, divided by the porosity n:

$$\frac{dr}{dt} = \frac{q_r}{n}$$

The time dt necessary for a water particle to travel over a distance dr is:

$$dt = \left(\frac{dr}{dt}\right)^{-1} dr = n\frac{dr}{q_r}$$

The time to travel from point A (at r_A) to point B (at r_B) is found by integration:

$$\int_{r_A}^{r_B} n\frac{dr}{q} = n\int_{r_A}^{r_B} -\frac{2\pi r H}{Q}\,dr = -\frac{\pi n H}{Q} r^2 \Big|_{r_A}^{r_B}$$

Thus:

$$T_{A\to B} = \frac{\pi n H}{Q}(r_A^2 - r_B^2)$$

This expression gives the travel time between two points in a radial flow field. Note that in the expression the conductivity no longer occurs.

For the present case we have $r_A = R = 2000$ m and $r_B = r_w = 0.2$ m and we obtain:

$$T_{A\to B} = 1589 \text{ year}$$

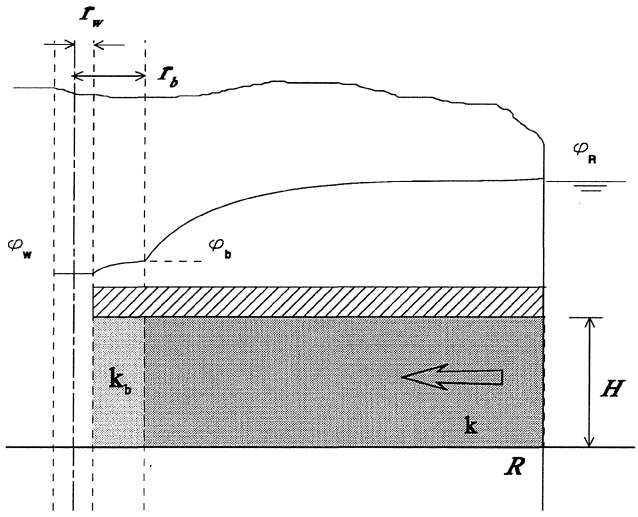

Exercise 6 ***Unconfined flow***

The figure below sketches a cross-section of an unconfined aquifer bounded by two parallel canals. The water-levels in the canals are respectively φ_1 = 8 m (left) and φ_2 = 4 m (right). The impervious base of the aquifer is taken as reference level. The distance between the canals is 200 m. The discharge Q, integrated over the height of the aquifer, is 0.60 m^2/day. (Note that Q represents the discharge per meter in the direction perpendicular to the cross-sectional plane). At first (section a and b) the groundwater recharge N is assumed to be very small and, therefore, it is neglected.

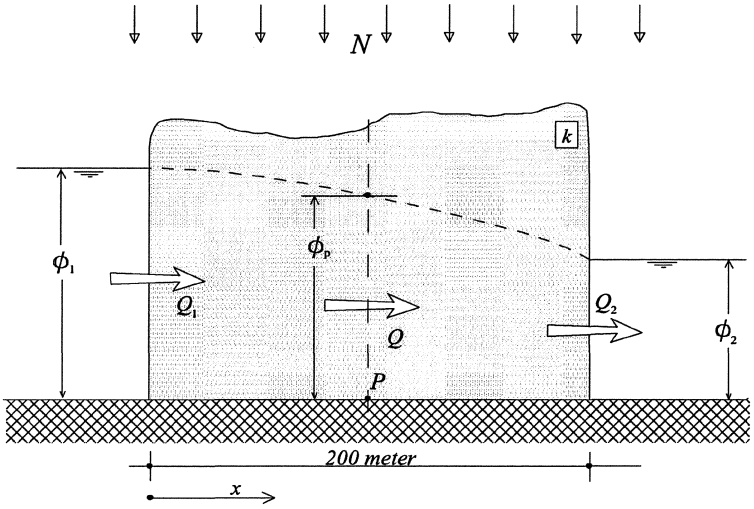

a) Calculate the permeability k of the aquifer (give the answer in m/day).

Answer: The discharge between two parallel canals in an unconfined aquifer is given by eq.(46)

$$Q = -\frac{k}{2}\frac{\varphi_2^{\,2} - \varphi_1^{\,2}}{x_2 - x_1}$$

or

$$0.6 = -\frac{k}{2}\frac{16 - 64}{200}$$

Thus k = 5 m/day

b) What is the piezometric head in a point P, halfway the two canals (i.e. at x = 100 m) ?

Answer: The distribution of the head is given by equation (45), where for the present case N may be taken zero. Substitution of all the given data leads to:

$$\varphi_p^{\,2} = \frac{\varphi_2^{\,2} + \varphi_1^{\,2}}{2}$$

or $\varphi_p = 2\sqrt{10} = 6.32m$

c) The rainfall increases dramatically due to the 'el Niño' phenomenon and the groundwater recharge N may no longer be neglected. If N becomes 0.015 m/day, what will now be the head in point P.

Answer: Equation (45) still holds, but the first term at the right hand side is now no longer equal to zero. Substitution of all know parameters yields:

$$\varphi_p^{\,2} = -\frac{0.015}{5}(100)(-100) + \frac{\varphi_2^{\,2}(100) - \varphi_1^{\,2}(-100)}{2} = 70$$

or $\varphi_p^{\,2} = \sqrt{70} = 8.37\ m$

d) What can be said about the direction of the flow in point P in the el Niño situation ? If chemicals are spilled into the aquifer around the point P, will they finally show up in the canal at the right hand side or in the canal at the left hand side.

Answer : The direction of the flow is opposite to the direction of the gradient. When we differentiate equation (45) we obtain:

$$\frac{d\varphi^2}{dx} = 2\varphi\frac{d\varphi}{dx} = -\frac{N}{k}(x - x_2) - \frac{N}{k}(x - x_1) + \frac{\varphi_2^{\,2} - \varphi_1^{\,2}}{x_2 - x_1}$$

For $x = x_p$ the first two terms at the right-hand side cancel and the third one is negative. Then, since φ is positive the gradient $d\varphi/dx$ must be negative and the flux positive. The flow is therefore in the positive x-direction (towards the right).
The spilled chemicals will end in the canal at the right hand side.

e) For the el Niño situation calculate the position (x-coordinate) where the flow reverses (the point where $d\varphi/dx$ = 0 and thus where $d\varphi^2/dx = 0$).

Answer: To simplify the algebra put the origin of the x-axis at the left canal. Then the expression for $d\varphi^2/dx$ becomes:

$$\frac{d\varphi^2}{dx} = -\frac{N}{k}(2x - x_2) + \frac{\varphi_2^{\,2} - \varphi_1^{\,2}}{x_2}$$

This expression is equal to zero when $2x$ = 200 – 24/0.3 , so x = 60 meter.

f) In the situation with no recharge Q_1 (the discharge from the canal at the left hand into the aquifer) is equal to Q_2 (the discharge from the aquifer into the canal at the right hand side). In the new situation this is no longer the case. Calculate Q_1 and Q_2 for the situation with N = 0.015 m/day.

Answer: The discharge Q in the aquifer is $-k\varphi(d\varphi/dx) = -(k/2)\ d\varphi^2/dx$, so using the expression found earlier we have

$$Q = \frac{N}{2}(2x - x_2) - \frac{k}{2}\frac{\left(\varphi_2^{\,2} - \varphi_1^{\,2}\right)}{x_2}$$

With $x = x_1 = 0$ this gives $Q_1 = -1.5 + 0.6 = -0.9$ m^2/day
With $x = x_2 = 0$ this gives $Q_2 = 1.5 + 0.6 = 2.1$ m^2/day

Note that Q_1 is negative, which means that at the left hand side the flow is no longer from the canal into the aquifer, but from the aquifer into the canal

Special Techniques

Superposition

From classical mechanics the superposition principle for velocity vectors is known. This principle can be applied as well in groundwater mechanics. It means, that when in an aquifer two wells are active and q_1 and q_2 are the velocities due to each well separately, then the velocity for both wells acting simultaneously is the vectorial sum of q_1 en q_2.

Superposition is allowed because of the linearity of the governing equations. The principle simply states that when two solutions $\varphi_1(x, y)$ and $\varphi_2(x, y)$ satisfy a linear equation, then each linear combination $A\varphi_1 + B\varphi_2$ satisfies the equation as well. This can easily be verified. Of course, the boundary conditions also have to be taken into account. In the case of groundwater flow towards a well the boundary condition is that ϕ is zero at a large distance of the well. Thus, addition of solutions for two wells does not change the boundary condition. For two wells in the point (x_1, y_1) and (x_2, y_2) with discharges Q_1 and Q_2, we apply eq (37) where the distance to the wells r_1 and r_2 is replaced by $\sqrt{(x-x_1)^2+(y-y_1)^2}$ and $\sqrt{(x-x_2)^2+(y-y_2)^2}$, respectively. We obtain:

$$\varphi = \frac{Q_1}{2\pi kH}\ln\sqrt{(x-x_1)^2+(y-y_1)^2} + \frac{Q_2}{2\pi kH}\ln\sqrt{(x-x_2)^2+(y-y_2)^2} + C \qquad (73)$$

For a system of N wells we may write:

$$\varphi = \frac{1}{2\pi kH}\sum_{j=1}^{N} Q_j \ln\sqrt{(x-x_j)^2+(y-y_j)^2} \quad + C \qquad (74)$$

where Q_j is the discharge of well j, located in the point (x_j, y_j). As usual the head is with respect to a reference level. Without specifying the reference, the constant C is unknown. C can be determined, if at a certain point the head is given. For example, if at (x_r, y_r) the head $\varphi = \varphi_r$, then C becomes:

$$C = \varphi_r - \frac{1}{2\pi kH}\sum_{j=1}^{N} Q_j \ln\sqrt{(x_r-x_j)^2+(y_r-y_j)^2} \qquad (75)$$

Well in uniform flow

The head distribution for a uniform flow with a constant discharge q along the positive x-axis is $\varphi = -(q/k)\,x$, which is Darcy's law integrated once. If in such a flow field a pumping well is placed at $(a,0)$ we obtain:

$$\varphi = -\frac{q}{k}x + \frac{Q}{2\pi kH}\ln\sqrt{(x-a)^2 + y^2} + C \qquad (76)$$

The flow lines for this case are shown in figure 11. The flow lines that separate water entering the well and water flowing further down gradient are called the *water divides* or *separating stream lines*. The area in between these separating streamlines is the intake region of the well, also called *capture zone*. Contaminants leaching from the surface within the capture-zone will reach the well sooner or later and may cause a pollution problem. Upstream (in the negative x-direction) the influence of the well vanishes and the streamlines will become straight lines. The width of the capture zone obtains a maximum L as $x \rightarrow -\infty$. Since here the well is far away its influence is small and may be neglected. The specific discharge may be approximated by q. The amount of water that flows between the separating streamlines is now LHq. This amount must be equal to the discharge Q of the pumping well Q. Then, the width of the capture-zone becomes:

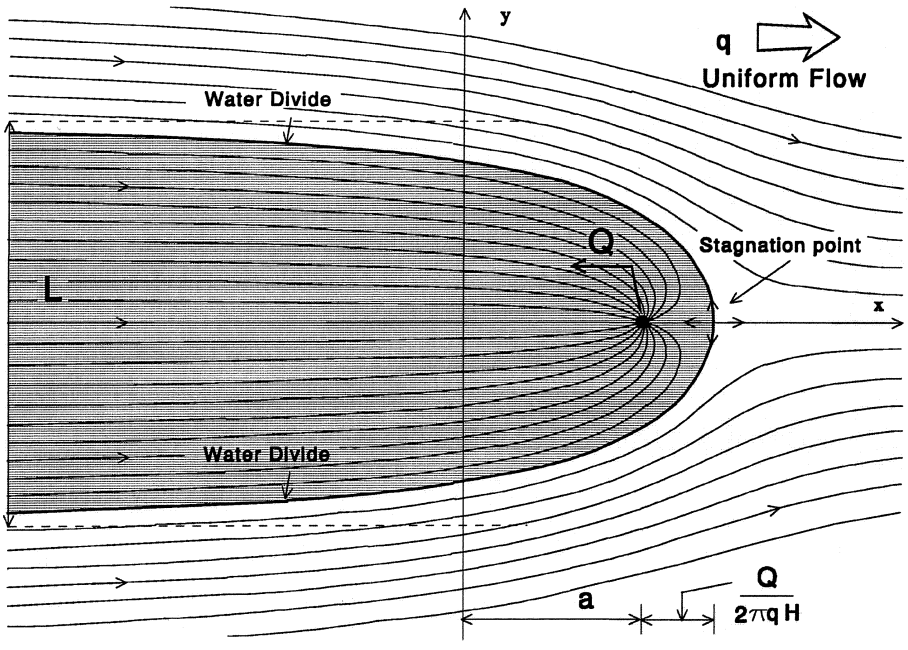

Figure 11 Streamlines for a well and a uniform flow

$$L = \frac{Q}{qH} \tag{77}$$

A point of interest is the location of the *stagnation point.* At this point both q_x and q_y are zero. It is obvious from (76) that q_y is zero only along the x-axis. Along this axis q_x is (differentiation of (76) to x and putting $y = 0$):

$$q_x = q - \frac{Q}{2\pi H(x-a)} \tag{78}$$

The x-coordinate of the stagnation point is by putting $q_x = 0$:

$$x = a + \frac{Q}{2\pi qH} \tag{79}$$

A groundwater particle further downstream from the stagnation point will definitively not enter the pumping well and move on in positive x-direction.

Method of images

An interesting technique based on the superposition principle is the *method of images*. Here, a solution for a particular problem is constructed by addition of one (or more) imaginary wells, the so-called *image wells*. The effect of the image well, which is placed outside the area of interest, is to fulfill the boundary condition. For further explanation we consider an example (see figure 12). Suppose a solution is sought for the flow towards a well near a river with a fixed head. For simplicity we assume that the river is located along the y-axis (the line $x = 0$) and the head in the river is zero. Then, the boundary condition along the river reads:

$$\varphi(0, y) = 0 \tag{80}$$

The extraction well with discharge Q is located on the x-axis at a distance a from the river. To satisfy the boundary condition, an infiltrating well is placed at $(-a,0)$, with a discharge $-Q$. The head for this situation is given by:

$$\varphi(x,y) = \frac{Q}{2\pi kH} \ln \frac{\sqrt{(x-a)^2 + y^2}}{\sqrt{(x+a)^2 + y^2}} \tag{81}$$

By substitution of $x = 0$ the fulfillment of boundary condition is easily verified. The method works because the line $x = 0$ (the river) is the set of points with equal distances to each of the wells and therefore, the heads cancel out. Thus, a river may be simulated by adding a well with an opposite discharge at the reflection point of the original. The solution is only valid in the region $x \geq 0$.

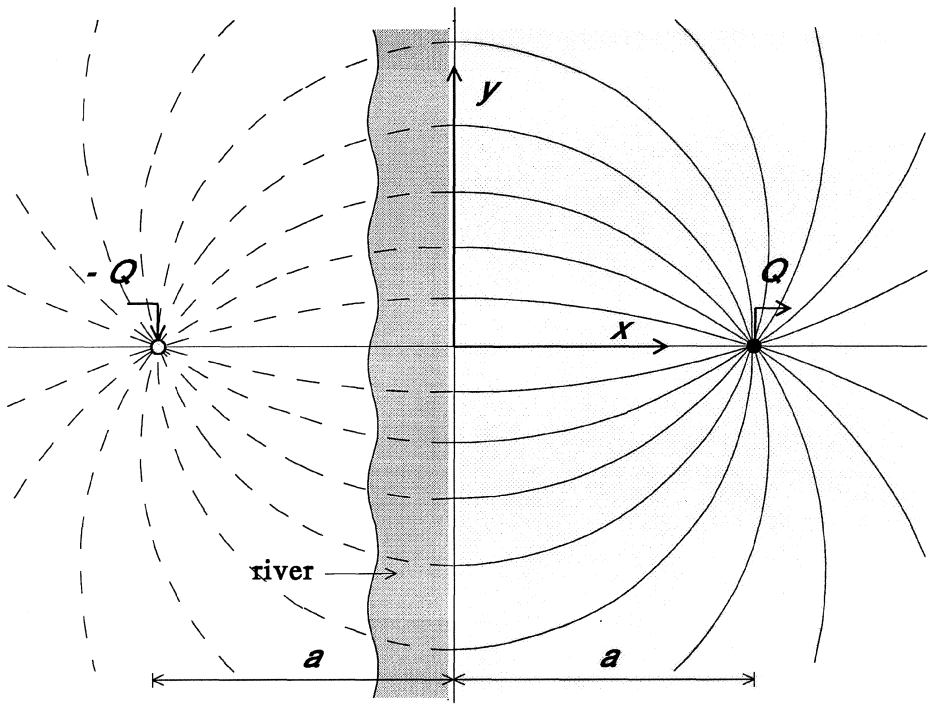

Figure 12 Well near a river; position of the original well and image well

The method of images can also be applied at a bend in the river. The following example (figure 13) shows a bend of 90 degrees along the x-axis and y-axis. A well is located at the point (a,b). The condition $\varphi(0,y) = 0$ is satisfied by an infiltration well at the reflection point with respect to the y-axis, i.e. $(-a,b)$. The second part of the boundary condition $\varphi(x,0) = 0$ is fulfilled by one more refection, this time with respect to the x-axis. Finally, a system of four wells arises: the original well, two infiltrating image wells and one pumping image well. The head is given by:

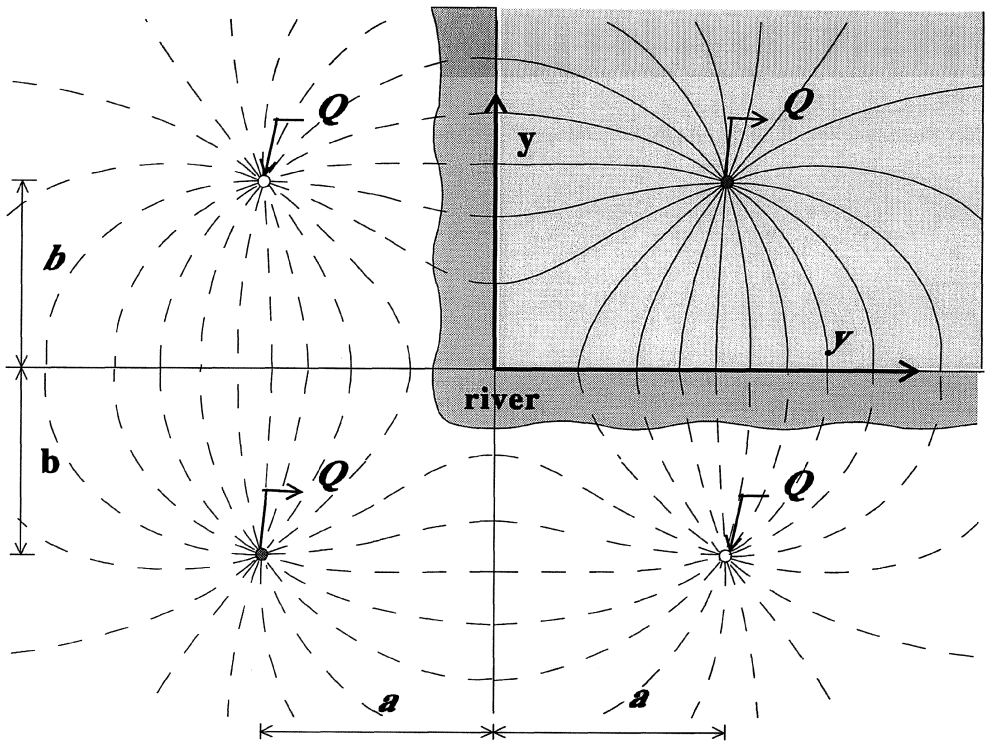

Figure 13 Well near a river bend; position of the original well and 3 image wells

$$\varphi(x,y)=\frac{Q}{2\pi kH}\ln\frac{\sqrt{(x-a)^2+(y-b)^2}}{\sqrt{(x+a)^2+(y-b)^2}}\frac{\sqrt{(x+a)^2+(y+b)^2}}{\sqrt{(x-a)^2+(y+b)^2}} \tag{82}$$

The method of images can also be used for a well near an impervious boundary (figure 16). Consider an impervious rock, located along the y-axis and a well in $(a,0)$. The boundary condition is of the Neuman type and reads:

$$\left.\frac{\partial\varphi}{\partial x}\right|_{x=0}=0 \tag{83}$$

This can be satisfied by a system of two extracting wells at $(a,0)$ and $(-a,0)$. The line $x = 0$ is an axis of symmetry and therefore the velocities in x-direction due to the original well are canceled out by the velocities due to the image well. The head distribution is:

$$\varphi(x,y)=\frac{Q}{2\pi kH}\ln\sqrt{(x-a)^2+y^2}+\frac{Q}{2\pi kH}\ln\sqrt{(x+a)^2+y^2}+C \tag{84}$$

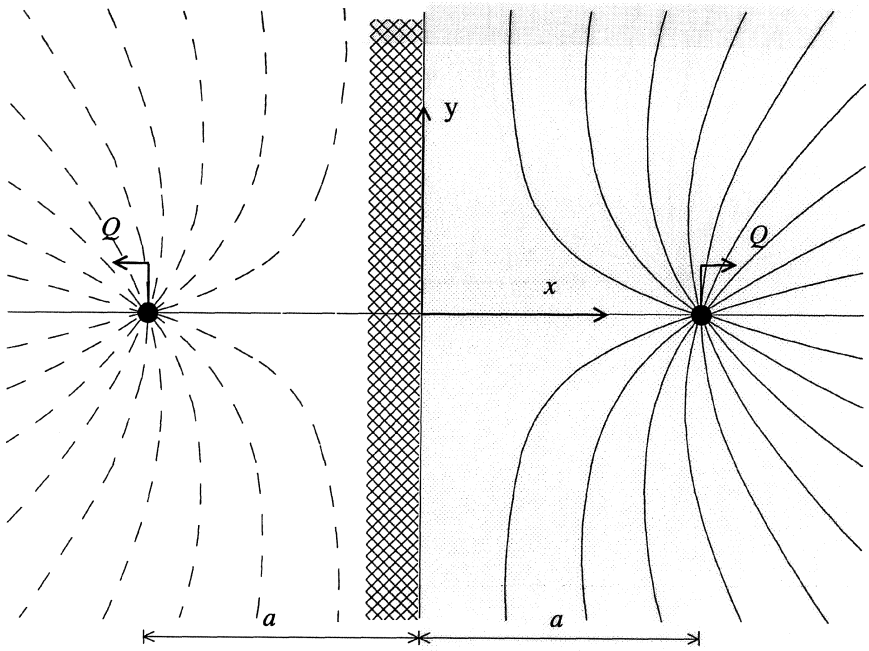

Figure 14 Well near an impervious wall; position of the original well and image well

Differentiation to x gives:

$$\frac{\partial\varphi}{\partial x}=\frac{Q}{2\pi kH}\left[\frac{x-a}{(x-a)^2+y^2}+\frac{x+a}{(x+a)^2+y^2}\right] \tag{85}$$

Along the y-axis (x = 0) the boundary condition is fulfilled. The examples given above refer to confined flow, but superposition in general and the method of images may also be applied for semi-confined flow. It is also applicable for phreatic flow, as long as we consider solutions for φ^2.

Exercise 7. Calculating travel time

From the point of quality control for the water in the well it is useful to know the travel time from the river to the well. For instance, when pollution occurs at the river, measures can be taken in time at least the travel time along the shortest streamline is known. From figure (12) one sees that the shortest streamline runs along the x-axis. To calculate the travel time T along the x-axis we have:

$$T = \int_{x=0}^{x=a} \left(\frac{dx}{dt} \right)^{-1} dx$$

The groundwater velocity $dx/dt = v_x = q_x/n$ can be found by Darcy's law:

$$\frac{dx}{dt} = -\frac{Q}{2\pi nH}\left[\frac{1}{x-a} - \frac{1}{x+a}\right] = \frac{aQ}{n\pi H}\frac{1}{(a^2 - x^2)}$$

Then

$$T = \frac{n\pi H}{aQ}\int_{x=0}^{x=a}(a^2 - x^2)dx$$

and, after integration:

$$T = \frac{2}{3}\frac{n\pi H}{Q}a^2$$

Note that in this expression the permeability does not occur.

Exercise 8. River-bank infiltration

A river is infiltrating with a rate q_i. A well with discharge Q is placed at a distance a from the river-bank (see figure). Suppose the river runs along the y-axis, while the well is located at the x-axis in the point (a, 0). Derive the expression for the position of the stagnation point and the travel time from the river to the well along the shortest streamline.

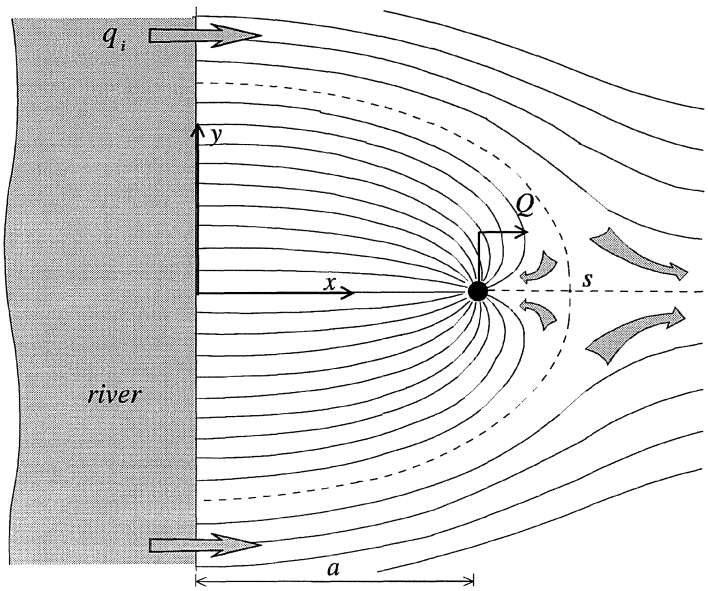

Stagnation point

If the head in the river is φ_r, the head distribution can be written as:

$$\varphi = \varphi_r - \frac{q_i}{k}x + \frac{Q}{2\pi kH}\ln\sqrt{(x-a)^2+y^2} - \frac{Q}{2\pi kH}\ln\sqrt{(x+a)^2+y^2}$$

To obtain the position of the stagnation point we examine q_x and q_y. According to Darcy's law:

$$q_x = q_i - \frac{Q}{2\pi H}\left\{\frac{x-a}{(x-a)^2+y^2} - \frac{x+a}{(x+a)^2+y^2}\right\}$$

and

$$q_y = -\frac{Q}{2\pi H}\left\{\frac{y}{(x-a)^2+y^2} - \frac{y}{(x+a)^2+y^2}\right\}$$

For $q_y = 0$ the only possibilities are the river itself ($x = 0$) or a point on the x-axis ($y = 0$). Since the river is infiltrating, originally with $q_x = q_i$ and this rate is increased by the presence of the well, we don't expect to find $q_x = 0$ along the river. Thus, we focus on the x-axis and investigate q_x:

For $y = 0$:

$$q_x = q_i - \frac{Q}{2\pi H}\left\{\frac{1}{x-a} - \frac{1}{x+a}\right\}$$

Putting $q_x = 0$ results in:

$$x^2 - a^2 - \frac{Qa}{\pi H q_i} = 0$$

The stagnation point evidently is on the positive side of the x-axis, so x_s becomes:

$$x_s = a\sqrt{1 + Q/(\pi a H q_i)}$$

Travel-time

Along the shortest streamline, which coincides with the x-axis, the velocity $v_x = q_x/n$ or:

$$v_x = \frac{q_i}{n}\left\{1 - \frac{Q}{2\pi H q_i}\left[\frac{1}{x-a} - \frac{1}{x+a}\right]\right\}$$

After writing $v_x = dx/dt$ and some rearrangement, this becomes:

$$\frac{dx}{dt} = \frac{q_i}{n}\left\{\frac{(x^2 - a^2) - Qa/\pi H q_i}{(x^2 - a^2)}\right\}$$

The travel time from the river to the well along the x-axis is given by:

$$T = \int_{x=0}^{x=a}\left(\frac{dx}{dt}\right)^{-1} dx$$

This leads to:

$$T = \int_{x=0}^{x=a}\left(\frac{x^2 - a^2}{x^2 - a^2 - Qa/\pi H q_i}\right) dx$$

or:

$$T = \int_{x=0}^{x=a}\left(1 - \frac{Qa/\pi H q_i}{Qa/\pi H q_i + a^2 - x^2}\right) dx$$

After writing $p^2 = Qa/\pi H q_i + a^2$ and integration:

$$T = \frac{na}{q_i}\left[1 - \frac{p^2 - a^2}{2pa}\ln\frac{p+a}{p-a}\right]$$

The term $T = na/q_i$ represents the travel time from the river to $x = a$, for the situation without a well. Evidently the travel time is reduced by the existence of the pumping well. Note that p is equal to the distance of the stagnation point towards the river.

Potential and stream function

General Theory

In the previous chapters we have shown pictures with flow patterns, displayed by a set of flow lines or streamlines. A flow line may be defined as the path a hypothetical particle follows in time. In addition to this set of lines we can also display the flow pattern by a set of isohypses or (equi)-potential lines. An equipotential line is a line along which the piezometric head is constant. In an isotropic aquifer the streamlines are always perpendicular to the equipotential lines. In the present chapter we discuss some general concepts on the theory of the potential function and the stream function.

For two-dimensional flow in a homogeneous and isotropic confined aquifer, we introduce the *velocity potential* Φ:

$$\Phi = k\varphi \tag{86}$$

Φ is also called the *potential* and has the dimension [$L^2\ T^{-1}$]. The derivative of Φ yields directly the specific discharge vector q (besides the minus sign):

$$q = -\nabla\Phi \tag{87}$$

If Φ exists and satisfies the Laplace equation, $\nabla^2\Phi = 0$, it is possible to define a 'conjugate' function Ψ, by the relations:

$$\frac{\partial\Phi}{\partial x} = \frac{\partial\Psi}{\partial y} \quad ; \quad \frac{\partial\Psi}{\partial x} = -\frac{\partial\Phi}{\partial y} \tag{88}$$

The function $\Psi(x,y)$ is called the *stream function*. The equations (88) are the *Cauchy-Riemann* relations. The dimension of Ψ is the same as that of Φ, i.e. [$L^2\ T^{-1}$]. With the Cauchy-Riemann relations the specific discharge can be expressed in Ψ:

$$q_x = -\frac{\partial\Psi}{\partial y} \quad ; \quad q_y = +\frac{\partial\Phi}{\partial x} \tag{89}$$

For Ψ to be a single-valued it is required that:

$$\frac{\partial^2 \Psi}{\partial x \partial y} = \frac{\partial^2 \Psi}{\partial y \partial x} \tag{90}$$

When Cauchy-Riemann is used to substitute Ψ by Φ, it gives:

$$\frac{\partial^2 \Phi}{\partial x^2} = -\frac{\partial^2 \Phi}{\partial y^2} \tag{91}$$

which is true, since we required Φ to satisfy Laplace. The term *stream function* becomes clear, when the properties of lines with constant Ψ-value are examined. For two nearby points on such a line we have:

$$\Psi(x_0 + \Delta x, y_0 + \Delta y) = \Psi(x_0, y_0) \tag{92}$$

Expansion of the left hand side in a Taylor series, gives:

$$\Psi(x_0 + \Delta x, y_0 + \Delta y) = \Psi(x_0, y_0) + \frac{\partial \Psi}{\partial x}\Delta x + \frac{\partial \Psi}{\partial y}\Delta y + O(\Delta x^2) + O(\Delta y^2) \tag{93}$$

For Δx and Δy infinitely small, the higher order terms may be ignored and (93) combined with (92) leads to:

$$\frac{\partial \Psi}{\partial x}\Delta x + \frac{\partial \Psi}{\partial y}\Delta y = 0 \tag{94}$$

For the ratio between Δy and Δx we find:

$$\frac{\Delta y}{\Delta x} = -\frac{\partial \Psi / \partial x}{\partial \Psi / \partial y} = \frac{\partial \Phi / \partial y}{\partial \Phi / \partial x} = \frac{q_y}{q_x} \tag{95}$$

Apparently, a line with constant Ψ has the direction of the specific discharge. In other words, it indicates the path of a water particle, which is why it is called a streamline and Ψ is called *stream-function.*

Another property of the stream function follows from the equality:

$$\frac{\partial^2 \Phi}{\partial x \partial y} = \frac{\partial^2 \Phi}{\partial y \partial x} \tag{96}$$

Using Cauchy-Riemann yields:

$$\frac{\partial^2 \Psi}{\partial x^2} + \frac{\partial^2 \Psi}{\partial y^2} = 0 \tag{97}$$

which shows that Ψ also satisfies the Laplace equation.

A relation exists between the stream function and the discharge. To see this, examine the total discharge through a line *A-B* (figure 15). The discharge is independent of the path from *A* to *B*, since any two different lines from *A* to *B* enclose a region, where no water is stored or generated. Thus, water that passes through the first line also passes through the second line. As the position of the line may be chosen freely, we may compose a line by two sections: one section along the *x*-direction from point *A* to *C* and the other along the *y*-direction from *C* to *B*. The total discharge Q_{AB} is now found by:

$$Q_{AB} = \int_{x_A}^{x_C} (-q_y) dx + \int_{y_C}^{y_B} q_x dy \tag{98}$$

With (89):

$$Q_{AB} = \int_{x_A}^{x_C} \left(-\frac{\partial \Psi}{\partial x} \right) dx + \int_{y_C}^{y_B} \left(\frac{\partial \Psi}{\partial y} \right) dy \tag{99}$$

or:

$$Q_{AB} = (\Psi_A - \Psi_C) + (\Psi_C - \Psi_B) = \Psi_A - \Psi_B \tag{100}$$

Thus, the discharge across the line between *A* and *B* is equal to Ψ_A - Ψ_B.

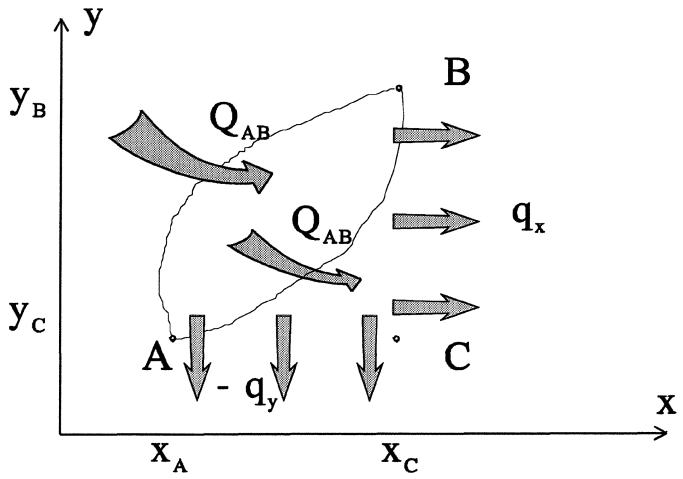

Figure 15 Relation between discharge and streamfunction

Streamlines are perpendicular to equipotential lines. This can be verified by considering two nearby points on a potential line, the same way as we examined the direction of the streamline. For two points on a potential line we have:

$$\Phi(x_0 + \Delta x, y_0 + \Delta y) = \Phi(x_0, y_0) \tag{101}$$

Taylor's expansion gives:

$$\Phi(x_0 + \Delta x, y_0 + \Delta y) = \Phi(x_0, y_0) + \frac{\partial \Phi}{\partial x}\Delta x + \frac{\partial \Phi}{\partial y}\Delta y + O(\Delta x^2) + O(\Delta y^2) \tag{102}$$

Combination of (101) and (102) gives, for Δx and Δy small enough to ignore second order terms:

$$\frac{\partial \Phi}{\partial x}\Delta x + \frac{\partial \Phi}{\partial y}\Delta y = 0 \tag{103}$$

or:

$$\frac{\Delta y}{\Delta x} = -\frac{\partial \Phi / \partial x}{\partial \Phi / \partial y} = -\frac{q_x}{q_y} \tag{104}$$

Equations (95) and (104) represent the tangent of the angle of the streamline and the potential line with the x-axis, respectively. Since their product is -1, these lines are orthogonal.

At introducing the stream-function, it was assumed that Laplace's equation holds. Hence, for horizontal flow in semi- and unconfined aquifers the theory on the stream function is not valid or has to be redefined. In 2-dimensional vertical flow, the situation is different and the stream-function still does exist. For horizontal flow in unconfined aquifers the stream function can be defined via the discharge potential.

Unconfined horizontal flow

Consider an unconfined homogeneous and isotropic aquifer. Instead of the specific discharge itself we consider the integral of q over the vertical, denoted by Q:

$$Q_x = \int_0^{\varphi} q_x dz \quad ; \quad Q_y = \int_0^{\varphi} q_y dz \tag{105}$$

Note that φ is here defined with respect to the base of the aquifer. Accordingly, a *discharge potential* Φ is defined as

$$\Phi = k\frac{\varphi^2}{2} \tag{106}$$

The dimension of the discharge potential is $[L^3 T^{-1}]$. The derivative yields the discharge vector:

$$\vec{Q} = -\nabla\Phi \tag{107}$$

Like the velocity potential, the discharge potential satisfies Laplace's equation $\nabla^2 \Phi = 0$, which follows from the continuity equation:

$$\frac{\partial}{\partial x}(Q_x) + \frac{\partial}{\partial y}(Q_y) = 0 \tag{108}$$

Note that this equation does not hold for an unconfined aquifer with rainfall. As in the case of confined flow a stream-function Ψ is introduced, by:

$$\frac{\partial \Phi}{\partial x} = \frac{\partial \Psi}{\partial y} \quad ; \quad \frac{\partial \Psi}{\partial x} = -\frac{\partial \Phi}{\partial y} \tag{109}$$

It is easily verified that again Φ is single valued and satisfies the Laplace equation.

Strack's comprehensive potential

Strack has proposed a so-called *comprehensive potential*, which can be used both in confined and in unconfined aquifers or even in aquifers where both types of groundwater occur simultaneously (see figure 16). For the comprehensive potential is defined as:

$$\Phi = kH\varphi - k\frac{H^2}{2} \qquad (\varphi \geq H) \tag{110}$$

$$\Phi = k\frac{\varphi^2}{2} \qquad (\varphi \leq H) \tag{111}$$

In confined flow the derivative of Φ yields the total discharge $Q = Hq$. The second term in (110), which vanishes in taking derivatives, is included to ensure that Φ is continuous at the transition from confined to unconfined flow.

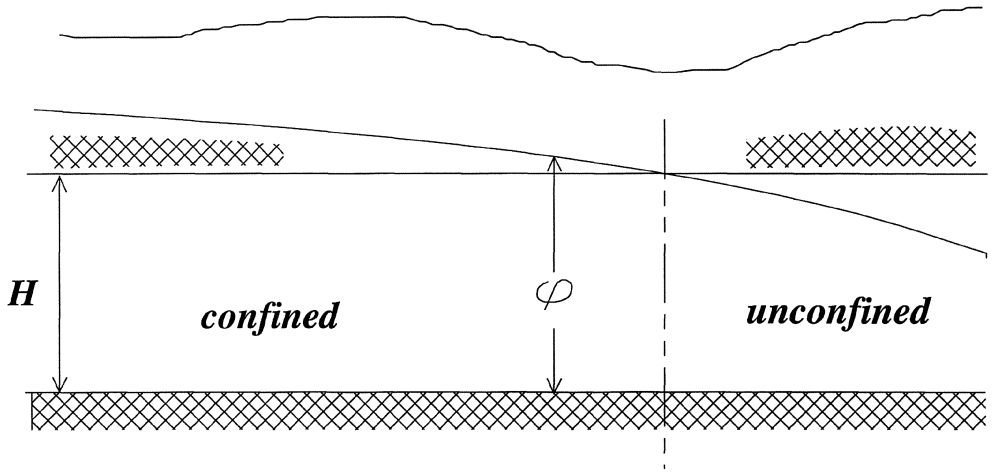

Figure 16. The comprehensive potential

The method of squares

The fact that potential lines and streamlines form sets of orthogonal lines is the basis of an approximate graphic method. In this method curvilinear field coordinates s and n are used (figure 17), related to the original x- and y-coordinates by:

$$s = x\cos\alpha + y\sin\alpha$$
$$n = -x\sin\alpha + y\cos\alpha \tag{112}$$

where α is the angle of the specific discharge vector q at a given point.

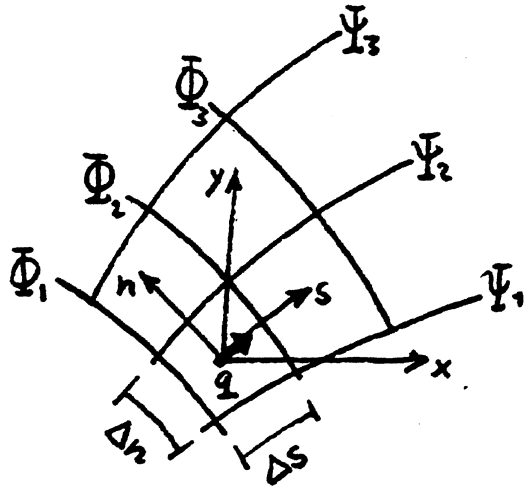

Figure 17 Curvilinear coordinates s and n

For q we can write:

$$q = -\frac{\partial\Phi}{\partial s} = -\frac{\partial\Psi}{\partial n} \tag{113}$$

A plot of streamlines and equipotential lines at constant intervals $\Delta\Phi$ and $\Delta\Psi$ is known as a *flow net*

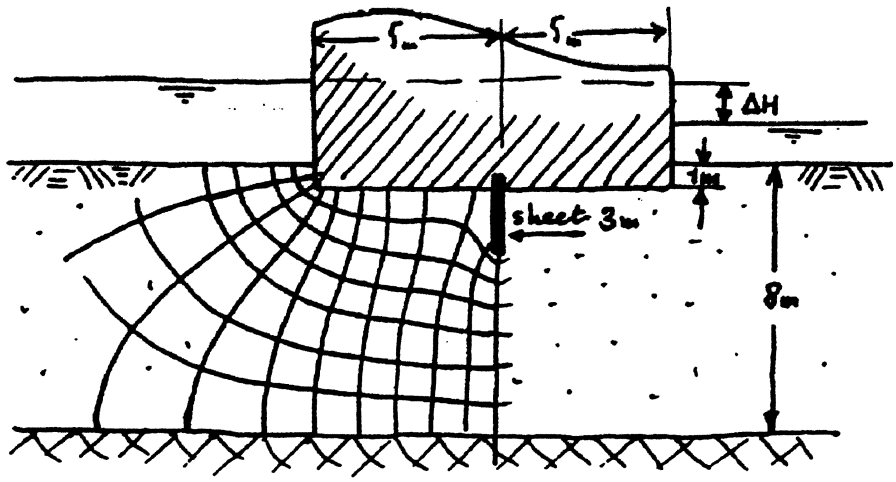

Figure 18 Example of method of squares

When such a flow net is drawn using $\Delta n = \Delta s$, then:

$$q = -\frac{\Delta\Phi}{\Delta s} = -\frac{\Delta\Psi}{\Delta n} \tag{114}$$

This means that we have the same increments for Φ and Ψ ($\Delta\Phi = \Delta\Psi$). The flow net consists of distorted squares. From $q = -\Delta\Psi/\Delta n$ follows that $q\Delta n = -\Delta\Psi$. The physical meaning of this is that the total discharge Q between two flowlines [$Q = q\Delta n$] is a constant since $\Delta\Psi$ is constant. The area between two flowlines can be considered as a tube that carries a certain (constant) amount of fluid. This is often called a streamtube.

Figure 18 shows the flow underneath a dam with a sheet pile. A flow net is sketched for half of the area. The other half is symmetric. Six streamlines are drawn, resulting in 7 flow-tubes, each representing 1/7 of the discharge Q, or $\Delta\Psi = Q/7$. From the equipotential lines it appears that the total drop in potential (kH) is divided over 20 equipotential intervals, or $\Delta\Phi = kH/20$. The total discharge follows from:

$$Q = 7\Delta\Psi = 7\Delta\Phi = \frac{7}{20}kH \tag{115}$$

Complex analysis

The previous chapter showed, that in a number of situations a two dimensional flow problem can be represented by a set of orthogonal lines: the *equipotential lines* and the *stream lines*. Then, each point in the (x, y) plane has, besides its Cartesian coordinates, a unique Φ and Ψ value, which can be considered as a second set of (curvilinear) coordinates. We may display these 'coordinates' in the (Φ, Ψ)-plane (figure 19). In most cases, the boundary conditions of a flow problem consist of given heads (an equipotential line) and impermeable walls (streamlines). This means that in the (Φ, Ψ)-plane the boundaries are represented by straight lines, e.g. like the rectangle ABCD in figure 19. The inside of the rectangle corresponds with the flow domain. The potential lines and stream lines in the (Φ, Ψ)-plane, are said to be *mapped* to the (x,y)-plane and solving a groundwater flow problem, is equivalent to finding a transformation that maps the (Φ, Ψ) plane into the (x,y)-plane. Of course, the transformation must be such that not only the boundary conditions fit, but also Laplace's equation must be satisfied. In the following section we shall show that such a transformation exists, based on the theory of functions of complex variables, and that these functions automatically satisfy Laplace's equation.

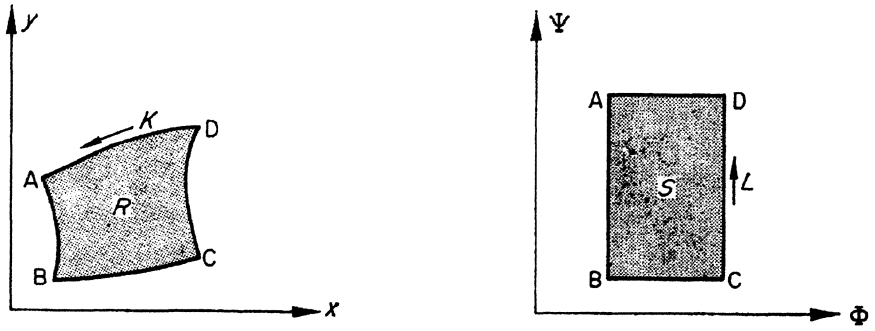

Figure 19 Mapping between (x,y)-plane and (Φ, Ψ)-plane

Complex functions

Consider two complex variables, one representing the physical plane $z = x + iy$ and the other, $\Omega = \Phi + i\Psi$, representing the (Φ, Ψ)-plane. Ω is called the *complex potential*. Let's assume that a

function exists between Ω and z, denoted by $\Omega = \Omega(z)$. Assume that the derivative $\Omega'(z)$ exists and has a unique value. $\Omega'(z)$ is defined as:

$$\Omega'(z_o) = \lim_{z_1 \to z_0} \frac{\Omega(z_1) - \Omega(z_0)}{z_1 - z_0} \tag{116}$$

$\Omega'(z_0)$ must be unique and, therefore, the limit must be independent of how z_1 approaches z_0. We compare two alternatives. First, z_1 approaches z_0 in the direction of the x-axis. In this case, we can write $\Delta z = x_1 - x_0 = \Delta x$. Secondly, z_1 approaches z_0 in the direction of the y-axis and $\Delta z = i(y_1 - y_0) = i\Delta y$. Thus, if $\Omega'(z_0)$ is unique, the following is true:

$$\frac{d\Omega}{dz} = \frac{\partial \Omega}{\partial x} = \frac{\partial \Omega}{i \partial y} \tag{117}$$

or with $\Omega = \Phi + i\Psi$:

$$\frac{\partial \Phi}{\partial x} + i\frac{\partial \Psi}{\partial x} = \frac{1}{i}\left(\frac{\partial \Phi}{\partial y} + i\frac{\partial \Psi}{\partial y}\right) \tag{118}$$

Separation of real and imaginary parts gives:

$$\frac{\partial \Phi}{\partial x} = \frac{\partial \Psi}{\partial y} \quad ; \quad \frac{\partial \Psi}{\partial x} = -\frac{\partial \Phi}{\partial y} \tag{119}$$

which are the Cauchy-Riemann relations. In other words, a function with a unique derivative automatically satisfies the Cauchy-Riemann relations. We have seen before, that when Cauchy-Riemann holds, also Laplace's equation holds, for Φ and for Ψ. Since the theory of complex functions requires that each function has a unique derivative, these functions automatically satisfy the Laplace equation. This is the crux of the method. The technique of complex functions only applies to groundwater problems that are described by the Laplace equation, i.e. confined flow in a uniform aquifer (or in vertical cross-sections of leaky or phreatic situations). The functions must be analytic, which most functions like exponentials, logarithms, sine and cosines are. A question that remains to be looked at is the fulfillment of the boundary conditions. In most cases the boundary conditions are given in terms of prescribed potential or prescribed stream function.

Complex velocity

Ω has been introduced as a *potential*. In analogy with the physical potential Φ we may introduce a *complex velocity* w as the derivative of this potential or:

$$w = -\frac{d\Omega}{dz} \tag{120}$$

The relation between w and q is as follows. Since $w = - d\Omega/dz = - \partial\Omega/\partial x$:

$$w = -\frac{\partial \Phi}{\partial x} - i\frac{\partial \Psi}{\partial x} = q_x - iq_y \tag{121}$$

Remarkable is that the direction of w does not coincide with the direction of q. The complex velocity represents the conjugate of q, denoted by *conj* (q). Since *conj* $(a + ib) = a - ib$, we have:

$$w = conj(q) = q_x - iq_y \tag{122}$$

When w is zero, both q_x and q_y are zero, so at this point there is no flow. Such a point is called a *stagnation point.*

Example: *The function* $\Omega = z^2$

Consider the function $\Omega = z^2$. The pattern of perpendicular lines in the Ω-plane (streamlines and equipotential lines) is mapped to a pattern of perpendicular *curves* in the z-plane. For these curves hold that Φ is constant or Ψ is constant, so these curves represent the potential lines and the streamlines in the z-plane The equations of these curves are found from $\Omega = z^2$ after separating real and imaginary parts:

$$\Phi + i\Psi = (x + iy)^2 \tag{123}$$

or:

$$\Phi = x^2 - y^2 \tag{124}$$

and

$$\Psi = 2xy \tag{125}$$

These are two sets of hyperbolas (figure 20).

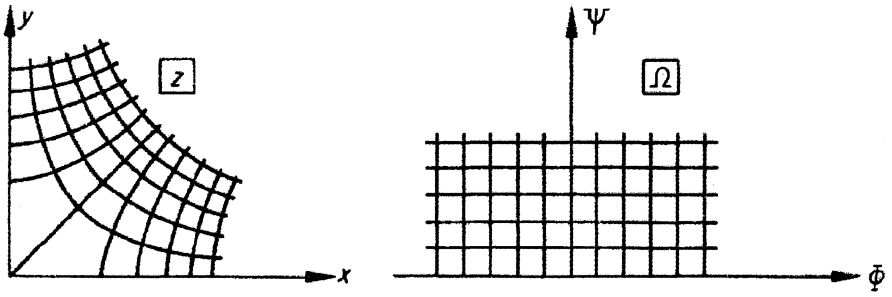

Figure 20 Mapping of $\Omega = z^2$

Example. Well in uniform flow near a river

A similar problem has been discussed in the section on superposition. With complex functions the problem can be solved in a more general way. Suppose the river runs along the y-axis and a natural background flow occurs towards the river with a rate q_n. The direction of the flow is under an angle θ with the positive x-axis. The x and y components of the flow are $q_x = |q_n| \cos\theta$ and $q_y = |q_n| \sin\theta$.

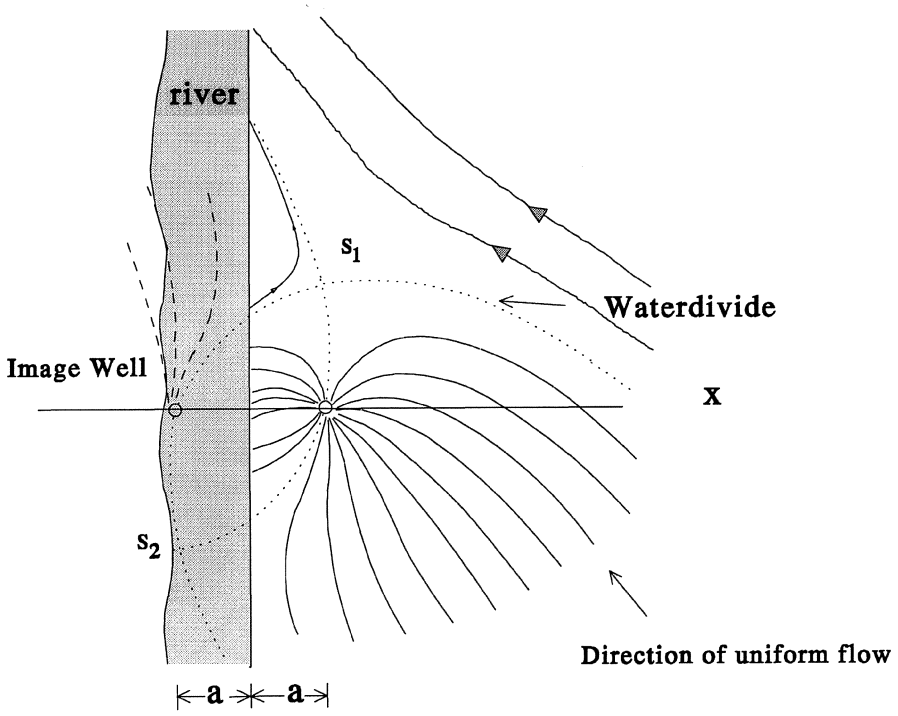

Figure 21 Well near draining river

The flow q_n is the complex variable $q_n = q_x + i\, q_y$ and the flow field (without the pumping well) can be described by:

$$\Omega = -conj(q_n)z \tag{126}$$

for the region $x \geq 0$. Note that along the river the potential is a linear function of y: $\Phi = -q_y y$. This can be verified by writing $\Phi = \text{Re}\,[\Omega] = \text{Re}\,[-conj(q_n)iy] = \text{Re}\,[-(q_x - iq_y)iy] = -q_y y$. A pumping well with discharge Q is placed near the river at a distance a, and an image well is added at a distance $-a$ from the y-axis to ensure that the potential in the river remains unchanged. The complete solution becomes:

$$\Omega = -conj(q_n)z + \frac{Q}{2\pi H}\ln\frac{z - z_p}{z - z_i} \tag{127}$$

where z_p denotes the location of the pumping well (here $x_p = a$, $y_p = 0$) and z_i the location of the image well ($x_i = -a$, $y_i = 0$). The stagnation points are found from $w = \Omega'(z) = 0$:

$$\frac{Q}{2\pi\pi H}\left[\frac{1}{z - z_p} - \frac{1}{z - z_i}\right] - conj(q_n) = 0 \tag{128}$$

This can be written as a second order algebraic equation with complex variables:

$$z^2 - (z_i + z_p)z + z_i z_p + \frac{Q}{2\pi H conj(q_n)}(z_i - z_p) = 0 \tag{129}$$

Two stagnation points s_1 and s_2 are found from

$$s_1, s_2 = \frac{z_i + z_p}{2} \pm \frac{z_i - z_p}{2}\sqrt{1 - 4\alpha} \tag{130}$$

where α is the complex parameter:

$$\alpha = \frac{Q}{2\pi Hconj(q_n)} \frac{1}{(z_i - z_p)} \tag{131}$$

Since z_i and z_p are symmetrical with respect to the y-axis, $z_i + z_p = 0$ and $z_i - z_p = -2a$, so:

$$s_1, s_2 = \pm a\sqrt{1 - 4\alpha} \tag{132}$$

Note that q_n and α are both complex variables.

Numerical methods

For a long time, analytical methods were the most used for groundwater problems, but since computers became available at a large scale, this position is taken over by numerical techniques. In numerical techniques the differential equation is not solved exactly, but approximately. Numerical solutions are often more realistic than analytical ones, since they do not require the high level of simplification necessary in analytical methods. Analytical methods remain important, for instance for the verification of numerical models. Also, they provide a better idea how system parameters influence the final solution of the problem and they are very appropriate to study, for instance, the asymptotic behavior of a problem.

In the following sections a brief introduction is given for two of the most popular numerical methods, the *finite difference* and the *finite element* method. These methods have a lot in common. Both methods transform the original differential equation into a set of algebraic equations, which accordingly is solved by the computer. The methods differ mainly in the way the algebraic equations are obtained.

Finite Difference Method

The first step in the Finite Difference Method is introduction of a grid covering the domain of the problem. Figure 22 shows an example of a simple grid: regularly spaced with a mesh size h equal in horizontal and vertical direction. The intersection of grid-lines is referred to as a *node*. The finite difference method provides a solution for the heads in the nodes. The smaller the mesh-size, the more accurate is the solution. However, as the number of nodes increases, so does the number of equations and calculation time and required computer storage.

If the head at a node with indices (i,j) is denoted by $\varphi_{i,j}$, then the derivatives $\partial\varphi/\partial x$ and $\partial\varphi/\partial y$ may be approximated by:

$$\frac{\partial\varphi}{\partial x} \approx \frac{\Delta\varphi}{\Delta x} = \frac{\varphi_{i+1,j} - \varphi_{i,j}}{h} \tag{133}$$

$$\frac{\partial\varphi}{\partial y} \approx \frac{\Delta\varphi}{\Delta y} = \frac{\varphi_{i,j+1} - \varphi_{i,j}}{h} \tag{134}$$

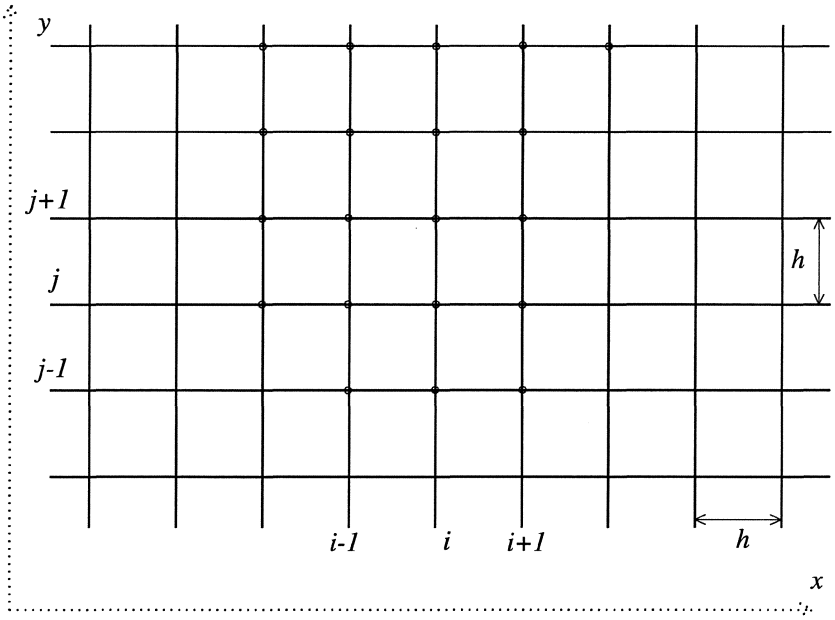

Figure 22 Finite Difference Grid

These expressions represent the derivative at a point halfway the nodes with coordinates (x_i+h/2, y_j) and (x_i+h/2, y_j+h/2), respectively. For the second derivative $\partial^2\varphi/\partial x^2$ at (x_i, y_j), we use the approximations of the first derivative at (x_i+h/2, y_j) and (x_i-h/2, y_j):

$$\frac{\partial^2\varphi}{\partial x^2} \approx \frac{\dfrac{\varphi_{i+1,j}-\varphi_{i,j}}{h} - \dfrac{\varphi_{i,j}-\varphi_{i-1,j}}{h}}{h} \tag{135}$$

which reduces to:

$$\frac{\partial^2\varphi}{\partial x^2} \approx \frac{\varphi_{i+1,j}-2\varphi_{i,j}+\varphi_{i-1,j}}{h^2} \tag{136}$$

Similarly, in the vertical:

$$\frac{\partial^2\varphi}{\partial y^2} \approx \frac{\varphi_{i,j+1}-2\varphi_{i,j}+\varphi_{i,j-1}}{h^2} \tag{137}$$

According to Laplace's equation, the sum of the second derivatives of φ to x and y is equal to zero. When we substitute the derivatives by the finite difference approximation we obtain

$$\varphi_{i+1,j} + \varphi_{i-1,j} + \varphi_{i,j+1} + \varphi_{i,j-1} - 4\varphi_{i,j} = 0 \tag{138}$$

or

$$\varphi_{i,j} = \frac{\varphi_{i+1,j} + \varphi_{i-1,j} + \varphi_{i,j+1} + \varphi_{i,j-1}}{4} \tag{139}$$

Equation (139) says that the head in each node is equal to the average of the heads in the surrounding nodes. This holds for all nodes that are not located on a boundary. In the next section we discuss the boundary nodes

Boundary Conditions

At the boundaries we may be dealing with a prescribed head (Dirichlet) or with a prescribed flux (Neumann). The equations for nodal points at a Dirichlet boundary are simply:

$$\varphi_{i,j} = \varphi_0 \tag{140}$$

where φ_0 represents the given head at the boundary. For the Neumann type we discuss only the case of an impermeable boundary, i.e. the flux perpendicular to the boundary is zero which is the same as the condition that the derivative perpendicular to the boundary is zero. This condition can be easily fulfilled by adding an imaginary node across the boundary with the same head as the first node inside the area opposite of the imaginary node. For instance, if the node (i,j) at a vertical boundary is located at the position (i,j), the imaginary node is at point $(i\text{-}1,j)$ and the node inside the problem domain is at $(i+1,j)$. With $\varphi_0 = \varphi_{i\text{-}1,j}$, the approximation of $\partial\varphi/\partial x$ at the boundary, for which we may write $(\varphi_{i+1,j} - \varphi_{i\text{-}1,j})/2h$, is clearly equal to zero. Thus for this node the equation reads:

$$\varphi_{i,j} = \frac{2\varphi_{i+1,j} + \varphi_{i,j+1} + \varphi_{i,j-1}}{4} \tag{141}$$

Gauss Seidel Iteration

When we require that Laplace's equation holds at all the nodes of the grid and as an approximation replace this by the requirement that the finite difference equivalent of Laplace's equation, eqs (139) (140) or (141) depending on the type of node, then we obtain a system of N equations. The solution to this set of equations is sought in an iterative way. Many algorithms exist that handle this job. Here we discuss the *Gauss Seidel* method. We work through the grid in a systematic way, starting with $i = 1$ and $j = 1$ (unless this nodes is at a Dirichlet boundary). This is called a sweep. Each time the head at a node is calculated by (139) or (141). The systematical order for handling the node is required, because we use newly computed values to determine the head at the adjacent node. The Gauss-Seidel procedure is well suited to be carried out by a computer.

To end the iteration process we need a stop-criterion. Usually, one considers the residual ε, just before the newly calculated value is imposed:

$$\varepsilon = \varphi_{i+1,j} + \varphi_{i-1,j} + \varphi_{i,j+1} + \varphi_{i,j-1} - 4\varphi_{i,j} \tag{142}$$

The sum of the absolute value of the residuals $|\varepsilon|$ over all the nodes tends to decrease at each iteration level. We may stop the program when the sum of $|\varepsilon|$ is at an acceptable low level.

Finite Element Method

As in the method of Finite differences, the domain of interest is divided into a large number of smaller spatial elements. The corners of the elements are called the *nodes*. The method is based on the following three ingredients.

(i) construct an approximate function $\hat{\varphi}$ using a large number N of parameters that may be varied freely. The approximation must be such that by changing the free parameters the function can take a large variety of shapes.

(ii) find a criterion that indicates how close the approximation approaches the exact solution, while the solution itself is not available. If there are N unknown parameters in the approximate solution (degrees of freedom), then the criterion must yield N conditions to be fulfilled. This leads to a system of N equations with N unknowns.

(iii) solve the system of N equations. Since in general N is large, the solution is normally carried out by a computer.

The approximation $\hat{\varphi}$

It is common to use a simple linear interpolation function, with the potentials φ_i in the nodes as unknown parameters. This is illustrated below for a 1-D situation. Suppose N nodes and N-1 elements are present. The element i contains the nodes with indices i and i+1. The coordinates are denoted by x_i and x_{i+1} and its potentials by φ_i and φ_{i+1}.

The linear interpolation of φ in element I [$x_i < x < x_{i+1}$] can be written as:

$$\hat{\varphi}(x) = \varphi_i \frac{-x + x_{i+1}}{x_{i+1} - x_i} + \varphi_{i+1} \frac{-x + x_i}{x_{i+1} - x_i} \tag{143}$$

or in more general terms as:

$$\hat{\varphi}(x) = \varphi_i N_i(x) + \varphi_{i+1} N_{i+1}(x) \tag{144}$$

The functions $N_i(x)$ are known as basis functions with φ_i and φ_{i+1} as free parameters. Figure 23 shows the shape of the basis functions. A function N_i is always equal to 1 at node i and zero at all other nodes, or:

$$\begin{aligned} N_i(x_i) &= 0 \quad for \quad i \neq j \\ N_i(x_i) &= 1 \quad for \quad i = j \end{aligned} \tag{145}$$

The elements i and i+1 are adjacent to node i. In these elements, $N_i(x)$ is defined as:

$$\begin{aligned} N_i(x) &= \frac{x - x_{i-1}}{x_i - x_{i-1}} \qquad for \quad [x_{i-1} < x < x_i] \\ N_i(x) &= \frac{-x + x_{i-1}}{x_{i+1} - x_i} \qquad for \quad [x_i < x < x_{i+1}] \end{aligned} \tag{146}$$

while $N_i(x)$ is zero in all elements not adjacent to node i.

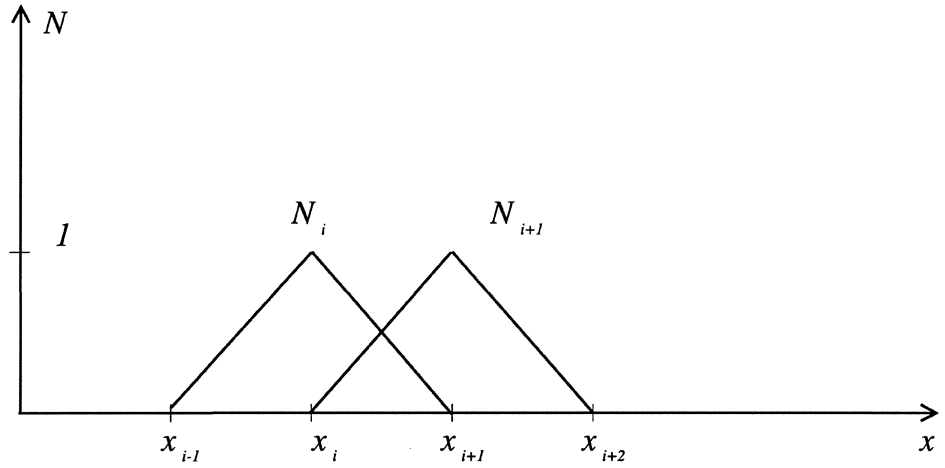

Figure 23 Example of basis functions

Using the basis functions we can write for the entire area of interest:

$$\hat{\varphi}(x) = \sum_{i=1}^{N} \varphi_i N_i \tag{147}$$

Similarly basis functions can be defined for 2-dimensional elements. Below an example is given for a mesh with rectangular elements (length l and height h):

$$N_i(x,y) = \frac{(l - |x - x_i|)(h - |y - y_i|)}{lh} \tag{148}$$

The essential property of these functions is that they are always equal to 1 at node i and zero at all other nodes. Further, they are defined only for the elements adjacent to node i. The approximate solution can now be written in the form:

$$\hat{\varphi}(x,y) = \sum_{1}^{N} \varphi_i N_i(x,y) \tag{149}$$

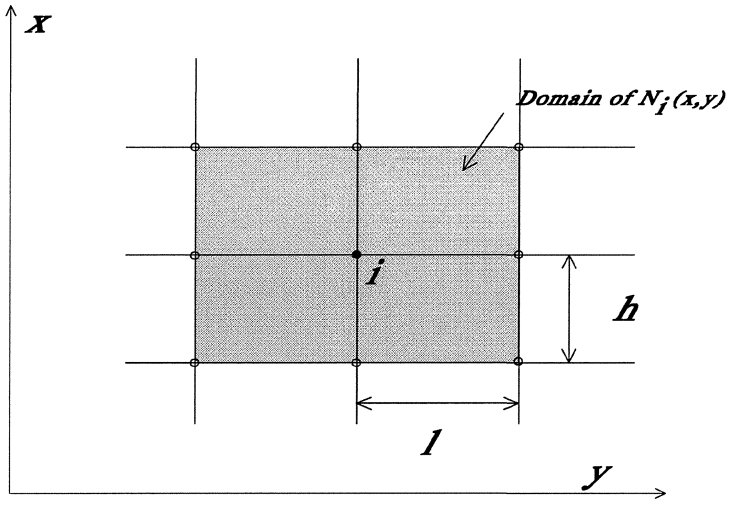

Figure 24 Domain of two-dimensional basis-functions

Criterion

There are several possibilities for the required 'criterion'. One is based on a so-called functional U defined by:

$$U = \frac{1}{2}\iint_V \left[\left(\frac{\partial \varphi}{\partial x}\right)^2 + \left(\frac{\partial \varphi}{\partial y}\right)^2\right] dxdy \qquad (150)$$

An existing theorem says that U has an absolute minimum, if φ satisfies the Laplace equation. If we substitute φ by $\hat{\varphi}(x)$, U will not obtain the absolute minimum, since $\hat{\varphi}(x)$ does not satisfy Laplace. However, we accept the lowest value possible when we vary the values φ_i, which are until now unknown parameters in $\hat{\varphi}(x)$, see eq (147). Then, when we find the lowest value possible we consider this $\hat{\varphi}(x)$ the best approximation to the Laplace equation (and boundary conditions). To obtain the set of φ_i's that produce the minimum of U, we require that $\partial U/\partial \varphi_i = 0$ for $i = 1, \ldots, N$. This yields a system of N algebraic equations with N unknowns. When we consider node i, it can be noticed that $\hat{\varphi}(x)$ depends only on φ_i in the elements adjacent to the node i because $N_i = 0$ in all other elements. Thus, in the elements not adjacent to node i, $\partial \hat{\varphi}/\partial \varphi_i = 0$ and consequently there $\partial U/\partial \varphi_i = 0$. This means that $\partial U/\partial \varphi_i$ only needs to be calculated for elements adjacent to node i. This results in an algebraic equation that expresses φ_i in the heads of the 8 surrounding nodes. With

N nodes this yields a set of N algebraic equations. The procedure of solving these equations is similar to that of the finite difference method.

PART 2

Groundwater Transport Fundamentals

General

Groundwater is moving slowly, but compared to other soil constituents it is quite mobile. Since water is also a good solvent, it is an ideal underground carrier for soluble substances. This explains the important role of groundwater in the spreading of contaminants. In this chapter we will discuss the major transport processes.

Transport mechanisms

When groundwater is flowing, it also displaces solutes. This type of transport is called *advection* or *convection.* In addition to pure displacement, spreading of the solutes occurs, due to differences in concentration. This process is known as *dispersion.* Advection and dispersion are essentially different. Advection causes no changes in the solute concentration. Dispersion, however, always leads to a decreasing concentrations and, therefore, is an *irreversible* process. The distinction between advection and dispersion is important from a mathematical point of view. The dispersive term gives the solute transport equation the properties of a parabolic differential equation. Advection gives it a hyperbolic character. This difference has numerical consequences. Standard methods such as the finite element or finite difference method are especially suited for parabolic differential equations. Applied to hyperbolic equations these methods create an artificial mixing, known as numerical dispersion. We will illustrate the origin of numerical dispersion for a simple one-dimensional case and discuss some alternative numerical procedures that avoid complication.

Advection

The amount of solutes displaced by advection follows directly from Darcy's law as the product of specific volume flux q times the solute concentration c [kg/m^3]:

$$\vec{F}^{adv} = c\,\vec{q} \tag{152}$$

Here, $\vec{F}^{adv}$ is the advective solute flux [M L^{-2} T^{-1}]. Advection may change the shape of a polluted region, but the concentration remains unchanged (figure 25).

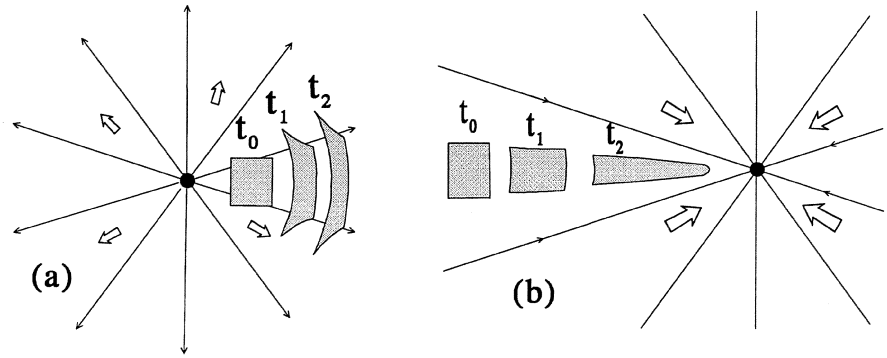

Figure 25 Displacement and deformation of a polluted area for diverging flow (infiltration well) and converging flow (pumping well)

On micro-scale the displacement is more complicated than it suggested by Darcy's law. Instead of straight flow lines, we observe a highly variable flow along curved flow lines

Reasons for this variability are (figure 26):

- the velocity in the middle of a pore is higher than at the grain surface (fig 26a)
- not all pores have the same diameter (fig 26b)
- not all pores have the same direction (fig 26c)

Consequently, the solute displaces not as regularly as suggested by eq. (152). In the first place mixing occurs by diffusion. Below, we first discuss mixing by diffusion and, accordingly, the combined effect of diffusion and the velocity variation.

Molecular diffusion

When a dye is added to a glass of water, it spreads and the color gradually fades away. This process is known as *molecular diffusion.* In figure 27 an illustration is given of diffusion in a porous medium with stagnant water. Figure 27*a* (top) shows the distribution of a tracer for various moments in time. These curves are known as Gauss-curves. The standard deviation σ of these curves increases with time, according to:

$$\sigma^2 = 2D_m t \tag{153}$$

where D_m [L^2/T] is the coefficient of molecular diffusion. For salt in pure water D_m is approximately 0.7 cm^2/day.

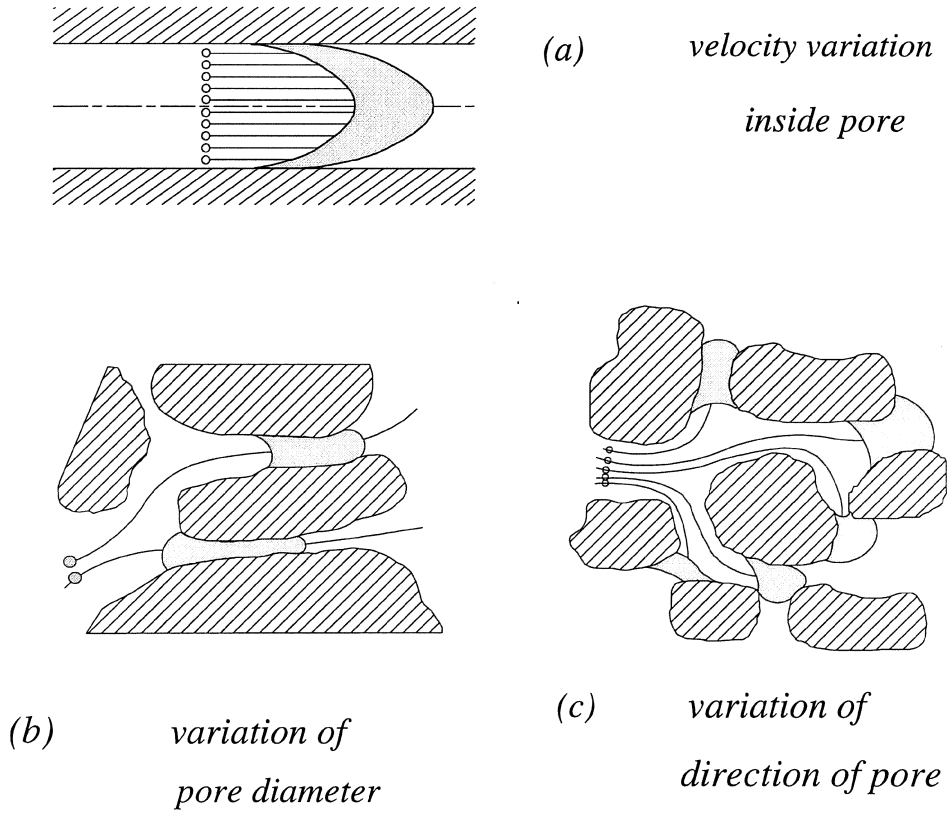

Figure 26 Variation of velocity on microscopic scale

The relation between the diffusive flux and the concentration gradient is given by Fick's law:

$$\vec{F}^{dif} = -D_m \nabla c \tag{154}$$

where $\vec{F}^{dif}$ is the diffusive mass flux [M L^{-2} T^{-1}].

Now consider the scale, in time and space, at which the contribution of diffusion is significant. Figure 27b shows a pore and a dye in the middle, which has just been injected ($t = 0$). In figures 27c and 27d a diluted 'cloud' of solutes is sketched after 45 sec and 3 minutes. The area of mixing has grown such, that the values of σ are respectively 0.25 and 0.5 mm. Evidently, mixing inside a pore is a matter of a few minutes. For comparison with the average advective movement in the same time interval, we consider a groundwater velocity of 2 cm/day. Under normal circumstances this velocity

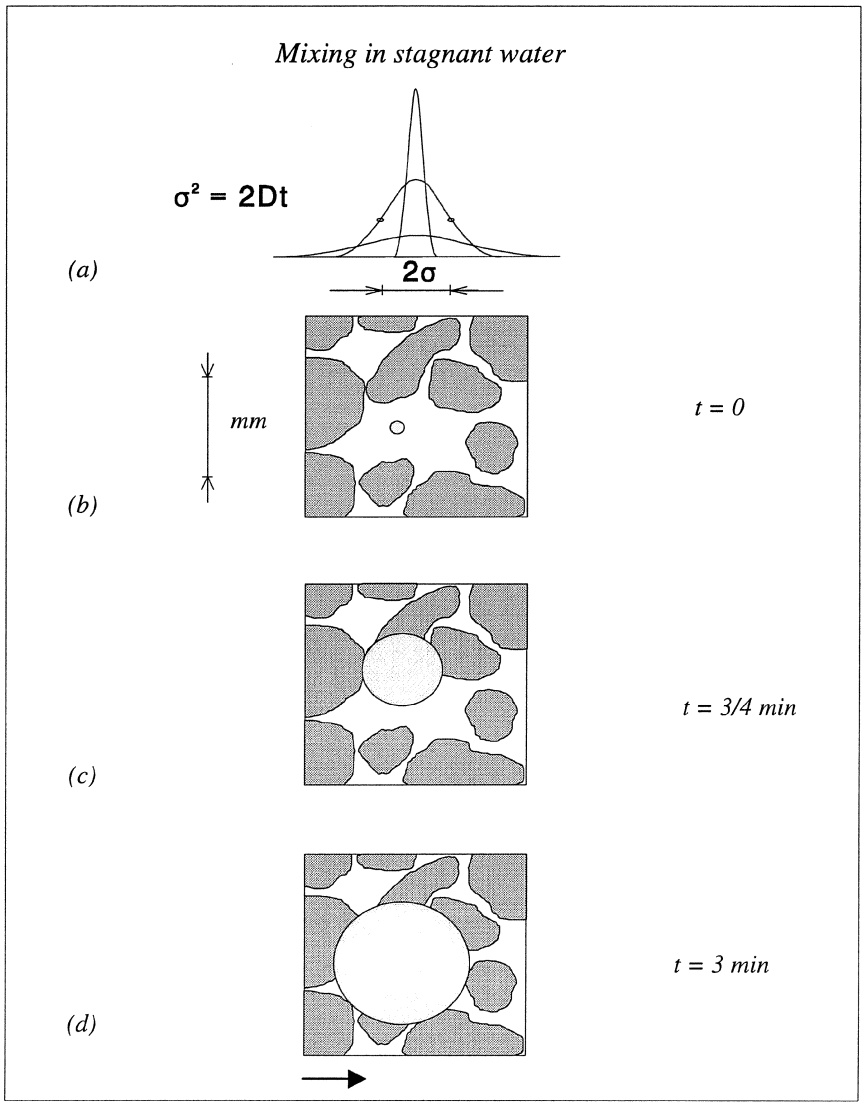

Figure 27 Diffusive mixing on microscopic scale

is not extremely low. The corresponding displacement by advection is 0.01 mm (figure 27c) and 0.04 mm (figure 27d). We conclude that at this time scale diffusion dominates. However, diffusive displacement is proportionally to the square root of time [$\sigma = \sqrt{(2D_m \Delta t)}$], while advection grows linearly with time ($\Delta x = vt$). Hence, the role of diffusion gradually reduces. After a year, with the same numerical values as above, we find:

$$\sigma = 0.22 \text{ m}; \qquad \Delta x = 7.3 \text{ m}$$

We may conclude that on a macroscopic level advection is predominating. As time increases diffusion contributes less and less to solute transport.

Micro-dispersion

When groundwater flows, diffusion is not the only mixing phenomenon. The actual (microscopic) velocity in the pores varies widely in space even when the Darcy (macroscopic) velocity is constant. Not all particles travel over the same distance or in the same direction. The result is a more intense mixing arises, which is called (hydrodynamic) dispersion or microdispersion. Figure 28 gives a schematic view of the tracer movement on a macroscopic level. Solutes are spreading over an area that has the shape of an ellipse, unlike the circle in case of diffusion. Concentration is Gaussian distributed over the axes of the ellipse. The standard deviations in longitudinal and transverse direction, σ_L and σ_T, increase in time according to:

$$\sigma_L^{\,2} = 2D_L t \tag{155}$$

$$\sigma_T^{\,2} = 2D_T t \tag{156}$$

where D_L and D_T [m^2/s] are the coefficients of longitudinal and transverse dispersion.

The macroscopic parameters D_L and D_T lump all information on microscopic heterogeneity that was lost by the use of the Darcy-velocity. The dispersion coefficients depend on the groundwater velocity:

$$D_L = \alpha_L |\vec{v}| + D_m \tag{157}$$

$$D_T = \alpha_T |\vec{v}| + D_m \tag{158}$$

where $\vec{v}$ is the groundwater velocity ($\vec{v} = \vec{q}/n$, n being the porosity). The parameters α_L and α_T are the longitudinal and transverse *dispersivity*, properties of the porous medium only. Their values must be determined by experiments. In the literature, dispersivities are given in the range from millimeters to centimeters. In general, longitudinal dispersivity is 5 until 10 times higher than the transverse dispersivity (de Josselin de Jong, 1958; Li and Lai, 1966).

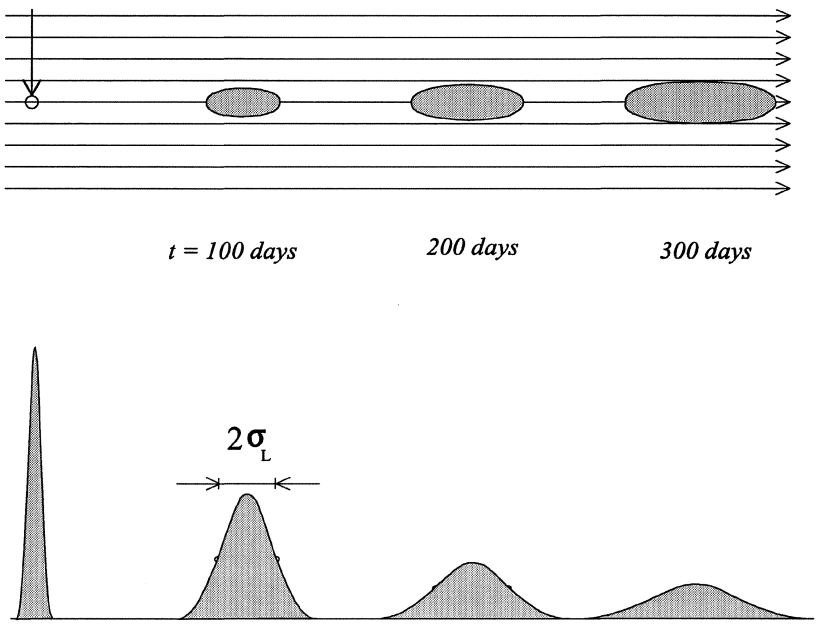

Figure 28 Microdispersion, observed at macroscopic scale

The dispersion tensor

For the dispersive flux of solute mass an expression similar to (154) is used:

$$\vec{F}^{dis} = -n\mathbf{D}\nabla c \tag{159}$$

The coefficient **D** is not a scalar as in Fick's law for diffusion, but a tensor. In 3-dimensional space **D** has 9 components:

$$\mathbf{D} = \begin{bmatrix} D_{xx} & D_{xy} & D_{xz} \\ D_{yx} & D_{yy} & D_{yz} \\ D_{zx} & D_{zy} & D_{zz} \end{bmatrix} \tag{160}$$

In matrix notation (159) is written as:

$$\begin{bmatrix} F_x^{dis} \\ F_y^{dis} \\ F_z^{dis} \end{bmatrix} = -n \begin{bmatrix} D_{xx} & D_{xy} & D_{xz} \\ D_{yx} & D_{yy} & D_{yz} \\ D_{zx} & D_{zy} & D_{zz} \end{bmatrix} \begin{bmatrix} \partial c/\partial x \\ \partial c/\partial y \\ \partial c/\partial z \end{bmatrix} \tag{161}$$

and in tensor notation:

$$F_i^{dis} = -nD_{ij} \frac{\partial c}{\partial x_j} \tag{162}$$

where summation is applied over j.

In the previous chapter we have seen that the dispersion coefficient depends on the groundwater velocity. A general relation between the components D_{ij} and v_i is given by Bear (1972):

$$D_{ij} = \frac{(\alpha_L - \alpha_T)}{|\vec{v}|} v_i v_j + (\alpha_T |\vec{v}| + D_m)\delta_{ij} \tag{163}$$

where δ_{ij} is the Kronecker delta, defined as δ_{ij} of $\delta_{ij} = 0$ for $i \neq j$ and $\delta_{ij} = 1$ for $i = j$. When the x_1-axis coincides with the flow direction all mixed terms are zero and we obtain:

$$D_{ij} = \begin{bmatrix} \alpha_L |\vec{v}| + D_m & 0 & 0 \\ 0 & \alpha_T |\vec{v}| + D_m & 0 \\ 0 & 0 & \alpha_T |\vec{v}| + D_m \end{bmatrix} \tag{164}$$

This corresponds to eqs (157) and (158).

The advection-dispersion equation

The advection-dispersion equation is derived from a mass balance (figure 29) over a time interval Δt for an elemental volume with dimensions Δx_i (i = 1, 2, 3). In the following expression we write Ω_i for the total solute flux, or:

$$\Omega_i = F_i^{adv} + F_i^{dis} \tag{165}$$

The amount of solutes that enters the elemental volume during Δt is:

$$(\Omega_1 \Delta x_2 \Delta x_3 + \Omega_2 \Delta x_1 \Delta x_3 + \Omega_3 \Delta x_1 \Delta x_2)\Delta t \tag{166}$$

The amount of solutes that leaves the control-volume is:

$$\left(\left[\Omega_1 + \frac{\partial \Omega_1}{\partial x_1}\Delta x_1\right]\Delta x_2 \Delta x_3 + \left[\Omega_2 + \frac{\partial \Omega_2}{\partial x_2}\Delta x_2\right]\Delta x_1 \Delta x_3 + \left[\Omega_3 + \frac{\partial \Omega_3}{\partial x_3}\Delta x_3\right]\Delta x_1 \Delta x_2\right)\Delta t \tag{167}$$

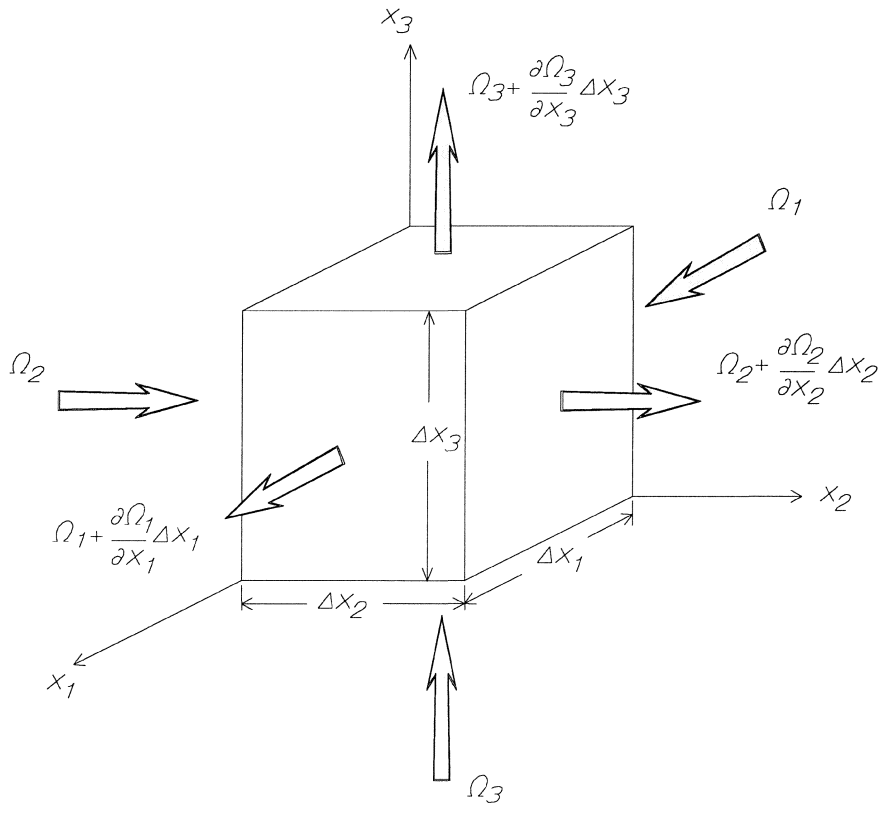

Figure 29 Control-volume with in- and outgoing solute flux

The principle of mass conservation says that the difference between (166) and (167) is equal to the increase of solutes stored in the volume. If the mass in a unit volume is denoted by M, we have $M\Delta x_1\Delta x_2\Delta x_3$ for the mass in our control volume and $(\partial M/\partial t)\ \Delta x_1\Delta x_2\Delta x_3\Delta t$ for the increase of stored mass during Δt. After elimination of Δx_1, Δx_2, Δx_3 and Δt the mass balance leads to:

$$\frac{\partial \Omega_i}{\partial x_i} = -\frac{\partial M}{\partial t} \tag{168}$$

For a species that does not adsorb or react with the grains, the mass in a unit volume becomes $M = nc$. Then, using (165), (152) and (159) we rewrite (168) into the *advection-dispersion equation*:

$$\frac{\partial}{\partial x_i}\left(D_{ij}\frac{\partial c}{\partial x_j}\right) - \frac{\partial}{\partial x_i}(v_i c) = \frac{\partial c}{\partial t} \tag{169}$$

This is also known as the *solute transport equation.* It has been assumed that porosity is constant. The first and second term at the left hand side represent dispersion and advection. The dispersive term consists of 9 components (summation over i and j) and the advective term of 3 components (summation over i).

Linear adsorption

For a species that adsorbs to the grains we may not use the relation $M = nc$, since this does not include the adsorbed mass, which also can change in time. Adsorption is the phenomenon that ions (generally positively charged) stick to the sand or clay particles and during some time do not participate in the transport. The amount of solutes adsorbed to the matrix is expressed by S, being the ratio of adsorbed mass and the mass of the solid grains:

$$S = \frac{M_a}{M_g} \tag{170}$$

S is dimensionless. In a unit volume of sand with porosity n the mass of the grains is $M_g = (1\text{-}n)\rho_g$, where ρ_g is the mass density of the grains. Then, the amount of adsorbed mass in a unit volume is:

$$M_a = (1-n)\rho_g S \tag{171}$$

Usually, the amount of adsorbed ions is a function of the concentration in the liquid c. If c increases, more ions are adsorbed and vice-versa. When c remains constant, the solutes in the liquid phase and in the adsorbed phase obtain a state of equilibrium. After changing the concentration a

new equilibrium occurs, which may take some time. However, compared to the low velocity of the groundwater, this new equilibrium may be assumed to occur without a delay. In this case we speak of *equilibrium adsorption*. The equilibrium between c and S is expressed by a so-called equilibrium isotherm:

$$S = f(c) \tag{172}$$

where the $f(c)$ is a function that depends on the type of solute. For many species the adsorption isotherm is described by a linear function of the type:

$$S = K_d c \tag{173}$$

Here K_d is the *distribution coefficient* [L^3 M^{-1}]. We are dealing now with *linear equilibrium adsorption*. Now, we consider the solute transport equation and extend the equation for the case of linear equilibrium adsorption.

Now we shall extend (169) and include adsorption. A more general formulation of (169) is:

$$n\frac{\partial}{\partial x_i}\left(D_{ij}\frac{\partial c}{\partial x_j}\right)-\frac{\partial}{\partial x_i}(nv_i c)=\frac{\partial M}{\partial t} \tag{175}$$

where M is the total mass in the control volume now including the adsorbed mass:

$$M = nc+(1-n)\rho_g S \tag{176}$$

More specifically for linear equilibrium adsorption we have:

$$M = nc+(1-n)\rho_g K_d c \tag{177}$$

With (177) substituted into (175) the transport equation becomes:

$$n\frac{\partial}{\partial x_i}\left(D_{ij}\frac{\partial c}{\partial x_j}\right)-\frac{\partial}{\partial x_i}(nv_i c)=\frac{\partial}{\partial t}\left(nc+[1-n]\rho_g K_d c\right) \tag{178}$$

Note that n, ρ_g and K_d are considered to be constants. After division by n, this becomes:

$$\frac{\partial}{\partial x_i}\left(D_{ij}\frac{\partial c}{\partial x_j}\right)-\frac{\partial}{\partial x_i}(v_i c)=R\frac{\partial c}{\partial t} \tag{179}$$

where R is called the *retardation-factor* (dimensionless)

$$R=\frac{nc+[1-n]\rho_g K_d c}{n} \tag{180}$$

The retardation factor is greater than or equal to 1. R = 1 corresponds to the case with no adsorption. We may notice that, when numerator and denominator are multiplied by c, R is the ratio between total solute mass M and solute mass in the liquid phase. The term retardation-factor indicates that adsorption retards the transport process, which is clearly seen by division of both sides of (179) by R:

$$\frac{\partial}{\partial x_i}\left(\frac{D_{ij}}{R}\frac{\partial c}{\partial x_j}\right)-\frac{\partial}{\partial x_i}\left(\frac{v_i}{R}c\right)=\frac{\partial c}{\partial t} \tag{181}$$

This suggest that the behavior of an adsorbed species is as an unadsorbed species with an apparent velocity v_i/R and an apparent dispersion coefficient D_{ij}/R.

Analytical Solutions

Point Injection (one dimensional)

The advection-dispersion equation can be solved analytically for some simple flow cases. In this section a few examples are discussed. For a homogeneous aquifer and a uniform groundwater flow along the x-axis the equation may be simplified. First, v and D are constants and secondly, the coordinates are exactly along the principal directions of the dispersion tensor. The solute transport equation now becomes:

$$D_L \frac{\partial^2 c}{\partial x^2} + D_T \frac{\partial^2 c}{\partial y^2} + D_T \frac{\partial^2 c}{\partial z^2} - v\frac{\partial c}{\partial x} = \frac{\partial c}{\partial t} \tag{182}$$

If the problem is one dimensional, the second and third term at the left hand side may be dropped. Now, a one-dimensional equation remains, for which a large number of solutions can be found in the literature (Kreft and Zuber, 1978; Bear, 1979; Van Genuchten and Alves, 1982). A very elementary solution is:

$$c(x,t) = \frac{M/n}{2\sqrt{\pi D t}} \exp\left(-\frac{[x-vt]^2}{4Dt} \right) \tag{183}$$

This is the classical solution for an instantaneous point injection of a solute mass M. When c is plotted versus x, we obtain a Gaussian curve with a standard deviation $\sigma = \sqrt{2Dt}$. If the solutes can also spread in the y-direction or in the y and z directions, we have the 2-dimensional and 3-dimensional variants:

2D:
$$c(x,y,t) = \frac{M/n}{4\pi t\sqrt{D_L D_T}} \exp\left(-\frac{[x-vt]^2}{4D_L t} - \frac{y^2}{4D_T t} \right) \tag{184}$$

3D
$$c(x,y,z,t) = \frac{M/n}{8\pi D_T t\sqrt{\pi t D_L D_T}} \exp\left(-\frac{[x-vt]^2}{4D_L t} - \frac{y^2}{4D_T t} - \frac{z^2}{4D_T t} \right) \tag{185}$$

It can be concluded from these solutions that the maximum concentration, c_{max}, always occurs at $x = vt$, so the peak of the concentration profile travels with the speed of the groundwater velocity. During this movement c_{max}.decreases in time. In the 1-D case the decrease rate is proportional to $1/\sqrt{t}$. Meanwhile, the standard deviation of this Gaussian curve grows in time: $\sigma = \sqrt{2Dt}$. Thus, in time the concentration profile displaces, becomes wider and reduces in height. For $t = 0$ the concentration goes to infinity, which is caused by the fact that mathematically the solute mass is distributed over an infinitely small line element. The mass in the aquifer, obtained by integration of $nc(x,t)$ from $x = -\infty$ to $x = +\infty$, must remain constant and equal to M at all t, also for $t \rightarrow 0$. The solution for $t = 0$ takes the form of the so-called dirac function $\delta(x)$, multiplied by M/n The function $\delta(x)$ has the following properties: $\delta(x) = 0$ for $x \neq 0$, $\delta(x)$ goes to infinity for $x = 0$, while the integral $\int_{-\infty}^{+\infty} \delta(x)dx = 1$

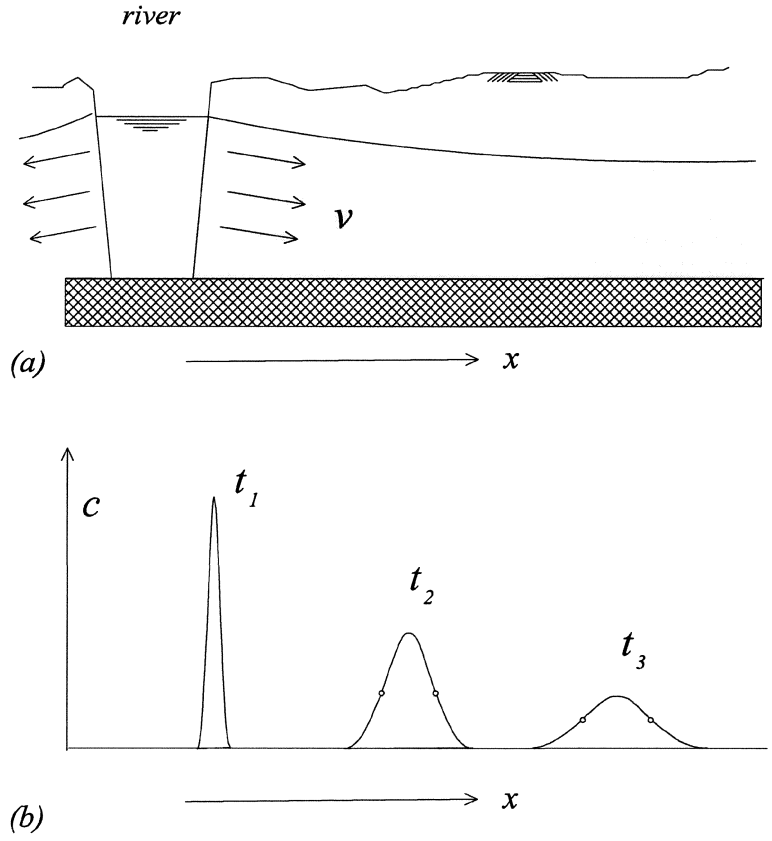

Figure 30 (a) Instantaneous pollution at an infiltrating river; (b) concentration profiles at several moments t_1; t_2; t_3.

Eq (183) describes, more or less, the case of an infiltrating river, where, due to a calamity during a very short period of time, pollution takes place. An illustration is given in figure 30. The x-direction is perpendicular to the river and M refers to the amount of (solute) mass that infiltrates per unit length of the river (perpendicular to the plane of the figure) and per unit length of aquifer thickness.

The erfc solution

With the elementary solution (183) new solutions can be constructed. We shall derive the solution for an infinite aquifer with a uniform flow and an initial constant concentration c_0 for $x < 0$, while for $x > 0$ the initial concentration is zero.

Consider a point $x = \xi$ on the negative x-axis. In a small line element between $x = \xi$ and $x = \xi + d\xi$ the contaminant mass dM initially is $n\, c_0\, d\xi$ (where n denotes the porosity). The concentration due initially present mass at $x = \xi$ becomes:

$$c(x,t) = \frac{c_0 d\xi}{2\sqrt{\pi Dt}} \exp\left[-\frac{[x-\xi-vt]^2}{4Dt}\right] \tag{186}$$

The solution we are finally looking for is obtained by adding point injections with dM, where the injection point varies from $\xi = -\infty$ to $\xi = 0$, thus:

$$c(x,t) = \int_{-\infty}^{0} \frac{c_0}{2\sqrt{\pi Dt}} \exp\left(-\frac{[x-\xi-vt]^2}{4Dt}\right) d\xi \tag{187}$$

This can be rewritten using the *complementary error function*, which is defined as:

$$erfc(z) = \frac{2}{\sqrt{\pi}} \int_{z}^{\infty} \exp(-\zeta^2) d\zeta \tag{188}$$

The function *erfc* is tabulated and can be found in many statistical or mathematical textbooks. After some algebra the final solution can be written as:

$$c(x,t) = \frac{c_0}{2} erfc\left(-\frac{x-vt}{2\sqrt{Dt}}\right) \tag{189}$$

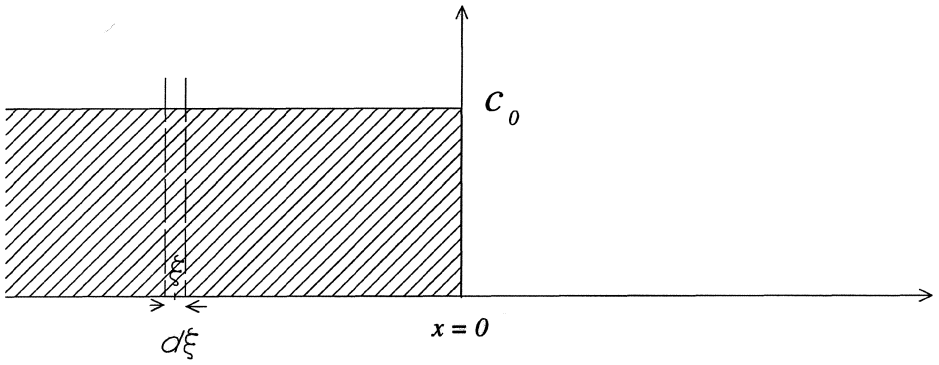

Figure 31 Construction of the erfc solution

The *erfc* solution can be considered as fundamental as (183). It may also be used to construct new solutions, using superposition. For instance, the case with initial concentration constant c_0 in the region $-a < x < a$ and zero in the region $|x|$, may be obtained by subtraction of two *erfc* solutions:

$$c(x,t) = \frac{c_0}{2}\left\{erfc\left(\frac{x-a-vt}{2\sqrt{Dt}}\right) - erfc\left(\frac{x+a-vt}{2\sqrt{Dt}}\right)\right\} \tag{190}$$

Point injection 2D

We can eliminate the advective term in (182) by the substitution $\bar{x} = x - vt$:

$$D_L \frac{\partial^2 c}{\partial \bar{x}^2} + D_T \frac{\partial^2 c}{\partial y^2} = \frac{\partial c}{\partial t} \tag{191}$$

This equation describes a dispersion process as seen by an observer traveling with velocity v. A second substitution $\bar{y} = y\sqrt{D_L/D_T}$ transforms (190) into:

$$D_L\left(\frac{\partial^2 c}{\partial \bar{x}^2} + \frac{\partial^2 c}{\partial \bar{y}^2}\right) = \frac{\partial c}{\partial t}, \tag{192}$$

which has an elementary solution:

$$c(\bar{x},\bar{y},t)=\frac{A}{4\pi t}\exp\left(-\frac{\bar{x}^2+\bar{y}^2}{4D_L t}\right) \tag{193}$$

The constant A can be obtained from the principle of mass conservation. Suppose at $t = 0$ an instantaneous injection of solute mass M takes place. The mass must be somewhere' in the aquifer at an arbitrary time t, so:

$$M = nH\int\int_{-\infty}^{\infty} c\,dx\,dy \tag{194}$$

where H is the aquifer thickness. This leads to $A = M\,(D_L D_T)^{-½}/nH$. After returning to the original variables we obtain:

$$c(x,y,t)=\frac{M/n}{4\pi Ht\sqrt{D_L D_T}}\exp\left(-\frac{(x-vt)^2}{4D_L t}-\frac{y^2}{4D_T t}\right) \tag{195}$$

Equation (195) describes a cloud of contaminants moving along the x-axis with the shape of an ellipse. While the cloud is moving the size grows and the concentration decreases. We have seen this case displayed in figure 28.

Continuous Point Injection

The description of a continuous pollution with a rate J [kg/sec] can be derived from (195). Consider the contribution of the pollution added to the aquifer at $t = \tau$ during a very short time interval $d\tau$. The amount of contaminant M is equal to $Jd\tau$. Since the interval $d\tau$ is infinitely short, the pollution may be considered as instantaneous. For the concentration at time τ due to an injection of $Jd\tau$ we apply eq. (195), with t replaced by t - τ and M by $Jd\tau$:

$$c(x,y,t)=\frac{Jd\tau/n}{4\pi H(t-\tau)\sqrt{D_L D_T}}\exp\left(-\frac{(x-v[t-\tau])^2}{4D_L(t-\tau)}-\frac{y^2}{4D_T(t-\tau)}\right) \tag{196}$$

Accordingly, eq. (196) is integrated from $\tau = 0$ until t. With $\theta = t$ - τ we can write:

$$c(x,y,t)=\frac{J}{4\pi nH\sqrt{D_L D_T}}\int_0^t \frac{1}{\theta}\exp\left(-\frac{(x-v\theta)^2}{4D_L\theta}-\frac{y^2}{4D_T\theta}\right)d\theta \qquad (197)$$

With the substitution $r^2 = x^2 + y^2 D_L/D_T$ this is rewritten as:

$$c(x,y,t)=\frac{J}{4\pi nH\sqrt{D_L D_T}}\exp\left(\frac{xv}{2D_L}\right)W\left(\frac{r^2}{4D_L t},\frac{rv}{2D_L}\right) \qquad (198)$$

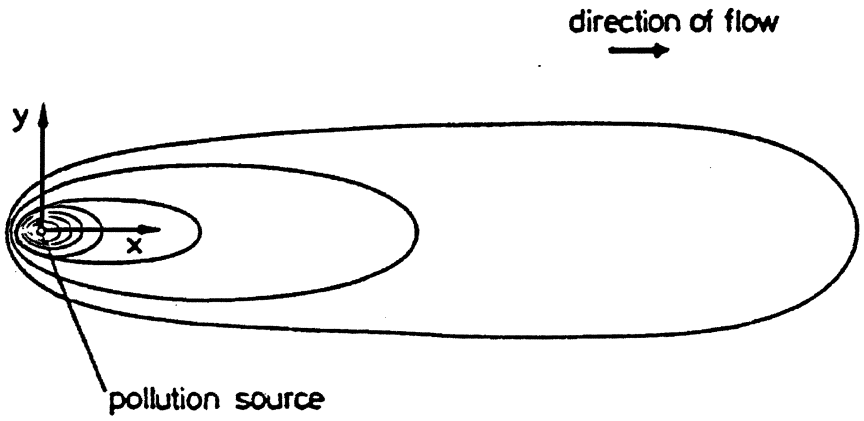

Figure 32 Continuous pollution in a uniform flow (non steady)

Here $W(u,b)$ is the Hantush Well function, well-known from pumping test theory:

$$W(u,b)=\int_u^\infty \frac{1}{\zeta}\exp\left(-\zeta-\frac{b^2}{4\zeta}\right)d\zeta \qquad (199)$$

Tables for $W(u,b)$ can be found in several textbooks on pumping tests (Kruseman and De Ridder, 1970). However, the exponential term is often large, while $W(u,b)$ becomes very small. Multiplication of these factors then leads to a loss of significant figures. Therefore, a table with values for the product $exp(b)\ W(u,b)$ is more convenient (appendix B). Here, u and b are dummy variables. The variable u represents $r^2/(4D_L t)$ and b stands for $rv/(2D_L)$ The values read from the table must be multiplied by $\exp(xv/2D_L - rv/2D_L$ In general this term is close to 1 and no additional loss of significant figures occurs by this multiplication.

Steady state

For large values of t, $u \rightarrow 0$ and $W(u,z)$ reduces to a modified Bessel function. The steady state solution becomes:

$$c = \frac{J}{2\pi nH\sqrt{D_L D_T}} \exp\left(\frac{xv}{2D_L}\right) K_0\left(\frac{rv}{2D_L}\right) \tag{200}$$

Table 3 (appendix C) gives the function $exp(z)\, K_0(z)$. The argument $rv/2D_L$ of K_0 is often sufficiently large to use an asymptotic approximation for K_0 (Abramowitz and Stegun, 1972):

$$K_0(z) \approx \sqrt{\frac{\pi}{2z}} \exp(-z) \tag{201}$$

[for $z > 5$ the error is smaller than 2.5 %]. This means that (201) may be approximated by:

$$c = \frac{J}{2nH\sqrt{\pi v r D_T}} \exp\left(\frac{(x-r)v}{2D_L}\right) \tag{202}$$

Note that along the x-axis ($r = x$) the concentration decreases proportionally to $1/\sqrt{x}$ and the rate of decrease only depends on D_T

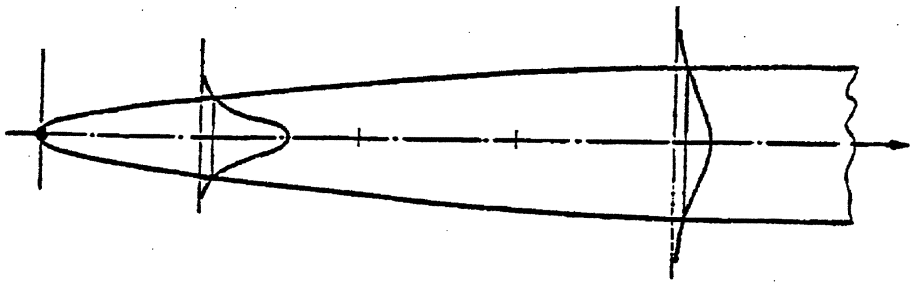

Figure 33 Continuous pollution steady state

Numerical Methods

Numerical dispersion

The finite difference and finite element methods, which are the most popular techniques for solving groundwater flow problems, are less successful in solving the solute transport equation. One of the reasons is a complication known as *numerical dispersion*. A 1-D finite difference scheme is discussed to illustrate the problem of numerical dispersion. The following equation is considered (D and v are assumed to be constant):

$$D\frac{\partial^2 c}{\partial x^2} - v\frac{\partial c}{\partial x} = \frac{\partial c}{\partial t} \tag{203}$$

In the finite difference method a grid is used. Let the grid be equidistant with a distance h between the nodes. Consider the Taylor series:

$$c(x+h) = c(x) + h\frac{\partial c}{\partial x} + \frac{h}{2}\frac{\partial^2 c}{\partial x^2} + O(h^2) \tag{204}$$

This gives for $\partial c/\partial x$:

$$\frac{\partial c}{\partial x} = \frac{c(x+h)-c(x)}{h} - \frac{h}{2}\frac{\partial^2 c}{\partial x^2} - O(h^2) \tag{205}$$

The first term at the right hand side is the finite difference approximation for $\partial c/\partial x$. The error made is given by the second and third term. The second term has the same form as the dispersive term. Thus, by using the finite difference approximation we introduce an error that looks like a mixing term. The 'dispersion coefficient' D^* for the artificial mixing equals $(h/2)\,v$, while for the physical dispersion we have $D = \alpha|v|$, α being in the order of cm's. Therefore, to prevent that artificial mixing becomes larger than physical mixing, we must use a small h. The Peclet number indicates how serious numerical dispersion is:

$$Pe = \frac{vh}{D} \tag{206}$$

For Peclet numbers smaller than 1 or 2 the error is limited. However, this leads to unacceptably small grid cells. The discussion above on numerical dispersion is far from complete. Several alternatives schemes exist that reduce the error. Nevertheless, the origin of numerical dispersion is explained: an error introduced by approximation of the advective term.

Method of characteristics.

The method of characteristics combines the particle tracking technique with a finite difference or finite element method. It uses the principle that an observer traveling with the advective velocity does not notice the advection displacement of the solutes. The particles act as traveling observers. The change in concentration as seen by these observers is described by the so-called moving or material derivative. Usually this is denoted by *Dc/dt*, but to avoid confusion with the dispersion coefficient *D* we use the notation $\bar{d}c/dt$ here. By the chain-rule we obtain:

$$\frac{\bar{d}c}{dt} = \frac{\partial c}{\partial t} + \frac{\partial c}{\partial x}\frac{dx}{dt} + \frac{\partial c}{\partial y}\frac{dy}{dt} + \frac{\partial c}{\partial z}\frac{dz}{dt} \tag{213}$$

or, in indicial notation (and after rearranging terms):

$$\frac{\partial c}{\partial t} = \frac{\bar{d}c}{dt} - v_i\frac{\partial c}{\partial x_i} \tag{214}$$

The second term at the right hand side can be rewritten. First, we know that:

$$\frac{\partial}{\partial x_i}(v_i c) = c\frac{\partial v_i}{\partial x_i} + v_i\frac{\partial c}{\partial x_i} \tag{215}$$

When we consider a steady groundwater flow or a non-steady and incompressible flow, we obtain from the continuity eq. $\partial v_i/\partial x_i = 0$. This means that the first term at the right hand side of (215) drops. Combining (214) and (215) gives:

$$\frac{\partial c}{\partial t} = \frac{\bar{d}c}{dt} - \frac{\partial}{\partial x_i}(v_i c) \tag{216}$$

Substitution of (216) into the advection-dispersion equation gives:

$$\frac{\bar{d}c}{dt} = \frac{\partial}{\partial x_i}\left(D_{ij} \frac{\partial c}{\partial x_j} \right) \tag{217}$$

Eq. (217) describes the change in concentration for a moving observer. The method is applied as follows. First, one introduces particles that will move along streamlines. The particle displacement is obtained by particle tracking. Particle tracking is a technique where the displacement of a water particle is determined by integration of the motion equations. Using vector notation the motion equations may be written as:

$$\frac{d\vec{x}}{dt} = \vec{v} \tag{218}$$

Several numerical schemes exist to integrate this set of motion equations: a simple Euler integration may do well, but better is to use Heun's rule or better still the Runge Kutta method. All these integration methods can be found in mathematical textbooks e.g. Wylie (1978).

The particles play the part of 'traveling' observers. After displacing the particles (advective step), equation (218) is solved using finite differences or finite elements (dispersive step). Because the advective term is absent in (218), no numerical dispersion occurs. A code based on the method of characteristics has been developed by Konikow and Bredehoeft (1972).

The random walk method

An alternative method to avoid numerical dispersion is the random walk method. The random walk is also based on particle tracking, but here particles represent solute mass instead of traveling observers. In the random walk method, a stochastic process is generated controlled by parameters that are chosen such that this process satisfies the transport equation. In this section, the method is explained for a uniform flow. For non-uniform flows a more formal approach is necessary, which will not be given in this syllabus.

Uniform flow

The random walk theory deals with the movement of a particle that is displaced subsequently by random steps S. It considers the probability to find the particle at time t at a location (x,y,z). Numerically we can estimate this probability by examining the frequency distribution of a large group of particles, assuming that the number of particles is large enough.

The most important parameters controlling the random movements are the mean μ_s and variance σ_s^2 of the steps S. The mean, or ensemble average, is often denoted by brackets $\langle\ \rangle$:

$$\mu_s = \langle S \rangle \tag{219}$$

and

$$\sigma_s^2 = \left\langle (S - \langle S \rangle)^2 \right\rangle \tag{220}$$

Consider a single particle in $x = 0$ at time $t_0 = 0$, displaced at t_k by a step $S(t_k)$. The position at $t = t_n$ is:

$$X(t_n) = \sum_{k=1}^{n} S(t_k) \tag{221}$$

We may write for the mean and variance of X:

$$\mu_x(t_n) = n\mu_s \tag{222}$$

$$\sigma_x^2(t_n) = n\sigma_s^2 \tag{223}$$

We use upper case X to indicate that the particle coordinate is a random variable.

For S we use a uniform probability distribution on an interval $[M\text{-}U, M\text{+}U]$ as shown in figure 34. The mean and variance of S are:

$$\mu_s = M \tag{224}$$

$$\sigma_s^2 = \frac{U^2}{3} \tag{225}$$

In figure 35 the probability density $P(x,t)$ is shown for X at $t = t_1$, t_2 and t_3. We can see the familiar bell-shape that resembles the Gauss after three consecutive steps. After n steps we obtain a probability density $P(x,t_n)$ that according to the central limit theorem can be

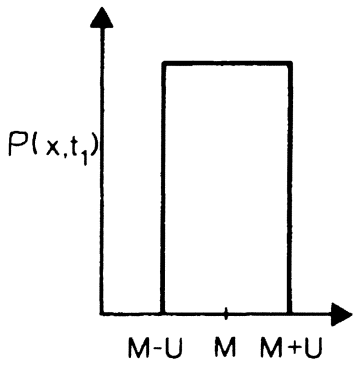

Figure 34 Probability density for a single step S

approximated by:

$$P(x,t_n) \cong \frac{1}{\sqrt{2\pi n\sigma_s^2}} \exp\left(-\frac{[x-n\mu_s]^2}{2n\sigma_s^2}\right) \tag{226}$$

for n sufficiently large. We compare eq. (226) with the solute concentration in a uniform flow (see eq. 183):

$$c(x,t_n) \cong \frac{1}{\sqrt{2\pi D t_n}} \exp\left(-\frac{[x-vt_n]^2}{4Dt_n}\right) \tag{227}$$

The similarity between (226) and (227) is clear. Writing τ for $t_k - t_{k-1}$ ($t_n = n\tau$) and using (224) and (225), we can write:

$$M = v\tau$$

and (228)

$$U = \sqrt{6D\tau}$$

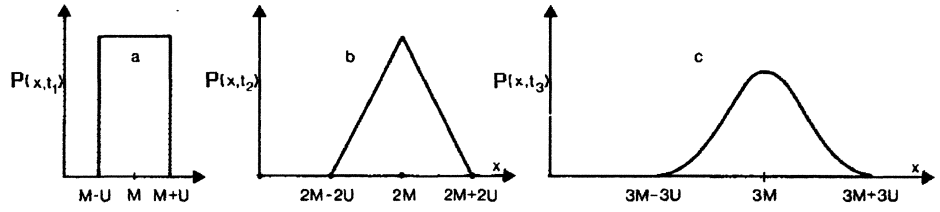

Figure 35 Probability density of x-coordinate after 1, 2 and 3 steps 2-D example

A large number of particles is considered with displacements S_i along the x_i-axis determined by:

$$S_i = M_i + U_i R_i \tag{229}$$

where R_i is a random number, between -1 and +1. For each random step a new R_i is being generated. M_i and U_i follow from (228). No advection occurs in transverse direction, so for the steps in the y-direction M is always zero. Figure 36 shows an example for a two-dimensional random walk simulation. Here, an instantaneous injection occurs, which is represented by 100 particles. The flow field is assumed to be uniform. The position of the particles is shown after 100, 200, and 300 days.

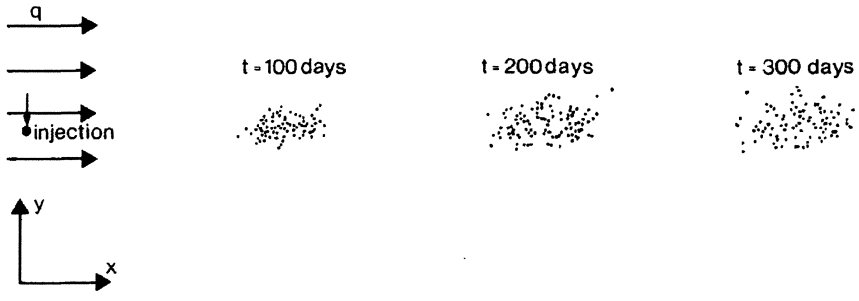

Figure 36. A two-dimensional random walk in a uniform flow

An example of non-uniform flow

The code POLLUTE (Uffink, 1990) applies particle tracking based on the random walk approach. Figure 37 (top) shows streamlines for a pumping well in a uniform flow field. Just outside the capture area a source of pollution is located. It is seen that polluted water reaches the well, though the pollution occurs outside the capture zone. This is clearly due to transverse dispersion. Although generally longitudinal dispersivity is higher than transverse dispersivity, the latter is more important since it may change the 'destiny' of the particles.

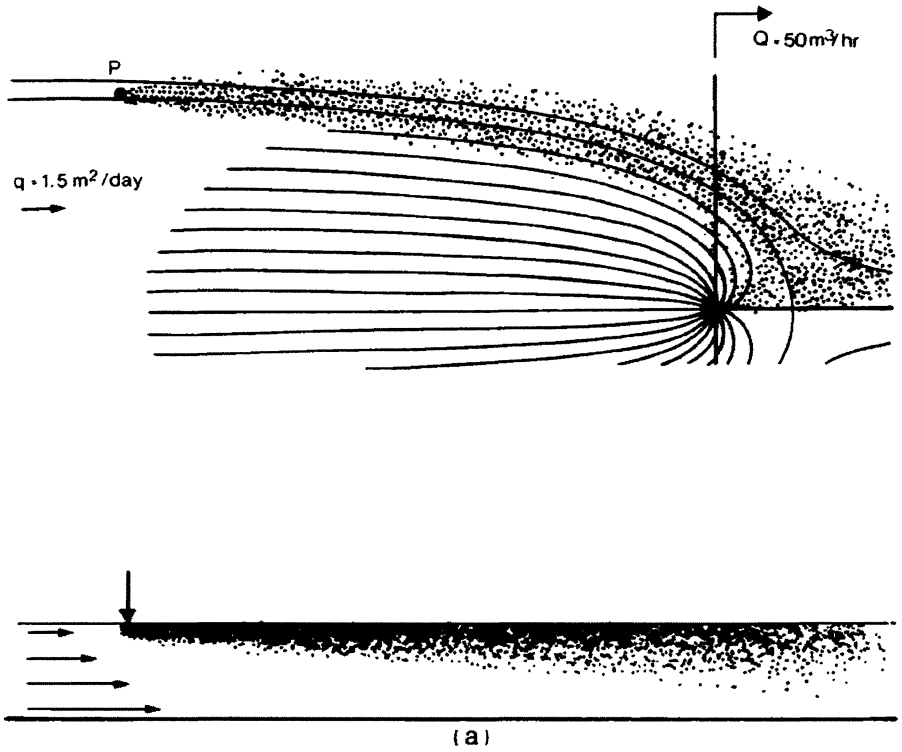

Figure 37 A two-dimensional random walk simulation in a non-uniform flow

(a) A plane view of a flow pattern for a pumping well in a uniform background flow. Outside the capture zone, at point P, a continuous pollution occurs. Due to transverse dispersion part of the pollution reaches the well.

(b) A cross section of a stratified aquifer. An instantaneous pollution (t=0) is given and the position of the particles after 1000 and 5000 days is shown. Due to transverse dispersion in the vertical direction, a number of particles migrate to the more permeable section of the aquifer where they obtain a greater horizontal displacement.

LITERATURE (part 1 and 2)

Abramowitz, M. and Stegun, I.A. 1972. Handbook of Mathematical Functions. Dover.

Bear, J. 1979. Hydraulics of Groundwater. McGraw-Hill.

De Josselin de Jong, G. 1958. Longitudinal and transverse diffusion in granular deposits. Transactions A.G.U. 39: 67-74.

Kreft, A. and Zuber A. 1978. On the physical meaning of the dispersion equation and its solutions for different initial and boundary conditions. Chemical Engineering Science, 33: 1471-1480.

Konikow, L.F. and Bredehoeft, F.D. 1978. Computer model of two-dimensional solute transport and dispersion in groundwater. From: Techniques of Water-resources Investigations of the United States Geological Survey. Government Printing Office, Washington.

Kruseman, G.P. and De Ridder, N.A. 1970. Analysis of Pumping Test Data. International Institute for Land Reclamation and Improvement. Bull. 11, Wageningen.

Li, W.H. and Lai, F.H. 1966. Experiments on lateral dispersion in porous media. Proc. Amer. Soc. Civil Engrs., 92, No. HY6.

Strack, O.D.L. 1989 Groundwater Mechanics. Prentice Hall, New Jersey.

Uffink, G.J.M. 1990. Analysis of dispersion by the random walk method. Thesis. Delft University of Technology.

Van den Akker, C. 1982. Numerical analysis of the stream function in plane groundwater flow. Thesis. Delft University of Technology.

Van Genuchten, M. Th. and Alves, W.J. 1982. Analytical solutions of the one-dimensional convective-dispersive solute transport equation. U.S. Department of Agriculture. Tech. Bull. No. 1661.

PART 3

Dike Technology

Introduction

The last millennium the Netherlands was created by land cultivation, by flood protection against sea and rivers and permanent water drainage from low land and polder areas. Large cities developed, including an intricate infrastructure of roads, railways, waterways and pipelines for sewerage, gas, and water and for underground transport. The main ports for shipping in Rotterdam and air transport in Amsterdam are a cradle for international industry and commerce. The protection of commercial and social values in the low land demand a continuous engineering effort. Tens of thousands of kilometers of sea dikes, river dikes and canal embankments, numerous sluices, bridges, harbours, tunnels, dams and closures and sophisticated monitoring and control systems form the backbone of the low land flood protection. The engineering skill could develop during centuries within a special legislative, social and political frame. The expertise has now settled in a vast range of laws, guidelines, handbooks and codes. At present new developments are required meeting the demands of the society of today. Demands related to multiple functioning and integral values. Moreover, the expectation of climate changes in terms of sea level rise, increasing rain intensity and high-peaked river discharges rings the bell for risk engineering in design and integral maintenance of water-defense structures.

History of the Dutch dike technology

Before building dikes
A large part of the Netherlands is situated under sea level. Without dunes and dikes half the country would be submerged. In general one speaks of low lands and the name "Netherlands" is appropriate. Since the last glacial period, which ended about 10.000 year ago, the sea level is rising and the coastline receding. This process took place by fits and starts. Repeatedly the sea was aggressive (transgression period), and other times relatively quiet (regression period). During the transgression periods the sea intruded deeply into the inland. During the regression periods large peat areas developed in the eroded parts (Holland, Utrecht). Natural sea walls along the coast could withstand the high storm surges, although the sea swallowed large areas. In the Roman era the possibilities for land cultivation improved and small villages arose at the borders of the peat marshes and inland creeks. One of the known gullies in that time was the Gantel running from the river Maes to the north, passing Delft. Shipping became feasible when in the year 47 the Roman warlord Corbulo ordered the digging of a channel connection to the river Rhine. Remnants of small dams and valve-sluices made from hollow trees have been found in the area. The higher dunes ascended only ten centuries ago. In the late Middle Ages the sea became more dangerous and aggressive. In the twelfth century an enormous gap was made in the Netherlands. The small lake Almere (in the Roman time called lake Flevo) was enlarged into a substantial inland sea, the Zuydersea. In that disaster many villages drowned.

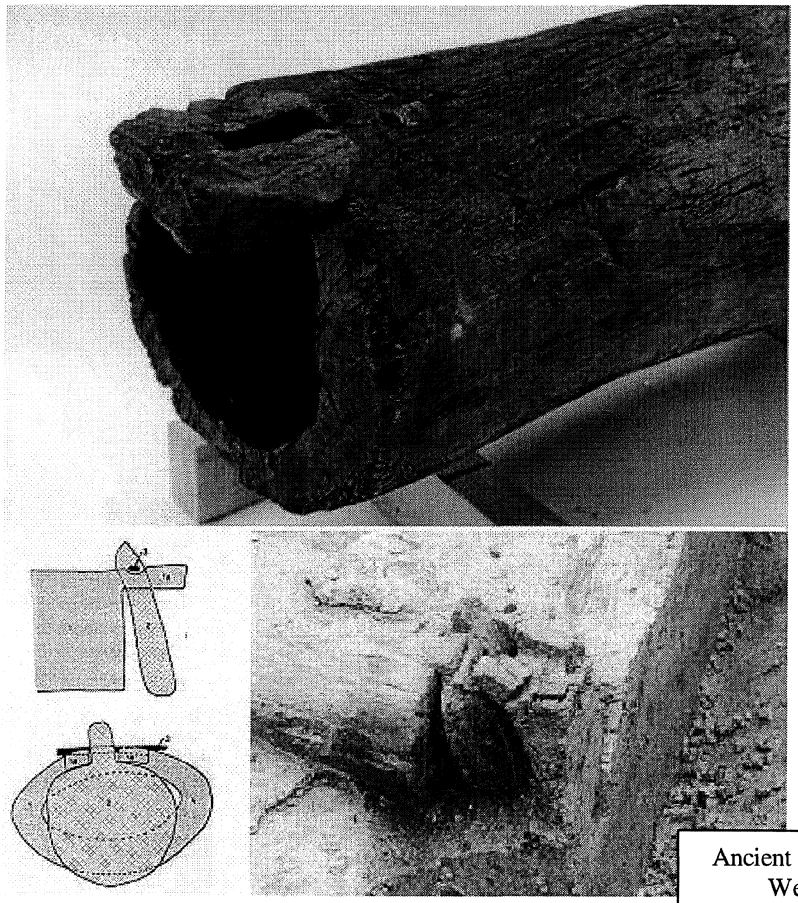

Ancient valve-sluice
Westland
Roman period

Early dike building

The oldest dike made from sods of turf was found in Friesland in 1996 and it is several hundreds meters long and dates from 200 B.C. The reclamation and exploitation of large peat-lands in the west and middle of the country created many large lakes, which are clearly shown on maps of the 16th and 17th century. In the 17th century large-scale land reclamation started to dry these lakes. Dikes surrounded low-lying areas and surplus water was drained out during low tides, or eventually by windmill power. These areas are called polders. In those times the discharges of the main rivers had increased significantly. Annual inundations and floods had serious consequences. Since the 11th century large efforts were undertaken to create defenses against the rising water. In many parts of the country dikes were build. The probability of inundation decreased and man started to settle on previously uninhabitable places. Formerly, this was only possible on hand-made mounds and sandbanks. Yet the danger of inundation was not over. Particularly, poor or unsystematic maintenance of the dikes frequently caused flooding. Pools along these dikes recall the many dike bursts. Frequently, enormous amounts of ice accumulated against the dikes causing collapse at the last. Not always was the water regarded as dangerous. In war times one breached the dikes deliberately to prohibit passage for the enemy. The Spanish and French, in particular, have experienced this strategic inundation during their invasions. The region Holland remained safeguarded against occupation. Until after the Second World War this Holland Water Line was maintained. At present, parts of it are a tourist attraction.

Land subsidence and sea-level rise

It is by no means certain that the Netherlands will always be inhabited, as it is now, by a large working population. There is evidence that a time will come when the sea will again inundate most

of the Netherlands, as they have already been on more than one occasion in the distant past. The level of the sea is rising, slowly but surely. If climatic changes should cause the polar ice caps to melt faster than at present, the rate at which the sea is now rising could increase and rapidly create a critical situation. It would only take one-tenth of today's polar ice to produce enough water to heighten the level of the sea by three meters. At present measurement indicate a rise of about 0.50 m per century. But it is not only a case of rise in sea level. Ground levels are getting lower at the same time. Besides a small tectonic subsidence, the weight of the upper layers of soil is compressing the softer peat ground underneath. And the intensified use of ground water means the ground is getting dryer, and dry soil compresses faster than wet soil. Dry peat oxidizes and vanishes. So the difference between sea level and ground level is increasing. This process proceeds with a decaying intensity, at present at a rate of about 0.50 m per century. In total, the low lands in the Netherlands may face a one-meter additional drop in the coming century.

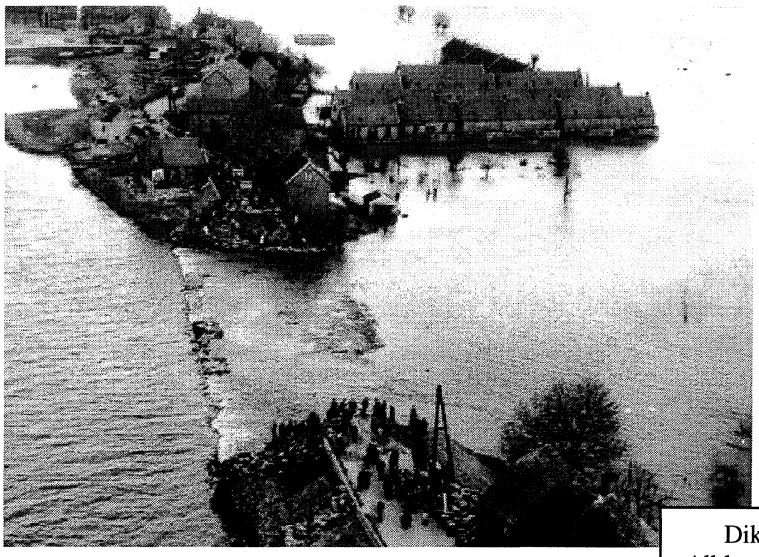

Dike breach at Alblasserdam in 1953

The Dutch approach

The method of flood defense that the inhabitants of the Netherlands have developed and applied - with varying degrees of success - throughout the centuries is dike building. Ever since the eleventh century, when the earliest primitive dikes and embankments were build, the task of keeping the hungry sea and rivers at arm's length has been a matter of dogged perseverance and trial and error. Since then the main outlines of the Dutch coast have changed very little. The Dutch success resulted in 1113 in a contract of the King-Bishop Frederik I of Bremen with a group of Dutchmen under leadership of Priest Heinricus to reclaim Northwest German lowlands in a Dutch style. Dutch engineers were invited by the Japanese Emperor (Ming dynasty) to assist in the regulation of complicated water management problems and land reclamation (Johannes de Rijke). As military history has demonstrated, the shorter the lines, the stronger the defenses. The first really major improvement in the Dutch coastal defenses came in 1932, when the Afsluitdijk (Zuydersea Barrier Dam) was build, linking the coasts of the provinces of North Holland and Friesland. This dike shortened the 1900-km coastline to 1300 km. It was a flood disaster in 1916 that gave the final impetus to the decision to link up the two coasts. After the Second World War plans were again made to improve the country's defenses against the sea and major rivers. But governments learn slowly, and it took another disaster to give the impetus to carry the Delta plan into the execution stage.

The Delta project

In February 1953 the dikes of the delta area in the southwest Netherlands were breached during a severe storm. 1835 people lost their lives and the material damage was enormous. The following Delta Act in 1956 provided for reinforcing the dikes and completely damming off the largest estuaries except for the Western Scheldt, which connects the sea with the harbour of Antwerp. In 1976, under the influence of the environmental lobby, which was then at the height of its strength, it was decided to keep the Eastern Scheldt partially open in order to conserve the tidal environment of this estuary. This was realized by building a very costly open dam. In 1983 the government wanted to cut public expenditure by back-pedaling on the river-dikes reinforcement program. There were sincere protests all round, but the most vociferous opposition came from the Water Boards, the public authorities responsible for managing the sea and river defenses. To relieve the cost of continuous inland dike maintenance the government decided to construct a moveable closure, the Maeslandt Barrier, in the main entrance canal to the harbour of Rotterdam, the only vulnerable open sea-connection left. This closure was completed in 1996. The government has kept its promise made in 1953 that the sea defenses will be of the required height and strength. A project that took 40 years! Billions of guilders have been spent on the job, and a gigantic amount of work has been done.

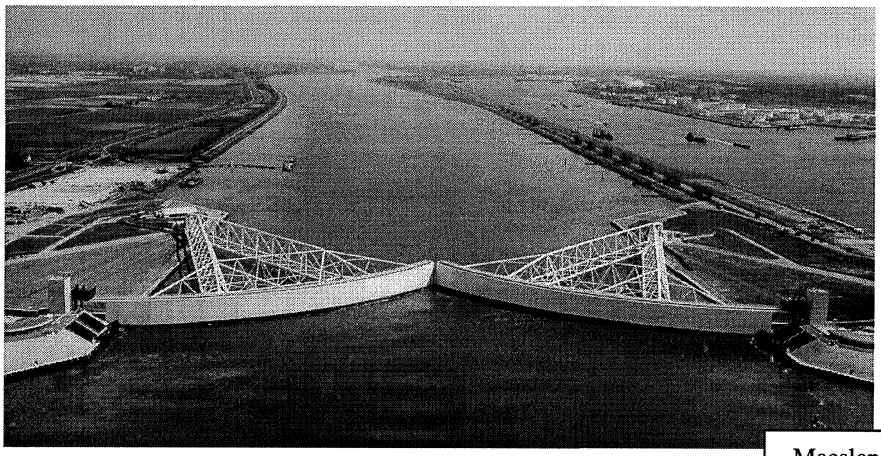

Maeslandt Barrier

The large-rivers project

The struggle against the water continues. Several hundreds of kilometer of river embankments, lake and canal dikes are waiting in turn for proper improvement. New insight uncovered the fact that design water levels have risen significantly. In the last decades public opinion changed. Landscape, nature and cultural values should be preserved in balance with safety requirements. The public protested fiercely against sacrifying old villages to dike enforcement measures. Several governmental Committees (Becht, Boertien) advised the parliament about acceptable lower norms and suggested development of sophisticated smart redesign methods and construction. Dike enforcement became subjected by law to the so-called MER-procedure (Environmental-Effect-Report Act), which delayed the river dike improvement program drastically. Water Boards did not have enough money, wanted to save maintenance costs and preferred a less expensive conventional technology. Latent danger lied in wait! When in 1995 and 1996 high-river water levels threatened again to destroy the weak dikes and a massive evacuation of some hundreds of thousands of man and cattle had to be undertaken, the government reacted quickly with special legislation. The Delta Act Large Rivers was lounged, and 370-km primary river dikes were reinforced in an accelerated tempo with a more integral design approach. With costs varying from 10 million

guilders per kilometer (conventional groundwork) to 30 million guilders per kilometer (smart methods) this project required an investment of more than ten billion guilders, completed in 2000.

What remains to be done
For the present, the attention focuses on problems related to polluted river beds, storage of contaminated sludge, restoring the natural habitat of rivers, estuary dikes, unstable sea-dike slope protection, introduction of the new integral approach and the development of a broad public and politic platform for a modern and consistent safety norm. A continuous great effort is dedicated to the improvement of the Dutch water-defense system by exploring new methods and ways, by developing new knowledge and experience and by inspiring a true and balanced political and social awareness about the matter of safety. There is consensus that a water-defense structure represents a multi-functional element, and that the safety demand – one of the primary functions - should be considered in relation with other aspects.

The philosophy behind the Dutch water-defence system

Organisation
The unique form of self-government - the "waterschap" - which may be regarded as having fostered the independent spirit of the western Netherlands, began to emerge in the first half of the twelfth century. Best translated today as "Water Board", the "waterschap" is authorized to 'manage' water levels in the western lowlands by building and maintaining embankments, dikes and sluices. The Water Boards have continued to function in much the same form to this day, when water has become a crucial factor in many aspects of life such as industry and recreation and their attendant problems, like water quality control. The Water Boards exercise authority over 1300 kilometers of sea dikes and 900 kilometers of main river dikes. It is difficult to estimate exactly the length of all the 'boezem' water embankments and dikes under Water Board control; it runs into the thousands of kilometers.
A Water Board's regulations mostly include detailed provisions for the recruiting and the functioning of the dike 'army'. When danger threatens, the 'troops' must be on alert, patrolling the dike and standing by with sandbags and equipment to stop occurring breaks. Members of the 'army' must be instilled with the need to defend their families, community and country and have an intimate knowledge of the lie of the land. By law, all male residents aged between 18 and 60 have, if necessary, to report for duty. An administrative and a technical department carry on the Board's everyday work. The administrative department prepares policy and gives legal and financial direction to all the work of water management to be carried out by the technical department. The technical department cares for the design, execution and management of dikes, pumping stations, purification plant, roads and buildings.

Dike technology
There are, roughly speaking, four types of dikes in the Netherlands: river, coastal, estuarine dikes and the embankments around *boezem*[1] waters, i.e. the canals and lakes used as storage basins to regulate polder water levels. These four types differ in design and construction. When, in the past, the authorities had to decide how high to build a dike, they took the highest known level as their standard. The many 'wielen', deep pits scoured out by water swirling through breaches, now to be seen as pools along the lines of the dikes, bear silent witness to our forefathers' failure to get their calculations right. After the terrible 1953 floods the authorities decided that the height to which the dikes ought to be raised, should conform, as far as possible, to scientifically calculated criteria. Their basic principle was not that flood water levels should never be able to exceed the height of the dike, since this would be impossible to finance, but rather that the likelihood of floodwater

[1] "*boezem* is best translated by *sinus*: any of various cavities which can contain water.

overflowing the dike would be quite small. This principle was laid down in the Delta Plan, drawn up in 1953.
In some areas, for example, an inundation risk of once in four thousand years is considered acceptable. The heights derived from these base levels are known as draft levels. Besides the draft level, the effect of surf rolling up the seaward slope must be taken into account when calculating the height of the dike crest. This seaward slope will, if properly designed, break the surf so it does not surge as high. Dikes in very exposed places are designed with a 'sill' built into the slope at storm tide level.

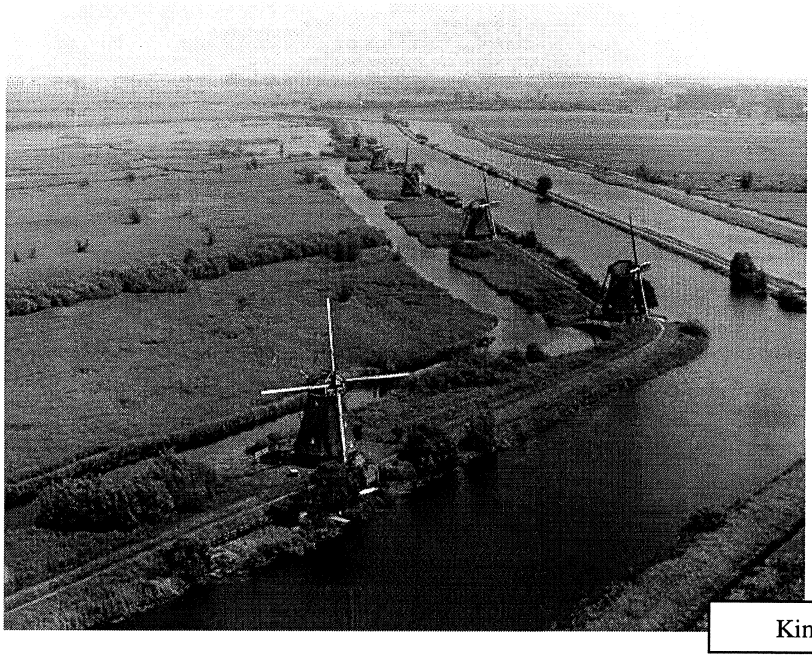

Kinderdijk

The body of the dike must be protected against the force of the waves and the effect of tidal currents. Dikes are mostly faced with turf as a basic covering. Depending on the angle of the slope and the force of the waves' attack, basalt, concrete blocks and/or asphalt are used as revetment. Fortunately, high tide levels never last long. A normal tide cycle lasts twelve hours; consequently the water hardly ever gets a chance to percolate deep into the dike so the angle of the inland slope can be allowed to be fairly steep, provide the subsoil allows for.
Water levels on the non-estuarine upper reaches of the rivers are determined by weather conditions upstream, such as rainfall and thaw. These days, the necessity of dike improvement is based on exceeding a certain river discharge occurring about once in two thousand years, a figure derived from statistics. High water on the upper river reaches lasts considerably longer than in a storm tide area, and waves do not generally play as great a role. These two factors are reflected in the design of the most desirable river dike cross-section. The riverside slope may, consequently, be angled more steeply and the revetment need not be of heavy quality as on the coast. The angle of the slope may not, however, be too steep for turf to grow properly grass cover or for a stone revetment to be satisfactorily placed. The longer periods of high water give the ground water table within the body of the dike more opportunity to rise. In order to prevent seepage, the inland side of the dike is often given a gentler slope. A peculiar phenomenon is uplift, occurring when ground water pressures are high enough to lift the covering ground layer at the lea side slope toe. In some cases local erosion arises in the form of sand boils, which undermine the foundation (piping). Another criterion is the overtopping, water gulping over the dike crest and loss of stability by subsequent erosion of the lee side.

The 'boezem' embankments are the smallest of all the four types of dike. They are mostly constructed of clay and peat. The core below the crest often consists of a great variety of materials as, in the course of time, local authorities have used sand, rubble, and clay as available to add to the dike's height. The strain which 'boezem' embankments have to withstand differs from other types of dike. They are, for example, subjected to a practically constant high water level. Their ground water table is, consequently, fairly high. The subsequent saturation forms a hazard, especially during periods of high rainfall, as earth-slides occurring along the inland slope might inflict inundation.

weed dike
1000 years old

Dike design

The most ancient dam is found at Jawa in Jordan, six millennia ago, built of earth with a protective coat of masonry. The dam of Kafara, on Wadi Garawi, south of Cairo, dates back 4.5 millennia. It is 12 meter high and 84 meter wide at the base, thus with a slope of 1:3.5, on either side, and its construction showed two distinct functions: stability by the two parallel outer embankments of rock and mortar, and imperviousness by the central filling of materials of the bed of the wadi. In ancient Netherlands a consistent dike design was developed by monks; it also consisted of the two separate functions: an impermeable part by densified sea weed, and a stabile part by an earth body of clay, reinforced by coupled rows of short wooden piles and a carefully placed stone toe against wave attack. Until 1850 dikes were made symmetric, just like the dam of Kafara, with slopes of about 1:2.5.

At present, a Dutch dike is faced with an impermeable layer. This is mostly clay but sometimes supplemented by asphalt or stone revetment. Apart from being impermeable, the layer must also resist scouring. A grass cover with a healthy layer of turf is usually sufficient for dikes on non-tidal river reaches. Dikes subjected to heavier attack are usually given a revetment of stone or concrete blocks. The core of a dike 'bears' the dike. It must provide support for the clay layer and give the whole dike sufficient volume and weight to resist the pressure of the water piled against it. It is never seen or felt, but a dike displaces horizontally for several decimeters when subjected to high water. Shear forces in the underground provide a further slip.

Other than the clay facing, the core should be permeable. Any water that does manage to percolate through must be allowed to flow away safely so the body of the dike does not become saturated and weaker, as higher saturation significantly decreases soil shear resistance. On the inland side the sand core is again faced with clay to prevent it being washed away, either by rain or by water overtopping the crest. Provision is made along the foot of the inland slope to allow water, which has penetrated the core to drain away safely. Such drainage is vital for the safety of the dike. It is to be said that many old river dikes have a clay core.

These general features may vary from place to place. Much depends on local factors, which can differ widely such as the type of ground below the dike, the materials available in the past, the pressure the dike must withstand, and the traditions and customs of the area. The evaluation of the relative importance of the various criteria of dike construction or dike improvement and subsequently the assessment of an economically optimal design is achieved by the application of the probabilistic approach, which involves a close inspection of water levels and corresponding failure

mechanisms, their probability and their coherence. This approach has gained national support in the last twenty years and has become the accepted design philosophy of modern dike design and maintenance in the Netherlands.

Dike-ring approach
The strength of the chain of defenses is never greater than their weakest link. This anticipates a safety norm of an area protected by a sequence of dikes, referred to as a dike-ring. For each zone surrounded by a dike-ring the safety norm is related to the economic, social and environmental values assigned to the protected area. The required safety of individual dike sections is related to the safety of the entire dike-ring area and to the specific role the considered dike plays. Dike technology is therefore based on three major elements:

- the safety philosophy; the dike-ring approach, application of probabilistic methods, and research on new economically and ecologically sound ways to retain the water.
- the design and the control of functions of water-defense systems; control-guidelines, technical elaboration of various failure mechanisms, and research on new ways of realisation of structural elements.
- rational maintenance; methods for preventive maintenance, methods for error detection and monitoring, and efficient techniques of maintenance.

Slope slide at Streefkerk 1984

Safety philosophy
Disasters due to technical failure seem always to be less acceptable than natural catastrophes. An important question is whether disasters due to technical failure can be avoided and whether damage due to natural catastrophes can be minimized. An observation is that in a society full with sophisticated technical systems disasters are unavoidable. Accidents are the logic consequence of a society that "lives" on technology. The discussion about safety mainly deals with probability theory and social acceptance. In a society, which is full of technical systems, there exists an apparent subjective safety during a period of absence of accidents. Safety assessment, therefore, comprises the evaluation of risk sensation involving objective personal and social acceptance and the analysis of probability of failure involving various realistic events.
The new Water Retainment Act provides the possibility to base the safety philosophy on likelihood of inundation. Three risk-components determine the relation between safety level and a probability of failure or malfunctioning:

- personally acceptable risk
- optimized economic risk
- social acceptable risk.

The personal acceptable risk is the probability of a casualty during an action while considering the personal factor (voluntary or involuntary activity). The optimized economic risk is the probability of exceeding expected cost of damage/maintenance, which may include the number of casualties in case of failure (inundation). The social acceptable risk is related to a balance of social costs and

benefits, including cultural, ethical and environmental aspects. The most critical or a combination of these three criteria is taken as the target reliability. This approach is still a subject of national debate.

Functional analysis
The basic function of a dike is to retain the water. Various elements can be distinguished each playing a characteristic role in the functioning of the dike. These principal elements are:
- the crest height should be above the design water level
- outer slope: a watertight cover in order to keep the inner groundwater table and leakage low and resistant against rapid draw down, ice and earthquake
- the core of the dike conveys the horizontal load due to the water to the subsoil
- inner slope: a permeable cover to keep groundwater table and leakage low and stable under overtopping and earthquake
- the subsoil provides suitable stability and has a water retaining function

In urban areas existing buildings in and on the dike can jeopardise its function. The watertight cover is locally interrupted, differential settlements can cause cracks and maintenance becomes more complicated. Using functional analysis two principal solutions can be defined for the situation of buildings on a dike: fully integrated, when the buildings and their foundations are also the water retaining structure or building and dike are functionally separated. This can be achieved by various measures. In these solutions the effects on the elements of the dike must be considered precisely and in detail (leakage, stability, erosion, etc.). For trees, cables and pipelines on and in the dike the same holds. Trey are admitted when they do not interfere with the principal dike function.
If the problems related to buildings and trees can be solved in a technical way, the question of control and maintenance is to be solved. When the water retaining function and building are fully integrated, frequent inspection is necessary. Uncontrolled changes in the buildings by their owners may be a danger to the dike function and a threat to the safety. It is recommended to plan the design for a period of 100 year. If buildings are outside the technical dike profile the inspection is more complicated, particularly when the fundamental elements (watertight screen) are not directly visible. The quality can be checked by adequate measurements during high waters. For buildings in the lee-side area a regular inspection of the cellars and the maintenance of the lee-side slope is required. The present-day development of houses in the river forelands, although officially prohibited, became lucrative and popular, but it raises a serious new political issue, as safety is at stake during high river discharges.

Dike maintenance
The technical component of management is maintenance, which consist of inspection, taking measures and allocation of personnel, materials and equipment. The condition of a water-defense system will degenerate in the course of time. Moreover, the loading conditions may change, and new insight in the evaluation of strength of elements in the system may arise. Two fundamental activities, periodical control and taking measures in time, form the backbone of a proper maintenance policy. Periodic control implies a comparison between actual condition and the minimum condition requested. The important question is how the system will behave until the next moment of inspection. The following steps are distinguished:
- determination of functional demands
- evaluation of the condition until the next inspection
- comparison with the norms
- choice of measures
- optimization.

Important aspects in this procedure are the concept of fixed and variable data, the degeneration model and the system of diagnosis. How to determine the actual strength of an existing dike? Pilot

studies have been performed to clarify the approach for practical purposes. Preliminary results are compiled in a concept control-guideline for a try out.

Failure mechanisms or malfunctioning

For a typical dike cross-section various failure mechanisms (limit states) can be distinguished. Traditionally, much attention is given to the mechanism of overtopping and wave overtopping. By the selection of a proper crest height with respect to the exceedence of design water levels and wave heights a safe dike profile can be accomplished. Breaches in the past have proved that overtopping was not always the cause of inundation. Piping, micro-instability and slope-slides have induced flood disasters. Also situations that did not happen so far could be added, such as collision during high water by a large ship. A similar consideration applies to structures in the dike (sluices, floodgates, locks, pumping stations), when they participate in the water-retaining function of the dike. Excess loading may also exceed the bearing capacity of the foundation causing large unacceptable displacements. History shows that structures in dikes present a major threat.

An aspect of special concern is the human factor, i.e. the manual operation of sluices, locks and floodgates during high waters. In the analysis the probability of the human error should be considered. For a dike-ring the probability of failure of any dike section and of any structure may lead to inundation of the area, as the total strength is not greater than its weakest link. Therefore, the probability of inundation increases with the length of dikes in a dike-ring.

Usually, a dike, which is well designed and performs the functions required, also satisfies the safety conditions of the various failure mechanisms. The function "water-retaining" demands a suitable "crest height", a suitable "water tightness" of the dike body and subsoil, a suitable "stability" to transfer the water level induced shear force, and a suitable "resistance" of the dike to all forces which are related to its existence (stream forces, wave loading, tourist damage). If the principal elements are well designed, i.e. the crest height, the outer slope, the core, the inner slope, and the subsoil, then the principle limit states or failure mechanisms are dealt with automatically.

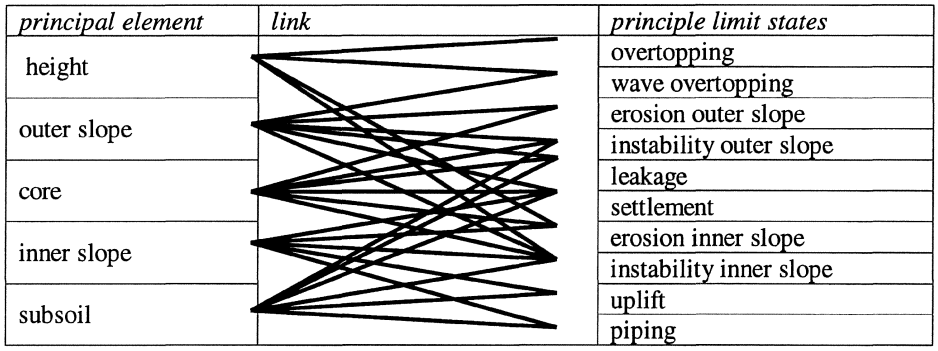

Dealing with uncertainties

The safety of a certain mechanism is controlled by investigation of the critical situation, the limit state[2], where loading and mobilized strength is in equilibrium, and any increase of loading causes collapse. Sometimes a limit state cannot be assessed by calculations. Physical tests and pilot tests or engineering experience is used. The probability method, in fact, elucidates and quantifies the relative importance of uncertainties. It is here, that conventional deterministic calculation methods apply as a cornerstone in an integral approach. Uncertainties are classified as intrinsic (related to nature: time, stochastic water levels, and space, soil heterogeneity) and epistemic (related to models: statistics, incomplete data, inaccuracy, scale). This is practically possible by the definition of dike-rings. For each ring a safety norm is determined and the safety norm of all other elements in the dike-ring system are related to this norm. The following scheme clarifies the relation between

[2] A distinction is made between ultimate limit state and service limit state. The former is the extreme situation when breaching occurs, the latter when any designed function is being jeopardized.

the conventional inundation safety approach and the new way as foreseen in the New Water Retainment Act. Four different levels can be distinguished. They are interconnected in a comprehensive manner, and they will give place to evaluating required and actual safety.

1. water level exceedence

loading = high water
strength = dike crest level
historic measure
INTUITION

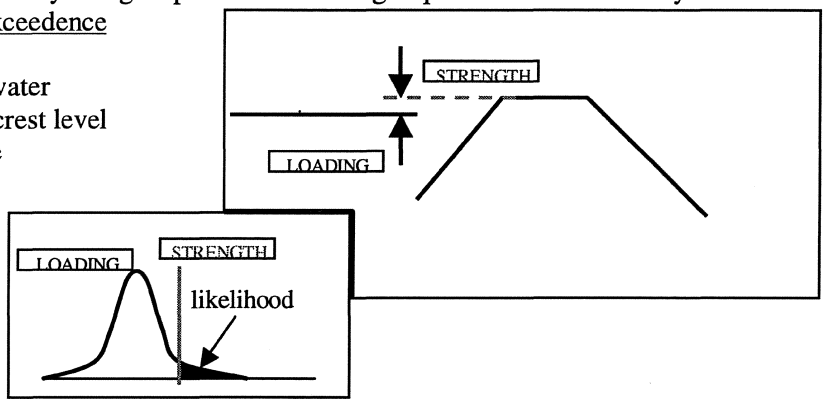

2. inundation likelihood = water level exceedence (loading) * failure likelihood (strength)

* (convolution)
each dike ring
each loading case
each failure mode
CONTEXT

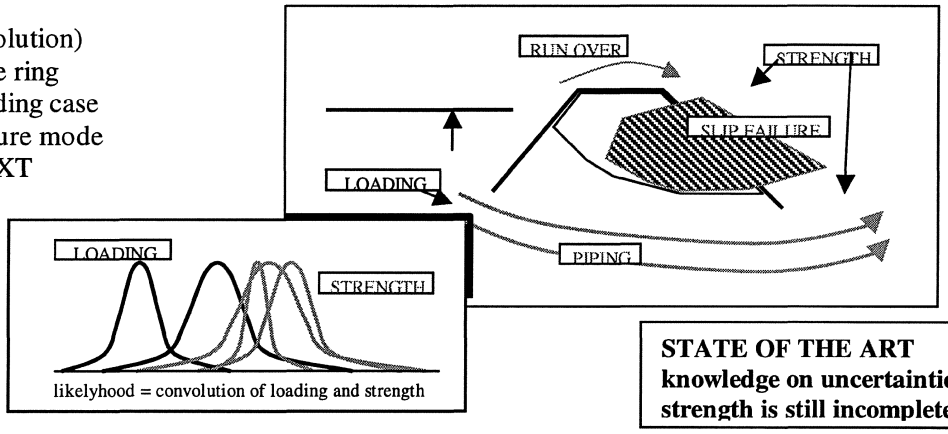

STATE OF THE ART
knowledge on uncertainties in strength is still incomplete

3. inundation risk = inundation likelihood * consequences (damage per dike ring)

consequences
integral evaluation
MEANING

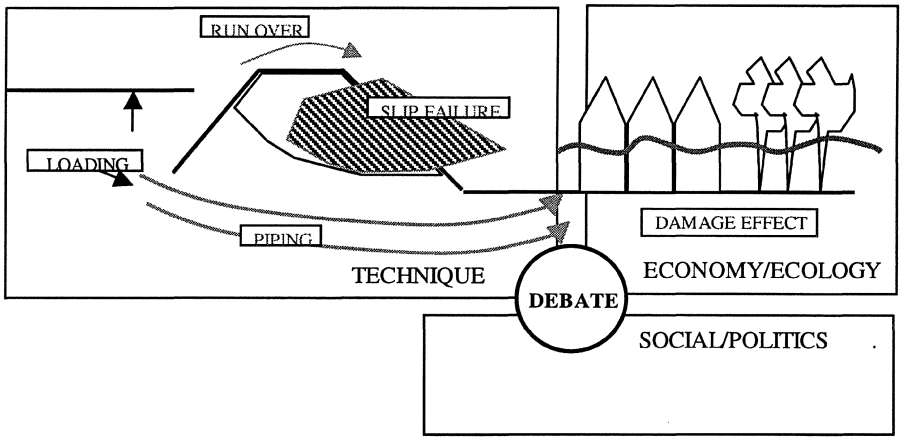

4. inundation safety = (actual inundation risk < accepted inundation risk) *(bolean)*

Hence, the inundation approach comprises the following aspects:
- loading (tides, waves, earthquakes)
- mechanisms (failure mechanisms per type of structure and element)
- calculation methods (probabilistic models, partial safety factors)
- inundation scenarios, damage evaluation
- decision models accounting for "values" and "loss" (damage).

The inundation approach requires the evaluation of the economic, social, and cultural damage caused by inundation. It requires awareness for natural and environmental values and a social acceptance of a change of the role that existing water-defence systems may play. The amount of damage is, in fact, a directive for the effort one should implement to keep the probability of this failure low. The calculation methods and decision models define how the information obtained can be used to make a rational decision.
Mere intuition and experience have in the past, addressed uncertainties. Today, it is possible to objectively quantify and qualify uncertainties for yet inexperienced but well-described scenarios. Societies do call for this approach being confronted with an increasing pressure on space allocation for work and living for a growing population with altering needs. In the coming decade the Dutch will face the issue how to handle uncertainties in an integral policy and decision making process for a prosperous development of their low lands.

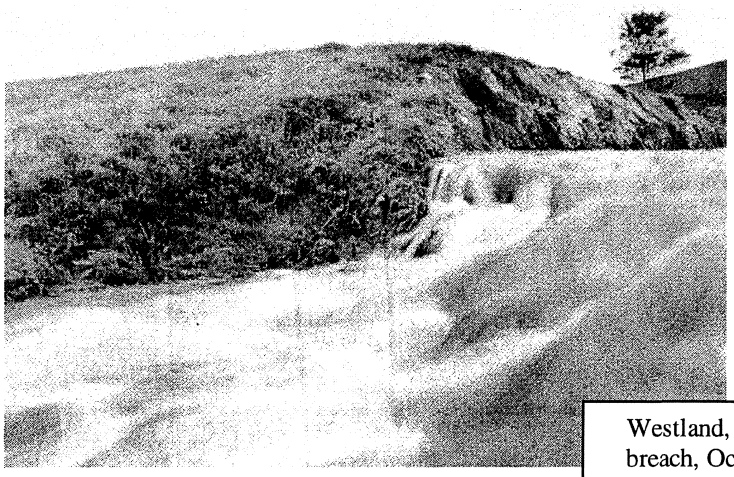

Westland, deliberate dike breach, October 4th, 1999
After severe rainfall

White spots and Dutch research initiatives.

Workshop Innovation
In 1998 GeoDelft, formerly Delft Geotechnics, organized a workshop Innovation, an open discussion in style of the British parliament. In introductions sharp inspiring statements on social versus scientific matters were prepared to stimulate a debate. Over eighty delegates from building, government and education communities participated as 'civilian' seated in the society bench, seated opposite in the scientific bench, or in the public seats behind the jury. The discussion took place between society and science, the public showed acclamation, while a small selected jury of wise and conscious men summarized and ascertained. Central themes were time and risk, essential to all our activities, as the general goal is the establishment of optimum environments in a safe and fast manner. This fits well in the geotechnical discipline with a focus on dike technology, road and railway design, underground construction, foundation and soil-quality management. The workshop Innovation evoked memorable sayings:

- The troubles are lying on the street. Due to the soft ground condition and an old-fashioned ownership structure Rotterdam is caught up with lingering costs for inefficient maintenance of roads and sewerage, spending millions of guilders yearly.

- The fundaments of soil behaviour are in dispute. Dilatancy is not a plastic, but a reversible behaviour of soil. Soft soil might be more resistant than anticipated.
- A firm coupling between social demand and scientific technology is essential. The social profit of R&D efforts can be guaranteed in the new form of collective research programs.
- Early involvement of geotechnical consultants in a design process stimulates the elaboration of alternatives in the early stage, alternatives that might accelerate the execution.
- The conventional structural separation of budget and responsibility for building and maintenance prohibits an integral approach.
- For the involvement of calculation and monitoring results as practical engineering tools it is the question how the behaviour in the building stage can be reliably extrapolated to the behaviour of the structure in use.
- The present-day monitoring is too much static. In fact, not the absolute results are important, but the effects and alterations in measured data. An appeal for dynamic monitoring.

The discussion and debate were vivid and pleasant. The mostly addressed subject was monitoring, which has a great potential seen in the light of the modern information technology. The workshop contributed to a consensus on social effects, scientific importance, objective priorities and a conscience to cooperate. Conclusions stated by the jury are:

- Monitoring in the construction and in-use stage makes sense only if possibilities exist to interfere in case of malfunctioning.
- Monitoring or close inspection by experts during the building phase may provide valuable information about weak links in the process.
- Monitoring might enhance building methods as new opportunities and innovations that may otherwise not come to life. This, in turn, may emphasize the value of monitoring.
- Parallel monitoring of specific vital parts of a construction process will provide new knowledge and information, which can be generalized in conceptual prediction models.
- Better performance later by monitoring now. Knowledge investment for future quality is a timeless wisdom.
- Knowing about or being involved in risks makes a great difference. Dedicated communication and clear information, dealing with social and political innocence and ignorance, is of essential importance. The profession needs more visualization.
- Legislation is decisive and fateful. A once fixed norm is inflexible and it can create its own rigid environment.

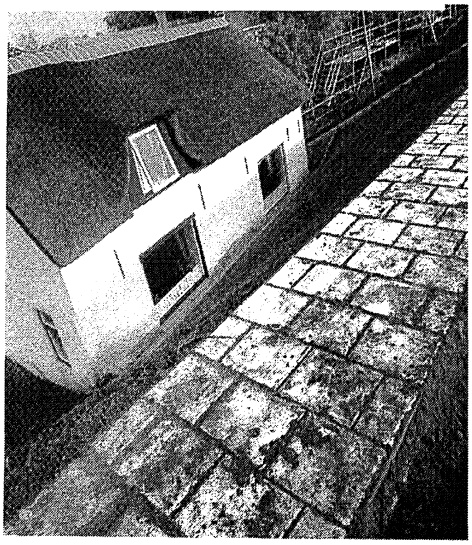

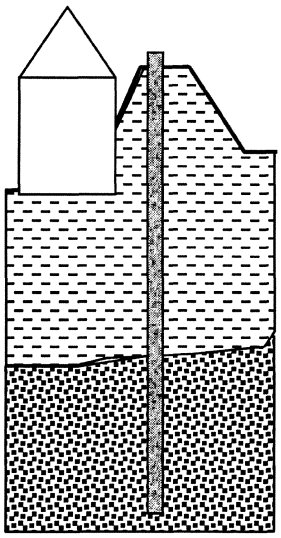

24 m concrete wall at Hardinxveld-Giessendam

One of the incentives for this workshop is a new professional role in national collective research programs enhanced by the Dutch government. Partial financing is available, 30 to 50%, for proactive and requested initiatives that focus on long term aspects of specific items, such as sustainable development of deltas (the *Delft Cluster Program*), sustainable development of the quality of the subsoil (the *Foundation Knowledge Transfer Subsoil*), underground construction (the *Center for Underground Building*), and multifunctional use of available living space (the *Center for Multiple Environmental Development*). The remainder of the financing is brought together by stakehoulders and by the research entrepreneur. Stakehoulders are the end users of the products and methodologies developed. The government itself is a stakehoulder for matters concerning safety against inundation. In the foregoing five years, 1994-1999, this new form of collective R&D programming was successful, and for the coming fifteen years new national R&D programs started recently, a great challenge for the Dutch engineering profession.

Recent achievements in knowledge and experience
Some of the most valuable achievements are compiled in comprehensive manuals and guidelines. They refer to earth and rubble stone dams and dikes constructed on soft ground.
soft ground engineering
CUR report 162 – Building on Soft Soils (1996). The Dutch knowledge and experience is gathered on design and construction of earth structures on and into highly compressible soils of low bearing capacity. The design process, including soil investigation, probabilistic methods and mechanical behaviours, is extensively discussed, and the construction, including fill materials, building methods and maintenance and management, are outlined. Special information is given on parameter correlations, software codes and validation methods of calculations, and practical cases are worked out. A special chapter deals with behaviour of peat and organic clays.
rubble mounds and stone revetments
CUR/CIRIA[3] report 154 – Manual on the Use of Rock in Coastal and ShoreLine Engineering (1991). Knowledge and experience obtained form several large projects, like the Delta Works, has been gathered by British and Dutch engineers. The manual includes data collection, design, construction and maintenance aspects. Chapter 4 describes the dynamic hydrogeotechnical stability of rubble mound structures and stone covers, in particular when exposed to wave attack and earthquakes. The manual contains various practical design concepts and formulas, and elaborated examples on the probabilistic approach. It also describes instruments and numerical tools, and the corresponding legislation.
dike technology
A long list of guide-lines and manuals, technical reports and fundamental studies is available, most of which published under the auspices of the TAW (Technical Advisory Committee for Water Defense Structures, founded in 1965), a committee that advises the Minister of Transport, Public Work and Water Management. Amongst its members resort representatives of the ministry, governmental departments (RWS, RIKZ, DWW, RIZA), the Water Boards, the provinces (IPO), the universities (TUDelft, IHE), and so-called knowledge institutes (Delft Hydraulics, GeoDelft). Technical guidelines and manuals in use are:

- Guide line River Dike Design, part I, lower river regime
- Guide line River Dike Design, part II, upper river regime
- Manual structural design river dikes
- Guide line Artifacts and Objects in on and near Dikes
- Guide line Audit of Dunes as Safe Water Defense System
- Guide line Sea and Estuary Dikes
- Manual Aspects of Clay
- Manual Asphalt as Cover

[3] CUR: Center for Civil Engineering Research and Codes (NL); CIRIA: Construction Industry Research and Information Association (UK)

- Manuak sand boils
- Guide line Environmental Effect Report
- Guide line Constructive Design
- Manual inventory and valuing LNC-aspects (LNC: Landscape, Nature, Culture)
- Guide line Water Defense Special Structures
- Guide line Sandy Coasts
- Guide line Auditing Safety
- Fundamentals for Water Defense
- Manual Water Defense Ground Structures

These guidelines are updated with a frequency of five years.
Some fundamental technical studies are:

- Waves of the Society in Hydraulic Engineering, H. Dubbelman, 1999
- Consolidation of Gassy Mud, B.G.H.M. Wichman, 1999
- Vertical Compression of Soils, E.J. den Haan, 1994
- On the Mechanism of Piping under Impervious Structures, J.B. Sellmeijer, 1988
- Rock Slopes and Gravel Beaches under Wave Attack, J.W. Van der Meer, 1988
- Advanced methods in groundwater flow computation, F.B.J. Barends, 1978

Boezem dike and groundwater flow

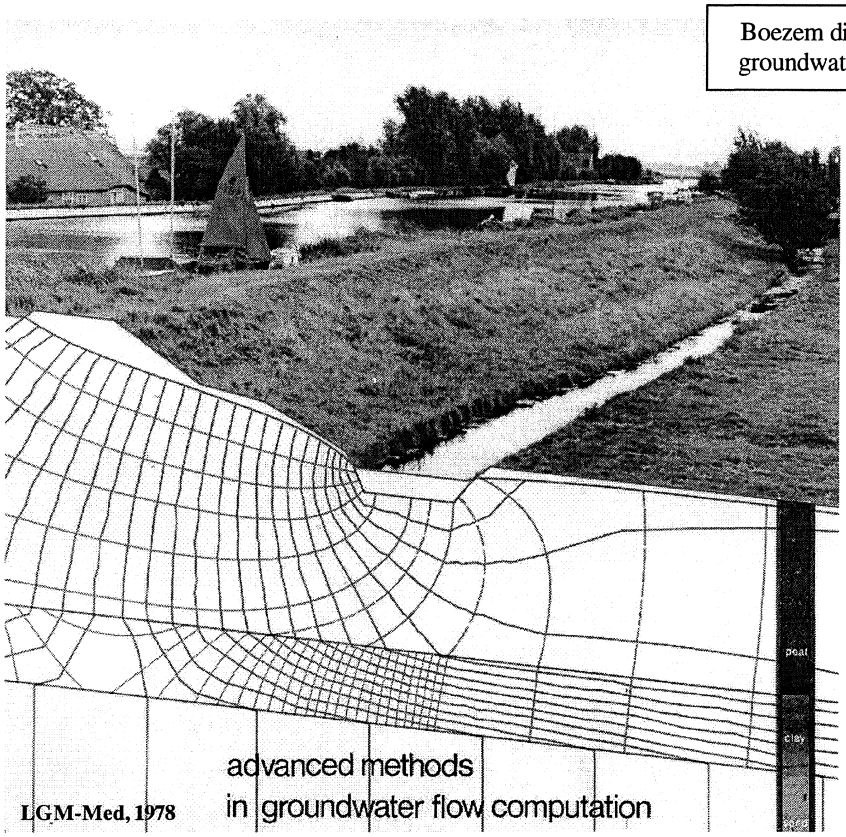

White spots
The national program WONS on research and support for water defense, with an annual budget of 25 million guilders, in the hands of the Ministry of Transport, Public Work and Water Management, covers three aspects: safety, rivers and coasts. The main issues for the coming period of five years are:

- The following efforts are planned for the aspect safety: inundation map covering the Dutch dike-ring areas with the inundation risk and the expected damage; adaptation of the guideline

Auditing Safety; the Boundary-Condition Book that contains hydraulic design conditions per dike-ring; the High Water Information system (HIS 2000) for the management task; updates of various guidelines and manuals; introduction of a safety philosophy based on inundation risks and corresponding norms.

- The following efforts are planned for the aspect rivers: improved prediction models for high water levels of the rivers Rhine and Maes; more accuracy in design discharge and water level; development of sustainability in water defense technology.
- The following efforts are planned for the aspect coasts: strategic report on dynamic coast management in relation to reclamation plans for enlarging Rotterdam harbour, building a new airfield in sea, and a wind-energy park; effects of climate dynamics on sea-level rise, currents, tides and storm frequency.
- A special effort is planned for studying the actual strength of dikes in close coherence with the national program Delft Cluster. Some locations are selected for a consistent monitoring of a dike section under (artificial) extreme conditions.

For the last subject, in a recent brainstorm session with representatives from different disciplines in the field of dike technology, the actual white spots in the present-day knowledge and experience were evaluated, with the emphasis on field monitoring. The following list shows the result, highest priority first.

Pore Pressures and the Phreatic Line in a Dike

The pore pressure is a crucial factor in the geotechnical stability, and a better prediction of these pore pressures result in higher safety. Pore pressures are also a critical factor during (re)construction of a dike. The dike composition, the soil heterogeneity and the time lapse of loading play an important role. Pore pressures should be evaluated in coherence with strength (plastic zones). Why do 'dry' dikes show slides?

Deformation and Strength

How crucial is deformation for the safety? There is a need for design norms related to deformation. What is the admissible rate of deformation in relation to safety? Do relations between strength- and deformation parameters exist and are they practically useful? There is a need for more validation of modern design and maintenance methods.

Breach Growth, Residual Strength, Transsafety factors

A recent study on breach growth of sandy dikes has provided a model of the so-called transsafety factor, i.e. the span between the initiation of failure and the complete breach. A study on the breach behaviour of a clay dike is due. Is instability of the inner slope a safety problem? A plead for a historic dike failure inventory with the emphasis on technical data in order to support information on actual strength. Modeling methods for large deformation and continuing failure.

Rigid Structures

What are the norms for sheet piling deformations when used against leakage? Measurement of the actual ground stresses (horizontal) is requested. The evaluation of existing alternative dike designs should get attention.

Overtopping and Infiltration (also Precipitation)

What is the contribution of surface, root-zone, and subsoil transport in the overtopping and infiltration through and on the lee-side slope of a dike? What is the sustainability of a grass cover? How to get a grip on the process of saturation and weakening of a dike body?

Erosion Outer Slope

What is the effect of rapid draw down in relation with the behaviour of the phreatic line for different types of revetments? Norms on this phenomenon do not exist.

Uplift and Outburst

The existing theory on this phenomenon should be tested in practice. By purpose creating some leakage just behind the dike inner toe, is that a useful remedy?

PART 4

Coastline Technology

Introduction

By the term hydro-mechanics of porous media a distinction is made with regard to standard geomechanics. It refers to the mechanical behaviour of porous structures when exposed to hydraulic loading, such as waves. Two facts make a difference: (1) multi-phase mechanics: air, water and rock/soil play a role; (2) dynamics: critical situations occur during dynamic loading. Both aspects render common geotechnical methods applicable with special considerations, which will be explained in this chapter. For common geotechnical methods reference is made to geotechnical handbooks (Verruijt, 1993; Van der Veen, Horvat, Van Kooperen, 1992; Lambe & Whitman, 1969; Terzaghi, Peck & Mesri, 1996).

Wave loading generates normal stresses (pressures) and shear stresses in the porous structure. The water phase in the porous structure can sustain pressures well, but not the shear stresses. For that part the granular skeleton of the porous medium gets involved. When shear stresses in the granular skeleton surpass a limit strength, the skeleton will slide and fail. This limit strength depends on the actual stress in the granular skeleton.

For the evaluation of hydro-mechanics in porous media the distinction between stresses in the granular skeleton and pore pressures is essential. The intergranular stresses determine the functioning of the structure. In hydraulic engineering the granular response is often disregarded resulting in incomplete understanding of the real process and in overestimation of the functionality. The procedure to assess the hydro-mechanical behaviour is compiled in the following table and checklist. The table contains the most essential processes and some characteristic parameters. The checklist refers to the most essential steps in an evaluation procedure.

Table I

inputdata		
GEOTECHNICAL DATA	HYDRAULIC DATA	EARTHQUAKE DATA
weight, geometry	set-up, waves	impacts, shakes
process		
internal flow by waves		accelerations
pore pressures		behaviour
response		
	STATE OF STRESS	
result		
STABILITY	DEFORMATIONS	DETERIORATION
slip surface	settlements	erosion
parameters		
mass	permeability	strength
grain type	storativity	stiffness
porosity	cohesion	dilatancy

CHECKLIST

Determination of:

- critical cross-sections, geometry, material parameters
- the design wave loading/design earthquake loading
- pore pressures (seepage pressures), transmission, internal setup
- the hydraulic stability of filters
- excess pore pressures
- the stability of the elements/structure
- settlements
- the dynamic stability
- residual deformations

Some of the above items are addressed in this chapter.

PARAMETERS

The hydro-mechanical processes are assessed by simulation techniques, by using models. Information is required to operate the models and formulae. Selection of critical cross-sections and geometry of material layers is one part. A provisional list of other material parameters, is presented below.

symbol	name	remark
D_i	grain size [m]	i (%) fraction < D
ρ	specific density [kg/m^3]	density of the bulk material
ρ'	specific density [kg/m^3]	density of granular material
ρ_w	specific density [kg/m^3]	density of water
γ	specific weight [N/m^3]	$\gamma = \rho g$ (also for γ' and γ_w)
S_h	grain shape	ratio maximum/minimum diameter
R_f	surface smoothness [mm]	irregularities grain surface
S	strength [N/m^2]	breaking strength grain
c'	cohesion [N/m^2]	interlocking, cementation
n	porosity	volumetric density granular skeleton
σ'	intergranular stress	
k	permeability [m/s]	$k(D, n, S_h, R_f,$ pressure gradient)
φ	friction angle	$d(R, n, S, \sigma', D)$
ψ	liquefaction potential	rate of excess pore-pressure
n_c	critical density	porosity at zero dilatancy
G	shear modulus [N/m^2]	$G(n, \sigma', S)$
K	bulk modulus [N/m^2]	$K(n, \sigma', S)$

Some additional specific information in relation to the above mentioned parameters are important for porous mound marine structures and are discussed next.

Cohesion c'

Cohesion is related to the fact that removal of a particle at zero effective stress requires some effort. For rock and artificial armour units cohesion is related to the interlocking. For sand cohesion is negligible. For clay it is related to electromechanical forces at microscale. Kobayashi (1987) suggests that for rock the use of an apparent cohesion to account for the dependence of friction to isotropic pressure or for the

overburden pressure (sand) should be assumed, particularly when applying a Bishop stability analysis. An average value for this apparent c' is 20 kN/m^2.

Porosity n

The porosity depends on the packing of the particles (skeleton structure). An average porosity value for large well-placed normally graded stones equals 42%. Randomly placed it may vary between 30% and 50%. In wide-graded mixtures this range is even larger. It is not practically possible to determine the porosity of existing coarse granular marine structures in a direct manner.

Permeability k

The hydraulic permeability depends on the flow regime (linear, turbulent). An approximate formula for linear flow is

$$k = 0.002 \frac{n^3 D^2 g}{(1-n)^2 \nu}$$

which is valid for uniform gradation with $D_{50} < 0.01$m. Here, ν is the kinematic viscosity of water, and g the gravitational acceleration. Hannoura & Barends (1981) describe various formulae. The apparent permeability is related to D^2 for linear flow and to $\sqrt{D}$ for turbulent flow (Fig. 1). The regime of flow

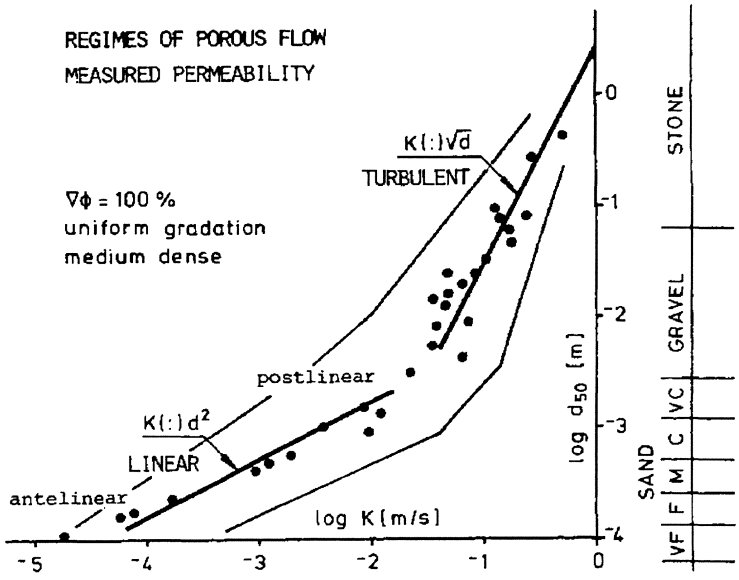

Fig. 1 Permeability versus grain size

depends also on the actual pressure gradient, which may vary in space and time (waves). Scaling problems are unavoidable in physical modelling.

Friction angle φ

The granular friction angle is a material constant for sands in the range of 35° to 45°. For stone/rock media the actual friction angle depends not only on various material characteristics, but also on the actual stress. Barton (1981) suggest:

$$\varphi = \varphi_0 + R\log(S/\sigma')$$

where φ_0 is a basic friction coefficient between polished surfaces, R a factor dependent on type, shape and packing, S the material strength and σ' the actual effective stress. φ_0 is in the range of 27° to 33°. The value for R is given in the diagram in Fig. 2. The effective stress can be determined by standard methods (stability or deformation models).

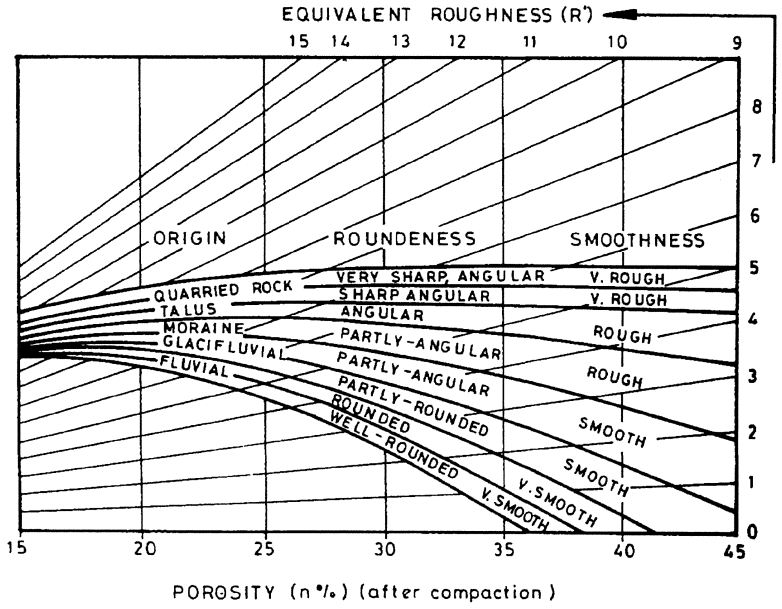

Fig. 2 Equivalent roughness R (Barton 1981)

Dilatancy

The sensitivity of a granular material to become liquefied is expressed by the so-called liquefaction potential. The liquefaction potential can be obtained by special laboratory tests (cyclic shear and cyclic triaxial tests) on samples from the site at various (manufactured) densities. Results should to be calibrated versus the in situ density. Excess pore pressures arise depending on the drainage capacity. Particularly fine loose sands ($D_{50} < 300\ \mu m$) are sensitive to excess pore pressure generation.

SCOPE OF HYDRO-DYNAMICS IN POROUS MEDIA

Hydro-mechanical aspects in porous media are important for those circumstances where the construction will not function properly, referred to as failure states. The manner in which such a state can occur is called a failure mechanism. Two major geotechnical mechanisms of a porous structure under dynamic loading are distinguished: excessive deformation and erosion of materials. Each mechanism is characterized by different aspects. The aspects are evaluated by applying models and formulae.

mechanism	aspect
excessive deformation	porous flow
	shear strength
	liquefaction
	accelerations
	excess pore pressures
	settlement of the fill
	residual deformation
erosion of materials	filter gradation
	change of material properties
	dynamic gradients
	local stability of elements

MODELLING AND SIMULATION

Models can be distinguished with respect to applicability, reliability, cost, sophistication, user-friendliness and accessibility. It is not possible to give a complete list of models, or to give a detailed picture of a particular model. Some general aspects are discussed and references are mentioned.
Four types of models (methods) are distinguished:

- sophisticated computer models, which provide a complete solution,
- uncoupled computer models, which solve a porous flow problem or a deformation/stability problem,
- simple models (hand-formulae) for particular phenomena, and
- engineering experience (intuition).

Loading

Geotechnical aspects of porous-mound marine structures concern the mechanical behaviour of rock/soil and the foundation being subjected to weight, to seepage forces, to pore pressures and to accelerations caused by waves and earthquakes. Wave pressures on the structure are usually measured in hydraulic models. The design loading essential for geotechnical failure is usually the maximum loading occurring during the lifetime of the structure. One could also design for a slightly lower load and accepting a certain amount of (repairable) damage. For the assessment of an optimum, most reliable and economic solution one may use probabilistic methods. The methods that are being discussed fit this purpose. For a probabilistic approach the probabilistic distribution of loading and the stochastic variation of material and geometrical parameters is required (CIAD 1985).

Geomechanical principles

The mechanical behaviour of a two-phase material (fluid and grains) is determined by loading (action) and by reaction, in terms of forces. In a porous medium the intergranular forces acting at the grain contacts are represented by the so-called intergranular or effective stress (σ', τ). This stress is equal to the average of all intergranular forces. It has normal and tangential components. Fluid pressures (p) in the pores present another force. It has normal components only. The reaction to a loading, expressed in terms of the total stresses ($\sigma = \sigma' + p$), comprises effective stresses and pore pressures. Because pore-pressure gradients cause flow, which in turn change the pore pressures with time, the part of the reaction by the pore pressures changes in time. Hence, effective stresses will vary to compensate for the

change in pore pressures. Deformations corresponding to these changing effective stresses are therefore time-dependent.

If the individual grains are relatively rigid, Terzaghi's effective stress rule applies: for normal stress components: $\sigma = \sigma' + p$, and for tangential stress components: $\tau = \tau'$. For example, the limit stress state along a slip failure surface is expressed by: $\tau = c' + (\sigma - p) \tan \varphi$ (Mohr-Coulomb criterion). The fact that p appears in the formula clarifies the importance of the flow field for the actual state of stress.

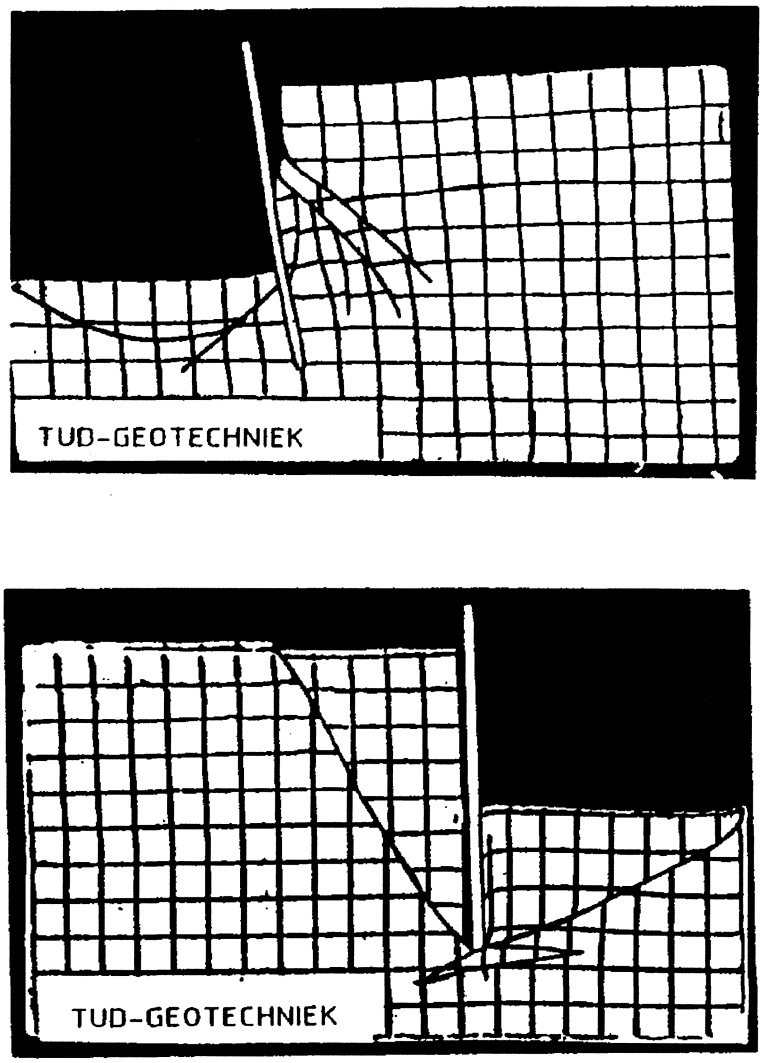

Fig.3 Geo-centrifuge

Modelling facilities

The state of the art assessment of the stability mainly consists of numerical methods varying from simple empirical formulae to sophisticated computer simulations. Physical model testing of geotechnical stability aspects is rarely performed because of difficulties to cope with non-linear behaviour and scale effects.

The description of physical processes with formulae, physical or numerical models, with graphs or engineering intuition can provide realistic approximations. The purpose of using a model is to optimise the design or a particular element of the structure.

It is difficult to make observations of hydrodynamic processes in a porous medium. Such a medium is not transparent. Beside measurement of pore pressures the response of the granular body should be recorded. However, the behaviour of one particular pore or one particular grain is not necessarily characteristic for the overall behaviour. In model studies not all scale effects can be accounted for simultaneously. An important geotechnical scale-effect that is difficult to match is the dependence of strength and stiffness to the absolute effective stress. A promising facility which could correct this deficiency is geo-centrifuge testing.

For the simulation of hydro-mechanical aspects empirical and numerical methods are common. The empirical methods are simple formulae taken from geotechnical practice and adjusted for the maritime environment. Numerical methods comprise computational models, suited for a schematic structure. Numerical methods have become common use in the last decade. In numerical models there are no scale effects, but a proper mathematical formulation of the material behaviour and an accurate solution procedure are a problem.

MATHEMATICAL BACKGROUND

The essence of numerical modelling is the mathematical description of the physical processes. A survey is presented in the form of basic equations and rules. Three media are involved: air, water and rock/soil. The influence of air is important because its entrainment affects compressibility and hence impact pressures. Practical information about air effects is limited.

Pore-water mechanics

For water and rock/soil two interrelated equations of state (mechanical equilibrium) are involved. The equation of state of the pore water yields (action = reaction):

$$-np_{,i} - n\rho g z_{,i} = n\rho \dot{v}_i + n^2 \rho g \frac{(v_i - u_i)}{k} \qquad (1)$$

pressure gradient — gravity — inertia — interaction

Here, v and u are the velocity vectors for the pore fluid and the granular matrix, respectively. The subscript i represents a coordinate direction. If preceded by a "," it is a partial derivative. The dot '°' above a variable represents a time-derivative:

$$\dot{v}_i = cv_{,t} + bv_j v_{i,j} + a\dot{u}_i \qquad (2)$$

local — convective — interaction

in which c includes virtual mass effects ($c > 1$) related to the unsteadiness of flow, b is the momentum distribution coefficient, and the last term represents mass effects in the flow field because of the presence of the granular phase. The last term in equation (1) includes viscous effects at pore size dimensions.

Granular matrix mechanics

The pore pressure p and the porous matrix velocity u are important to the deformation behaviour of the granular skeleton, which is described by an equation of motion for the porous matrix. This equilibrium is governed by the second equation of state (action = reaction):

$$-(1-n)p_{,i} - (1-n)\rho' z_{,i} = (1-n)\rho' \dot{u}_i + \sigma'_{ij,i} - \frac{n^2 \rho g}{k}(v_i - u_i) \qquad (3)$$

pressure gradient — gravity — inertia — effective stress — interaction

For the inertia term an expression like equation (2) can be formulated. Beside the two equilibrium equations the conservation of mass and material behaviour are required to complete the mechanical description. For a rock/sand granular media the individual grains are considered incompressible. For high stresses this assumption has to be reconsidered because it leads to other relations. The pore-water mass-conservation equation yields:

$$(\rho v_{,i})_{,i} + (n\rho)_{,t} = 0 \qquad (4)$$

in/out flow — storage

A compressibility law for the pore fluid can be introduced accounting for the presence of entrained air.
A stress-strain constitutive law describes the relation between the porous matrix stresses and the deformations (elastic, plastic, creep). For practical application rigorous concessions are made with regard the stress-strain behaviour, for example linear elastic or elasto-pure-plastic. Equations (1) to (4) represent a complete description of the mechanical process in a saturated rock/soil porous medium subjected to dynamic loading. Sophisticated numerical models exist covering these equations. In most applications much simpler approaches will do. Simplification is possible when interaction is disregarded. Then the porous flow is independent from the porous matrix behaviour. The opposite, however, is not the case: the effective stress depends on the pore pressure in all cases.

Consolidation, liquefaction and porous flow

Introduction of the filter velocity: $q_i = n(v_i - u_i)$ and a potential function: $\rho g \Phi_{,i} = p_{,i} + \rho g z_{,i}$ renders equation (1) into a familiar flow law:

$$\Phi_{,i} = -cq_{i,t} - \frac{q_i}{k(|q|)} \qquad (5)$$

gradient — unsteadiness — Forchheimer/Darcy

Substitution into the conservation equation (4) disregarding the unsteadiness yields after some elaboration the so-called storage equation:

$$\left(\frac{K}{\rho g}\right)\Phi_{,ii} = n\beta\,\dot{p} + \dot{e} \qquad (6)$$

The term e represents volumetric strain. It is important for soft slowly-draining layers (consolidation), for example in the foundation, and for loose sand deposits, which may show dilatancy. Then the last term of (6) is replaced by $-n\psi$, where ψ is the liquefaction potential. If e is assumed constant and the compressibility of the pore-water is disregarded ($\beta = 0$), the familiar equation for potential flow remains.

Wave transmission

In the case of a phreatic surface (internal water table) the motion of this surface under time-variant loading has to be considered. Local flow and storage determine the position, mathematically described by the so-called moving boundary condition. Saturation, airflow, and capillarity complicate the simulation of phreatic motion. In coarse porous media the unsteadiness and the inertia effects become significant. A simple way to address this phenomenon is by the averaging and integration of equation (1) and (4) over the vertical coordinate (like the shallow wave approach), and disregarding the interaction with the skeleton deformation. The following equations are obtained:

$$nc_m(v)_{,t} + v(v)_{,x} = -n^2 g(c_p D)_{,x} - \frac{n^2 g v}{k} \qquad (7a)$$

$$nD_{,t} + (Dv)_{,x} = 0 \qquad (7b)$$

where D is the local water depth and v the mean velocity, c_m and c_p are correction factors for vertical mass and pressure distribution, respectively.

Simple approach

Simplification of the equation of state of the granular matrix is obtained by adding equations (1) and (3) while disregarding inertial terms. The result is:

$$-p_{,i} - \rho'' gz + \sigma'_{ij,i} = 0 \tag{8}$$

with

$$\rho'' = n\rho + (1-n)\rho'$$

or with Terzaghi's rule :

$$\sigma_{ij,i} - \rho'' gz_{,i} = 0$$

In a practical approach the stress field is simplified rigorously by only considering vertical stresses: a direct relation between local stress and overburden:

$$\sigma_{zz} = \rho'' gz \tag{9a}$$

and by adopting a simple stress-strain law, assuming negligible deformations until a failure state given by Coulomb's law:

$$t < c' + \sigma' \tan\varphi = c' + (\sigma' - p)\tan\varphi \tag{9b}$$

where c' is the (apparent) cohesion and φ the internal friction angle.

MODELS

Sophisticated models

Sophisticated models deal with non-linear multi-phase deformation and dynamics. The core of the model is the solution of equations (1) to (4) simultaneously with appropriate constitutive relations and initial/boundary conditions. Complicating features are the formulation of non-linear behaviour and dynamic interaction, the determination of the initial state and the dynamic effect of air. Sophisticated models are applied in special situations: for unique or large structures, when a high degree of safety is required, and for the qualitative understanding of certain phenomena. The application of sophisticated models is relatively costly. It requires an extensive parameter collection (site investigation and laboratory testing). The results of numerical models should be validated by physical modelling. A sophisticated model is the TITAN code (Hölscher, 1995). It is suited to simulate non-linear dynamic behaviour of two-phase soil structure interaction utilizing the finite element technique. A Darcy-Biot approach is used for the water-soil interaction. The pore-water is compressible. Non-linear soil deformation behaviour is implemented. The code is tested and applied to various comprehensive dynamic problems.

Simplified (uncoupled) models

The behaviour of the water and the rock matrix can sometimes be separated, which simplifies the modelling significantly. For some phenomena a static geotechnical approach is sufficient, such as for settlements of the subsoil. For structures in a maritime environment the dynamic character of wave loading or earthquakes is essential. Uncoupled models simulate the porous flow without consideration of the influence of the rock/soil deformation, or they simulate the stability with a simplified pore pressure field.

Porous flow

Wave loading generates internally a pore-pressure field. Differences in pore pressures generate porous flow. For the determination of effective stresses the internal flow field must be known. The flow in coarse porous media is non-linear (turbulent). A moving boundary represents the fluctuating water table inside the structure. For mainly horizontal flow the equation (7) can be used. Specific features are the precise boundary conditions: the moving water table, overtopping, air entrainment, and the formulation of the wave action on the slope. Few models suited for wave-generated dynamic porous flow are known,

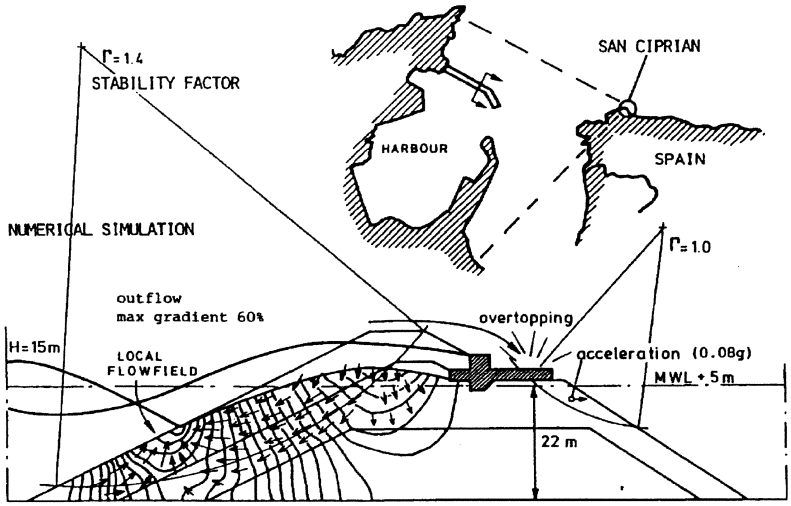

Fig. 4 Simulation of porous flow field by MBREAK

one of which is the MBREAK code (Hölscher & Barends 1990) and the ODIFLOCS code (Van Gent, 1972). An application is shown in Fig 4.

Deformation

The deformation behaviour of rock and soil is typically non-linear and irreversible. It is not easy to find a simple proper description of this behaviour. Field and laboratory tests are indispensible for the characterization of the soil/rock behaviour. The deformation can be obtained in a semi-uncoupled fashion. The pore-pressure field must be known. Simulation of deformations of a porous mound structure itself is seldom performed. Most deformation takes place during construction. For large structures deformation analysis is important. Settlements of compressible layers in or under the structure due to the overburden weight are a common feature in soil mechanics practice (consolidation). Various methods and models are available. Retarded settlements can be expected. Non-linear behaviour must be used to model squeezing (plasticity).

Stability

Effective stresses are responsible for deformations of the granular matrix. Significant deformations may occur in a narrow band, a slip surface conditioned by shear strength and kinematics, or deformations may occur throughout the structure (plastic strain). Various numerical models dealing with elasto-plastic

deformations can handle these phenomena. Models suited to simulate two-dimensional elasto-plastic consolidation are few in number.

Liquefaction

Dilatancy expresses a volume change of granular material under shear deformation; dilatancy (increase) and contractancy (decrease). This volume change is related to a change in the granular structure, by sliding and rolling of the particles in a different composition. Because water, which is trapped in the pores, cannot be expelled immediately, excess pore pressures are generated, negative for dilatancy and positive for contractancy. At the so-called critical density the material is volume constrained; then the shear deformation just does not cause a pore-volume change. The sensitivity to dilatancy-contractancy depends on the actual in-situ density; in fact on how much the actual density differs from the critical density.

In an ultimate state the skeleton structure collapses. Particles are freely floating in a pore fluid that does not fit in the available pore volume. This is a state of so-called liquefaction; a thick fluid without significant shear resistance appears, sometimes suddenly. The character of this phenomenon depends on the type of loading. A sudden loading (earthquake, solitary wave) may cause a rapid decrease of pore volume and a corresponding decrease of shear strength due to excess pore pressures, in less than a second. The dissipation of the pore pressures may take some minutes or more, and in the intermediate period catastrophic consequences may occur. Also constant cyclic loading may cause slow build-up of excess pore pressures with similar consequences. Both situations may occur simultaneously.

The suggested assessment of wave-induced liquefaction of seabed sand is according to the state of the art (Seed & Rahman 1978) referred to as the uncoupled approach. In the uncoupled approach the phenomenon is divided into two interrelated problems: (1) the wave induced state of stress without cyclic excess pore pressures, and (2) excess pore pressures by the cyclic stress ratio including dissipation. The actual liquefaction potential can be determined when the actual porosity and the critical porosity (at zero dilatancy) are known. The first one has to be determined at the site the second in the laboratory. A practical method is described (Barends & Calle 1985). It is particularly useful at the toe of a coastal defence structure, where local failure subsequently jeopardizes the entire structure.

Dynamic effects

During wave impacts and earthquakes the changes in rapid loading changes induce inertial effects in the pore fluid and the porous matrix. In some cases accelerations have to be taken into consideration. For the dynamic reaction, whether in the pore-water or in the granular skeleton, the permeability plays a significant role (Barends 1985). Realistic behaviour under earthquake loading can be obtained by a dynamic model based on a consistent stress and deformation state. Fig. 5 shows the result of such an analysis where the residual deformation has been calculated as the result of a complete earthquake loading. For coarse porous media the earthquake stability analysis can be employed without taking the pore water weight into consideration. This is permitted, because the sliding soil mass will not convey the pore water in its motion. This approach yields a reduction of the driving momentum.

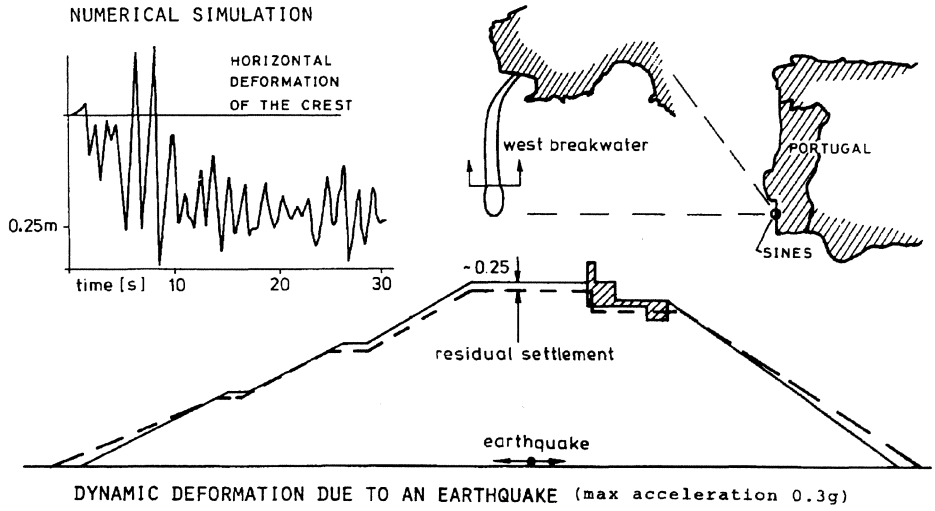

Fig. 5 Simulation of earthquake response

SIMPLE MODELS (FORMULAE)

Wave penetration/transmission

Wave loading causes time-dependent porous flow. The time dependency is due to storage. One kind of storage occurring in coarse granular media is phreatic storage. The storage acts as a damping mechanism which attenuates the wave effect inside the structure. A formula is derived based on conservation of mass and on a simplified flow field. The volume of water penetrating equals the volume of water stored:

$$Qdt = \frac{kAH}{\lambda} dt = nH \frac{\lambda_{t+dt} - \lambda_t}{2} \qquad (10a)$$

which gives:

$$n\lambda_{,t} = 2\frac{kA}{\lambda}$$

and integrated:

$$\lambda = \eta\sqrt{\frac{kAT}{n}} \qquad (10b)$$

where λ is the penetration length [m], η: parameter dependent on the loading (2.0 for a sudden constant water level change, 0.5 for cyclic water level changes), A: drainage surface through which water seeps [m], and T: elapse time for a sudden constant water lever change or period of cyclic loading. By this formula the significance of rapid or slow varying wave loading for the geotechnical stability can be evaluated. For coarse sand with $n = 0.20$, $k = 0.0001$ *m/s* and $A = 10$ *m*, the following is found:

water waves	$T = 10$ *s*	$\lambda = 0.11$ *m*
tides	$T = 12$ *hr*	$\lambda = 7.35$ *m*
rain river (constant)	$T = 3$ *day*	$\lambda = 72.00$ *m*

Internal phreatic set-up

The slope of a porous marine structure (rubble mound breakwater) subjected to waves, swell or tides represents a geometric-non-linear effect. The inflow surface along the slope at the moment of a high level

is larger than the outflow surface at the moment of a low water level. Moreover, the average path for inflow is shorter than the outflow path. Hence, during cyclic water level changes more water will enter the structure than will leave. Consequently, there will be a state, in which the outflow of the surplus of water is realized by an average internal set-up of the water level inside the structure (Barends 1988). The slope steepness causes an extra storage of water volume every cycle in comparison to a linear situation with a vertical slope (dashed area). This extra volume can be expressed as an average infiltration, according to:

$$I = I_0 \exp\left(-\frac{x}{\lambda}\right)$$

with (11a)

$$I_0 = c\frac{H^2}{2\lambda T \tan\alpha}$$

using the simplified formula for penetration length λ. Solving a schematic flow problem gives the expression for the average water height h as a function of x. The solution is:

$$h = Ax + B - \xi D^2 \exp\left(-\frac{x}{\lambda}\right) \tag{11b}$$

with $$\xi = 0.1\frac{cH^2}{4n\lambda D \tan\alpha}$$

where A and B depend on boundary conditions. The resulting formula is:

$$\frac{S}{D} = \sqrt{(1+\xi F)} - 1 \tag{11c}$$

where S is the maximum set-up, D the mean water depth, c a constant depending on the effects of air entrainment and rush-up/run-down ($c > 1$), H water level amplitude at the slope, λ penetration length, and α the slope angle. The function F is presented in Fig. 6 for two cases: (1) a closed, and (2) an open lee side. In the first case the maximum set-up occurs at the backside. In the second case the maximum

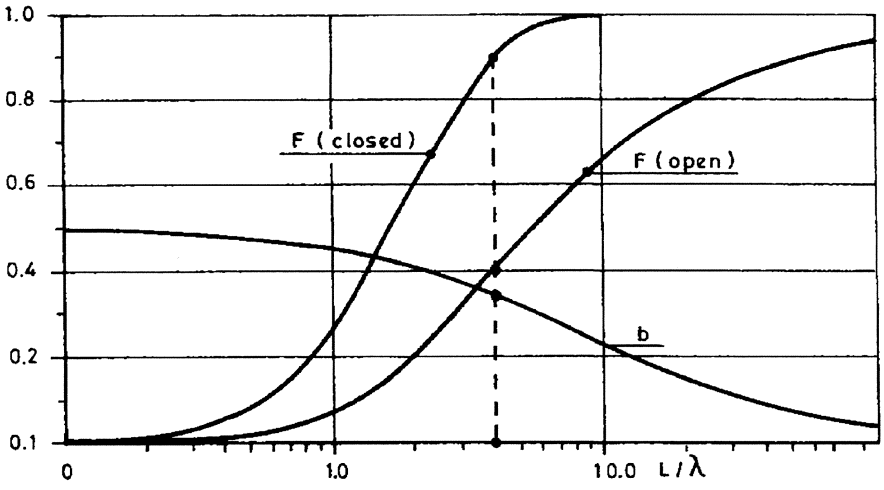

Fig.6 Diagram of internal set-up

set-up occurs at bL with L the length of the inner water table. For the real water table inside the structure the cyclic motion must be superimposed on the set-up. An example of the effect of internal set-up for a breakwater with a back-fill is shown in figure 7. The set-up is such, that for high waves the drain, which is intended to dissipate overtopping water, cannot function properly.

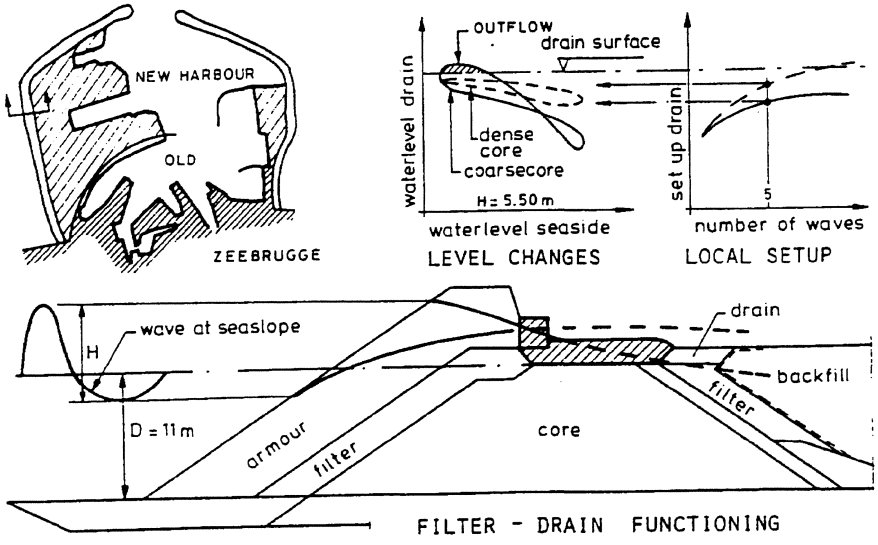

Fig. 7 internal set-up in a coastal structure

Slip circle analysis

The evaluation of the stability of rock marine structures is standard procedure. Usually, a failure state is simulated by the choice of a critical kinematical system assuming continuous deformation surfaces (slip surfaces), and comparing the mobilized force with the exposed one. Key factors are internal friction and cohesion. The stress state along the slip surfaces is determined by wave-induced pore pressures or earthquake-induced accelerations and a simplified effective stress field according to equation (9) (Bishop's method). Local excess pore-pressures (liquefaction) can be accounted for by adjusted pore pressures or a reduced friction angle. Several studies have shown that this method is sufficiently accurate for porous rock slopes when proper values for friction and cohesion are applied.

Bishop's method is most commonly used because of its convenience and its wide spread in simple computer codes. The most critical circle of sliding is calculated by considering the moment of weight and the shear resistance along the sliding surface. The soil mass is divided into several slices. The mechanical equilibrium of each of them is considered. Horizontal forces between adjacent slices are approximated. The error due to these simplifications in the safety factor is 2-6 %. The stability of the soil mass is expressed as a safety factor *F*. If F is larger than 1 the structure is safe. Usually an extra margin is taken into account to allow for uncertainties, for example. $F > 1.25$. The slip-circle analysis is based on effective stresses. Hence, pore pressures are important, even more when they vary in time. The typical rock friction angle dependent on the actual stress can be incorporated easily. Wave induced porous flow have shown an effect up to 25% of the safety factor (Fig. 8).

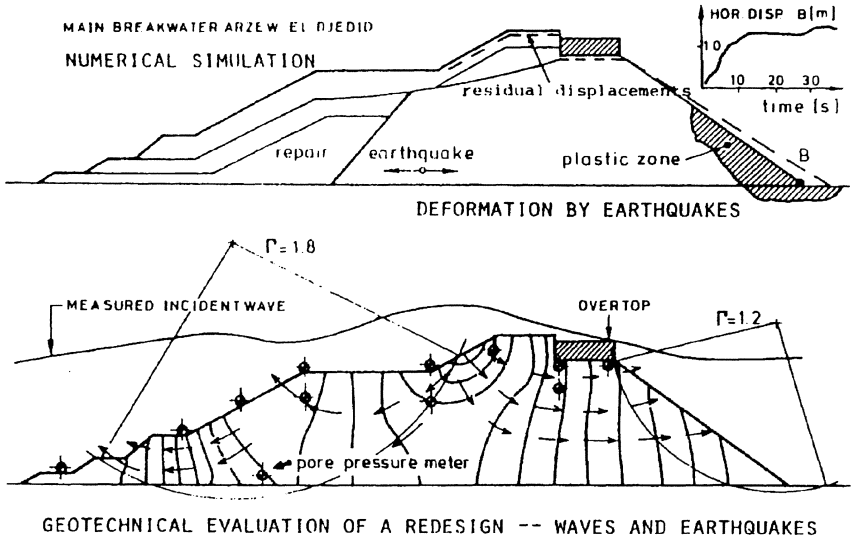

Fig. 8 Stability under wave attack >

The stability of slopes subjected to earthquakes is commonly simplified by the introduction of an additional inertial force, whose magnitude is equal to the product of the mass of the slice in failure and its horizontal acceleration. Usually vertical acceleration is not considered. The horizontal acceleration can be allowed for in a Bishop stability analysis. Morgenstern presented stability charts to facilitate the computation of the factor of safety of earth slopes during rapid draw down based on Bishop's stability analysis. A homogeneous structure with uniform *c'* and *d* is considered on a firm impervious bed. After drawdown no dissipation has yet occurred. Two graphs are presented in Fig. 9 left for a slope a of 2:1 and right 3:1 for a draw-down *L* of original height *H*. Heavy lines refer to $c'/qH = 0.025$ and dotted lines 0.0125.

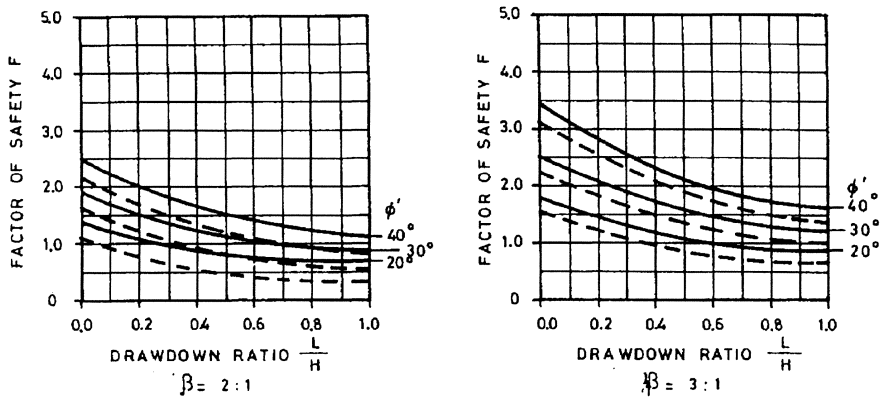

Fig. 9 Stability factors during rapid draw down

In some cases the most likely sliding face is not circular, but rather along weak strata or along strong rock surfaces. The interface between different rock layers may reveal lower internal friction because of different stone sizes. A reduction of the internal friction up to 30% may be expected. In this case one divides the sliding soil mass in an active wedge, a central block and a passive wedge. The factor of safety is the ratio between the active driving force and the passive resistance force. In the classical soil mechanics approach the conventional stability analysis assumes that the peak shear strength of the soil is fully mobilized simultaneously along the total length of the potential sliding plane. This is not always the case, a progressive failure can occur. Particularly under certain conditions slides in overconsolidated plastic clays and clay shales are preceded by the development of a continuous failure surface by a mechanism of progressive failure. Such situations have to be analysed with special care.

Filter stability

Granular filters are applied to protect against erosion by scour and migration (mixing fines in coarse). The filter stability is characterized by filter rules. The classic filter rules are (Terzaghi 1922):

Migration	uniform material		$D_{50f}/D_{50b} < 5$
	wide graded	1.	$D_{15f}/D_{85b} < 5$
		2.	$5 < D_{50f}/D_{50b} < 20$ to 60
permeability			$D_{20f}/D_{20b} > 5$

Suffix f and b relate to the filter (coarse) and basic (fine) material, respectively. Thanikachalam & Sakthivadivel have suggested less strict filter rules, which take into consideration the gradation:

$$D_{10f}/D_{10b} < 2.50\ D_{60b}/D_{10b} + 5.00$$

$$D_{60f}/D_{10f} < 0.94\ D_{10f}/D_{10b} - 5.65$$

$$D_{50f}/D_{50b} < 2.41\ D_{60f}/D_{10f} + 8.00$$

The internal stability of a wide graded material covering more orders of grain sizes must be treated in a different way. Kenney (1985) refers to a normalized steepness of the grain size distribution curve to express the internal stability. A minimum of 1.5 is advised. The application of this approach is validated for sand, gravel, and mine stone. A geo-textile on a fine granular bed is designed to prevent migration through the textile, which may be caused by "driving gradients". The following criteria are determined for the evaluation of the tightness of the geo-textile weave (fabric):

cohesive beds

$$O_{90}/D_{90b} < 10;\ O_{90}/D_{90b} < 1;\ O_{90} < 0.1\ mm$$

non-cohesive beds

- stationary loading	$O_{90}/D_{90b} < 1$	regular woven mattresses
	$O_{90}/D_{90b} < 1.8$	nonregular non-woven
- cyclic loading	$O_{98}/D_{15b} < 1$	no-clogging, not-widely graded
	$O_{98}/D_{85b} < 1$	clogging, widely graded

In some situations the fines from the bed may clog in the fabric and decrease the permeability significantly, causing high-pressure gradients. An acceptable criterion is that the geo-textile pressure gradient equals the gradient in the bed under design load conditions. Since the flow through the textile can be turbulent, the precise definition of the permeability needs careful attention. The strength of geo-textiles is important when sliding of soil masses may occur through the textile, or when settlements are opposed by the geo-textile. The required strength of a fabric can be determined by a modified Bishop stability analysis. For more information reference is made to literature (Geo-textiles 1986).

Dynamic excess pore-pressure

A pore-pressure build-up in a porous marine structure is possible due to external time-dependent loading and local deformation of the granular matrix. Pore pressure build-up dissipates by porous flow and by unloading. For the evaluation of the possibility of a local cyclic pore pressure build-up the order of magnitude of the dissipation period has to be considered. If the dissipation period is small compared to the relevant loading period, a cyclic pore pressure build- up will not occur.

Three phenomena need to be considered:

1 phreatic storage,
2 propagation of dynamic disturbance along the inner water table, and
3 field storage (elastic storage).

For (1) the phreatic storage effect see the section on wave penetration. A perturbation in the pore pressure will decay due to dissipation according to: $p(t) = p_0 \exp(-Bt)$ where p_0 is sudden pressure excitation and B is a decay factor depending on the phenomenon considered: (2) $B=ng/K$ for a dynamic disturbance along the inner water table, and (3) $B = 3c/rl$ for elastic field storage.

An example.

A structure has the following properties: porosity $n = 0.4$, gravity acceleration $g = 10\ m/s^2$, permeability $k = 0.05\ m/s$ (coarse gravel), elastic storage coefficient $c = kK/\gamma$ with bulk modulus $K = 3\ MPa$ and $\gamma = 15\ kN/m^3$ giving $c = 10\ m^2/s$, average drainage path $l = 4\ m$, hydraulic radius $r = V/A$ with volume $V = 140\ m^3$ and drainage surface $A = 15.6\ m^2$ giving $r = 9\ m$. Applying the formula yields: for (2) $B = 80$ and for (3) $B = 0.8\ 1/s$. In conclusion, a local pore-pressure build-up will not occur, if the relevant loading return period exceeds $1/3\ B$, which yields for (2) $0.0125\ s$ and for (3) $1.2\ s$. Therefore, for this example, excess pore pressures are expected (breaking waves and wave impacts), but cyclic accumulation is unlikely.

ENGINEERING EXPERIENCE (INTUITION)

Settlement of rock fill

The natural settlement (densification) of rock fill subjected to gravity, hydraulic or earthquake loading is sometimes important. Little is known about this aspect. For earth reservoir dams usually an increase of height of 0.2 to 0.5 % is applied, but during the construction densification activities are executed and controlled carefully.

In marine structures controlled densification is rarely performed. Loose dumped gravel and rock fill can be increased in density by special methods, such as the falling weight and shaking plate method. The Menard method is popular and densification effects to a depth of 10 *m* have been reported. For gravel a 10 - 15 % densification can be achieved and for rock fill 10/60 *kg* up to 15 %.

For large stones heavy mechanical densification causes crushing. As a first estimate one may compare the energy of natural causes to that by machines. Densification equipment produces an acceleration of 10 *g* maximum. Earthquakes may produce up to 2 *g* in the entire structure, which will, therefore, lead to a densification of 2 % to 4 %.

The result of failure by internal sliding is not considered. Large wave impacts may generate in the structure on average an acceleration of the order of 1 *g*. The average densification will be of the order of 1 %. Slamming waves may, however, produce locally higher accelerations and higher densifications. This can be observed along coastal defence structures around the storm waterline.

Internal erosion/fatigue

Local pore fluid velocities may convey fine particles through the pores of the coarse. This may lead to internal erosion and become the onset of deterioration of the structure. The occurrence is controlled by so-called filter rules, which define limits of adjacent coarse and fine layer grain sizes. Artificial armour and rock fill degenerate with time, break at the contacts, and the fines are washed out. If not washed out, the skeleton fills up and behaves differently. This process can be characterized as material fatigue (Fookes & Poole 1981). Water may convey free sediments that settle in the pores and change the hydraulic permeability. It may become a serious problem under critical loading conditions (suffocation). Growth of marine organisms in pores may have a similar effect.

Local stability of rock fill

The hydraulic loading imposed on individual particles by waves, internal friction and interlocking of randomly placed stones cannot be described properly. Physical tests provide some general understanding

of the stability of a stone at the border subjected to hydraulic gradients. The experiments show that for a compacted granular medium porous outflow first activates a group of coherent particles to expand, creating a loose packing, until one favourable surface particle starts moving (boiling), giving way to outflow. This surface particle seems to possess a self-healing stability potential due to the inhomogeneity, which is induced by the motion. The space generated by the lifting decreases the extrusion pressure. This behaviour has been observed in tests on sand and gravel (turbulent porous flow). The lift can, however, be a catalyst for the erosion, since a lifted extruding particle can be conveyed more easily by the parallel free surface flow.

References

Barends, F.B.J. et al. (1983) Westbreakwater - Sines - Dynamic - geotechnical stability of breakwaters, *Proc. Conf. Coastal Structures*, Arlington.

Barends, F.B.J. (1985) Geotechnical aspects in breakwater design, chapter 6 in *Developments in Breakwaters*, Thomas Telford PC, London.

Barends, F.B.J and E.O.F. Calle (1985). A method to evaluate the geotechnical stability of off-shore structures founded on a loosely packed seabed sand under wave loading, BOSS '85, Delft.

Barends (1993) CUR-CIRIA Manual.

Barends (1994) Handbook for coastal/marine structures.

Barton, N. & Kjaernsli (1981) Shear strength of rock fill, Proc. ASCE. Geot. Eng. DN, Vol. 107 (GT7).

CIAD (1985) Computer aided evaluation of the reliability of a breakwater design (ed. Barends), CIAD Assoc., Zoetermeer, Holland.

Fookes, P.G. & Poole, A.B. (1981) Some preliminary consideration on the selection and durability of rock and concrete materials for breakwaters and coastal protection works. *Q. Jl. Engl. Geol.* Vol 14.

Geotextile (1986) IIIrd Int. Conf. on Geotextiles, Vienna.

Hannoura, A. & Barends, F.B.J. (1981) Non-Darcy flow; a state of the art, Euromech-143, Flow and Transport in Porous Media, Balkema PC, Rotterdam.

Hölscher, P. & F.B.J. Barends (1990) Finite difference schemes for wave transmission in rubble mounds, to appear in *J. Num. Meth. in Eng.*

Kenney, T.C. et al. (1985) Internal stability of granular filters, *Canadian Geotech Jl*, 22.

Kobayashi,M et al. (1987) Bearing capacity of a rubble mound supporting gravity structure, Rp 26(5) Port and Harbour Research Institute, Ministry of Transport, Nagase,Yokosuka.

Lambe, T.W. & R.V. Whitman (1969) Soil mechanics, J. Wiley, New York.

Seed H.B. & M.S. Rahamn (1978) Wave induced pore pressure in relation to ocean floor stability of cohesive soils, *Jl Marine Geotech.* 3(2).

Terzaghi, K (1943) Theoretical soil mechanics, J. Wiley, New York.

Van Gent, M.R.A. (1992) Formulae to describe porous flow. Comm. Hydr. & Geol. Eng., ISNN 0169-6548: 92(2), Univ, Delft.

Appendices

APPENDIX A Table 1 Bessel functions

x	$I_0(x)$	$I_1(x)$	$K_0(x)$	$K_1(x)$
0.0	1.0000	0.0000	∞	∞
0.1	1.0025	0.0501	2.4271	9.8538
0.2	1.0100	0.1005	1.7527	4.7760
0.3	1.0226	0.1517	1.3725	3.0560
0.4	1.0404	0.2040	1.1145	2.1844
0.5	1.0635	0.2579	0.9244	1.6564
0.6	1.0920	0.3137	0.7775	1.3028
0.7	1.1263	0.3719	0.6605	1.0503
0.8	1.1665	0.4329	0.5653	0.8618
0.9	1.2130	0.4971	0.4867	0.7165
1.0	1.2661	0.5652	0.4210	0.6019
1.1	1.3262	0.6375	0.3656	0.5098
1.2	1.3937	0.7147	0.3158	0.4346
1.3	1.4693	0.7973	0.2783	0.3726
1.4	1.5534	0.8861	0.2437	0.3208
1.5	1.6467	0.9817	0.2138	0.2774
1.6	1.7500	1.0848	0.1880	0.2406
1.7	1.8640	1.1963	0.1655	0.2094
1.8	1.9896	1.3172	0.1459	0.1826
1.9	2.1277	1.4482	0.1288	0.1597
2.0	2.2796	1.5906	0.1139	0.1399
2.1	2.4463	1.7455	0.1008	0.1228
2.2	2.6291	1.8280	0.0893	0.1079
2.3	2.8296	2.0978	0.0791	0.0653
2.7	3.8416	3.0161	0.0493	0.0577
2.8	4.1573	3.3011	0.0438	0.0511
2.9	4.5028	3.6126	0.0390	0.0453
3.0	4.8808	3.9534	0.0347	0.0356
3.2	5.7472	4.7342	0.0276	0.0316
3.3	6.2426	5.1810	0.0246	0.0281
3.4	6.7848	5.6701	0.0220	0.0250
3.5	7.3782	6.2058	0.0196	0.0222
3.6	8.0277	6.7927	0.0175	0.0198
3.7	8.7386	7.4358	0.0156	0.0176
3.8	9.5169	8.1404	0.0140	0.0157
3.9	10.3690	8.9128	0.0125	0.0140
4.0	11.3019	9.7595	0.0112	0.0125

APPENDIX B Table 2 The function $exp(b)\ W(u,b)$

$b \rightarrow$	10	20	30	40	50	60	70	80	90
u ↓									
1.00	.7833	.5571	.4558						
1.25	.7833	.5571	.4558	.3951					
1.50	.7832	.5571	.4558	.3951					
1.75	.7831	.5571	.4558	.3951	.3536				
2.00	.7823	.5571	.4558	.3951	.3536				
2.25	.7798	.5571	.4558	.3951	.3536				
2.50	.7740	.5571	.4558	.3951	.3536	.3229			
2.75	.7628	.5571	.4558	.3951	.3536	.3229			
3.00	.7447	.5571	.4558	.3951	.3536	.3229	.2991		
3.25	.7187	.5571	.4558	.3951	.3536	.3229	.2991		
3.50	.6849	.5571	.4558	.3951	.3536	.3229	.2991		
3.75	.6440	.5571	.4558	.3951	.3536	.3229	.2991	.2798	
4.00	.5975	.5571	.4558	.3951	.3536	.3229	.2991	.2798	
4.25	.5473	.5571	.4558	.3951	.3536	.3229	.2991	.2798	
4.50	.4951	.5570	.4558	.3951	.3536	.3229	.2991	.2798	.2639
4.75	.4427	.5569	.4558	.3951	.3536	.3229	.2991	.2798	.2639
5.00	.3916	.5567	.4558	.3951	.3536	.3229	.2991	.2798	.2639
5.25	.3430	.5562	.4558	.3951	.3536	.3229	.2991	.2798	.2639
5.50	.2977	.5553	.4558	.3951	.3536	.3229	.2991	.2798	.2639
5.75	.2563	.5538	.4558	.3951	.3536	.3229	.2991	.2798	.2639
6.00	.2189	.5515	.4558	.3951	.3536	.3229	.2991	.2798	.2639
6.25	.1857	.5479	.4558	.3951	.3536	.3229	.2991	.2798	.2639
6.50	.1566	.5429	.4558	.3951	.3536	.3229	.2991	.2798	.2639
6.75	.1312	.5362	.4558	.3951	.3536	.3229	.2991	.2798	.2639
7.00	.1094	.5274	.4558	.3951	.3536	.3229	.2991	.2798	.2639
7.25	.0908	.5164	.4558	.3951	.3536	.3229	.2991	.2798	.2639
7.75	.0617	.4874	.4557	.3951	.3536	.3229	.2991	.2798	.2639
8.00	.0506	.4695	.4557	.3951	.3536	.3229	.2991	.2798	.2639
8.25	.0413	.4496	.4556	.3951	.3536	.3229	.2991	.2798	.2639
8.50	.0336	.4278	.4554	.3951	.3536	.3229	.2991	.2798	.2639
8.75	.0273	.4045	.4552	.3951	.3536	.3229	.2991	.2798	.2639
9.00	.0221	.3801	.4547	.3951	.3536	.3229	.2991	.2798	.2639
9.25	.0179	.3550	.4541	.3951	.3536	.3229	.2991	.2798	.2639
9.50	.0144	.3294	.4532	.3951	.3536	.3229	.2991	.2798	.2639
9.75	.0116	.3038	.4519	.3951	.3536	.3229	.2991	.2798	.2639

Table 2 (continued) The function $exp(b)\ W(u,b)$

$b \rightarrow$	10	20	30	40	50	60	70	80	90
u ↓									
10.00	.0093	.2785	.4501	.3951	.3536	.3229	.2991	.2798	.2639
12.50	.0009	.0876	.3839	.3946	.3536	.3229	.2991	.2798	.2639
15.00	.0001	.0185	.2279	.3819	.3536	.3229	.2991	.2798	.2639
17.50	.0000	.0030	.0903	.3168	.3517	.3229	.2991	.2798	.2639
20.00	.0000	.0004	.0256	.1976	.3336	.3227	.2991	.2798	.2639
22.50	.0000	.0000	.0056	.0898	.2732	.3189	.2990	.2798	.2639
25.00	.0000	.0000	.0010	.0308	.1768	.2977	.2984	.2798	.2639
27.50	.0000	.0000	.0002	.0084	.0882	.2423	.2927	.2797	.2639
30.00	.0000	.0000	.0000	.0019	.0346	.1615	.2698	.2785	.2638
32.50	.0000	.0000	.0000	.0004	.0110	.0863	.2192	.2711	.2636
35.00	.0000	.0000	.0000	.0001	.0029	.0373	.1495	.2475	.2617
37.50	.0000	.0000	.0000	.0000	.0007	.0133	.0842	.2010	.2529
40.00	.0000	.0000	.0000	.0000	.0001	.0040	.0393	.1399	.2292
42.50	.0000	.0000	.0000	.0000	.0000	.0011	.0154	.0821	.1864
45.00	.0000	.0000	.0000	.0000	.0000	.0002	.0052	.0407	.1319
47.50	.0000	.0000	.0000	.0000	.0000	.0001	.0015	.0172	.0801
50.00	.0000	.0000	.0000	.0000	.0000	.0000	.0004	.0063	.0418
52.50	.0000	.0000	.0000	.0000	.0000	.0000	.0001	.0020	.0188
55.00	.0000	.0000	.0000	.0000	.0000	.0000	.0000	.0006	.0074
57.50	.0000	.0000	.0000	.0000	.0000	.0000	.0000	.0002	.0026
60.00	.0000	.0000	.0000	.0000	.0000	.0000	.0000	.0000	.0008
62.50	.0000	.0000	.0000	.0000	.0000	.0000	.0000	.0000	.0002
65.00	.0000	.0000	.0000	.0000	.0000	.0000	.0000	.0000	.0001

Table 2 (continued) The function $exp(b)\ W(u,b)$

$b \rightarrow$	100	200	300	400	500	600	700	800	900
u ↓									
10.00	.2504	.1771	.1447						
12.50	.2504	.1771	.1447						
15.00	.2504	.1771	.1447						
17.50	.2504	.1771	.1447						
20.00	.2504	.1771	.1447						
22.50	.2504	.1771	.1447						
25.00	.2504	.1771	.1447						
27.50	.2504	.1771	.1447						
30.00	.2504	.1771	.1447	.1253	.1121				
32.50	.2503	.1771	.1447	.1253	.1121				
35.00	.2503	.1771	.1447	.1253	.1121				
37.50	.2499	.1771	.1447	.1253	.1121				
40.00	.2472	.1771	.1447	.1253	.1121				
42.50	.2374	.1771	.1447	.1253	.1121				
45.00	.2139	.1771	.1447	.1253	.1121				
47.50	.1743	.1771	.1447	.1253	.1121				
50.00	.1252	.1771	.1447	.1253	.1121	.1023	.0947		
52.50	.0783	.1771	.1447	.1253	.1121	.1023	.0947		
55.00	.0425	.1771	.1447	.1253	.1121	.1023	.0947		
57.50	.0202	.1771	.1447	.1253	.1121	.1023	.0947		
60.00	.0085	.1771	.1447	.1253	.1121	.1023	.0947		
62.50	.0032	.1771	.1447	.1253	.1121	.1023	.0947	.0886	.0835
65.00	.0011	.1771	.1447	.1253	.1121	.1023	.0947	.0886	.0835
67.50	.0003	.1771	.1447	.1253	.1121	.1023	.0947	.0886	.0835
70.00	.0001	.1771	.1447	.1253	.1121	.1023	.0947	.0886	.0835
72.50	.0000	.1771	.1447	.1253	.1121	.1023	.0947	.0886	.0835
75.00	.0000	.1771	.1447	.1253	.1121	.1023	.0947	.0886	.0835
77.50	.0000	.1771	.1447	.1253	.1121	.1023	.0947	.0886	.0835
80.00	.0000	.1770	.1447	.1253	.1121	.1023	.0947	.0886	.0835
82.50	.0000	.1766	.1447	.1253	.1121	.1023	.0947	.0886	.0835
85.00	.0000	.1752	.1447	.1253	.1121	.1023	.0947	.0886	.0835
87.50	.0000	.1719	.1447	.1253	.1121	.1023	.0947	.0886	.0835
90.00	.0000	.1651	.1447	.1253	.1121	.1023	.0947	.0886	.0835
92.50	.0000	.1532	.1447	.1253	.1121	.1023	.0947	.0886	.0835
95.00	.0000	.1357	.1447	.1253	.1121	.1023	.0947	.0886	.0835
97.50	.0000	.1134	.1447	.1253	.1121	.1023	.0947	.0886	.0835
100.00	.0000	.0886	.1447	.1253	.1121	.1023	.0947	.0886	.0835
125.00	.0000	.0001	.1445	.1253	.1121	.1023	.0947	.0886	.0835
150.00	.0000	.0000	.0723	.1253	.1121	.1023	.0947	.0886	.0835
275.00	.0000	.0000	.0000	.0000	.0018	.1006	.0947	.0886	.0835
175.00	.0000	.0000	.0005	.1248	.1121	.1023	.0947	.0886	.0835
200.00	.0000	.0000	.0000	.0626	.1121	.1023	.0947	.0886	.0835
225.00	.0000	.0000	.0000	.0012	.1110	.1023	.0947	.0886	.0835
250.00	.0000	.0000	.0000	.0000	.0560	.1023	.0947	.0886	.0835
300.00	.0000	.0000	.0000	.0000	.0000	.0512	.0947	.0886	.0835
325.00	.0000	.0000	.0000	.0000	.0000	.0025	.0924	.0886	.0835
350.00	.0000	.0000	.0000	.0000	.0000	.0000	.0474	.0886	.0835

APPENDIX C Table 3 The function $exp(x)\ K_0(x)$

x	$exp(x)\ K_0(x)$	x	$exp(x)\ K_0(x)$	x	$exp(x)\ K_0(x)$
.100	2.6823	5.100	.5426	10.100	.3897
.200	2.1408	5.200	.5376	10.200	.3979
.300	1.8526	5.300	.5327	10.300	.3860
.400	1.6627	5.400	.5280	10.400	.3842
.500	1.5241	5.500	.5233	10.500	.3824
.600	1.4167	5.600	.5188	10.600	.3806
.700	1.3301	5.700	.5144	10.700	.3789
.800	1.2502	5.800	.5101	10.800	.3772
.900	1.1972	5.900	.5059	10.900	.3755
1.000	1.1445	6.000	.4979	11.100	.3705
1.300	1.0210	6.300	.4902	11.300	.3689
1.400	.9881	6.400	.4865	11.400	.3673
1.500	.9582	6.500	.4828	11.500	.3657
1.600	.9309	6.600	.4793	11.600	.3642
1.700	.9059	6.700	.4758	11.700	.3627
1.800	.8828	6.800	.4724	11.800	.3612
1.900	.8615	6.900	.4691	11.900	.3597
2.000	.8416	7.000	.4658	12.000	.3582
2.100	.8230	7.100	.4595	12.200	.3553
2.300	.7894	7.300	.4565	12.300	.3539
2.400	.7740	7.400	.4535	12.400	.3525
2.500	.7595	7.500	.4505	12.500	.3511
2.600	.7459	7.600	.4476	12.600	.3484
2.800	.7206	7.800	.4420	12.800	.3470
2.900	.7089	7.900	.4393	12.900	.3457
3.000	.6978	8.000	.4366	13.000	.3444
3.100	.6871	8.100	.4340	13.100	.3431
3.200	.6770	8.200	.4314	13.200	.3418
3.300	.6580	8.400	.4264	13.400	.3393
3.500	.6490	8.500	.4239	13.500	.3381
3.600	.6490	8.600	.4215	13.600	.3368
3.700	.6322	8.700	.4192	13.700	.3356
3.800	.6243	8.800	.4168	13.800	.3344
3.900	.6167	8.900	.4145	13.900	.3333
4.000	.6093	9.000	.4123	14.000	.3321
4.100	.5953	9.200	.4079	14.200	.3298
4.300	.5887	9.300	.4058	14.300	.3286
4.400	.5823	9.400	.4036	14.400	.3275
4.500	.5761	9.500	.4016	14.500	.3264
4.600	.5701	9.600	.3995	14.600	.3253
4.700	.5643	9.700	.3975	14.700	.3242
4.800	.5586	9.800	.3955	14.800	.3231
4.900	.5531	9.900	.3936	14.900	.3221
5.000	.5478	10.000	.3919	15.000	.3210